Meteoritics & Planetary Science 44, Nr 9, 1287–1322 (2009)
Abstract available online at http://meteoritics.org

Compositional and lithological diversity among brecciated lunar meteorites of intermediate iron concentration

Randy L. KOROTEV[1*], Ryan A. ZEIGLER[1], Bradley L. JOLLIFF[1], Anthony J. IRVING[2], and Theodore E. BUNCH[3]

[1]Department of Earth and Planetary Sciences and McDonnell Center for the Space Sciences, Washington University, 1 Brookings Drive, Saint Louis, Missouri 63130, USA
[2]Department of Earth and Space Sciences, University of Washington, Seattle, Washington 98195, USA
[3]Department of Geology, Northern Arizona University, Flagstaff, Arizona 94035, USA
[*]Corresponding author. E-mail: korotev@wustl.edu

(Received 08 April 2008; revision accepted 15 July 2009)

Abstract–We present new compositional data for 30 lunar stones representing about 19 meteorites. Most have iron concentrations intermediate to those of the numerous feldspathic lunar meteorites (3–7% FeO) and the basaltic lunar meteorites (17–23% FeO). All but one are polymict breccias. Some, as implied by their intermediate composition, are mainly mixtures of brecciated anorthosite and mare basalt, with low concentrations of incompatible elements such as Sm (1–3 μg/g). These breccias likely originate from points on the Moon where mare basalt has mixed with material of the FHT (Feldspathic Highlands Terrane). Others, however, are not anorthosite-basalt mixtures. Three (17–75 μg/g Sm) consist mainly of nonmare mafic material from the nearside PKT (Procellarum KREEP Terrane) and a few are ternary mixtures of material from the FHT, PKT, and maria. Some contain mafic, nonmare lithologies like anorthositic norites, norites, gabbronorites, and troctolite. These breccias are largely unlike breccias of the Apollo collection in that they are poor in Sm as well as highly feldspathic anorthosite such as that common at the Apollo 16 site. Several have high Th/Sm compared to Apollo breccias. Dhofar 961, which is olivine gabbronoritic and moderately rich in Sm, has lower Eu/Sm than Apollo samples of similar Sm concentration. This difference indicates that the carrier of rare earth elements is not KREEP, as known from the Apollo missions. On the basis of our present knowledge from remote sensing, among lunar meteorites Dhofar 961 is the one most likely to have originated from South Pole-Aitken basin on the lunar far side.

INTRODUCTION

About half of the approximately 65 lunar meteorites (meteorite count, not stone count) are breccias from the highlands that, with 70–90% normative anorthite, are highly feldspathic (Korotev et al. 2003a). Feldspathic lunar meteorites have high concentrations of Al_2O_3 (>25%) and low concentrations of FeO (<7%; Fig. 1) and other elements associated with ferromagnesian minerals (Mg, Sc, Ti, V, Cr, and Mn). Most also have low concentrations of Sm (Figs. 2 and 3) and Th, two incompatible elements for which concentrations have been determined both in samples and regions of the lunar surface from orbit (Elphic et al. 2000; Lawrence et al. 2000). A quarter of lunar meteorites are either unbrecciated basalts or breccias consisting mainly (>90%) of basalt (Korotev 2005; Day et al. 2006a, 2006b; Haloda et al. 2006, 2009; Joy et al. 2006; Greshake et al. 2008; and references therein; Korotev et al. 2008; Sokol et al. 2008; Zeigler et al. 2007a, 2007b). These meteorites have low concentrations of Al_2O_3, (typically 8–12% for the basalts), high concentrations of FeO (17–23%), Sc, Cr, and other elements carried by mafic silicates, and low to intermediate concentrations of incompatible elements (Fig. 2). This paper focuses on the remaining quarter of the lunar meteorites, those with compositions intermediate between the anorthositic breccias and the basalts. Specifically, it deals mainly with meteorites having 13–20% Al_2O_3 and 7–17% FeO (Fig. 1a) or which are feldspathic but have concentrations of Sm that are greater than the 0.3–2 μg/g typical of feldspathic lunar meteorites (Fig. 2; Table 1). The well studied or, at least, well known meteorites in this category are Calcalong Creek, QUE (Queen Alexandra Range) 94281, SaU (Sayh al Uhaymir) 169, Yamato 793274/981031 (paired stones), Yamato 983885, and, marginally, EET 87/96 (the Elephant Moraine 87521 and 96008 pair), which may contain up to 10% nonmare material (Koeberl et al. 1991; Warren and Kallemeyn 1991; Arai and Warren 1999; Hill and Boynton 2003; Korotev et al. 2003b; Gnos

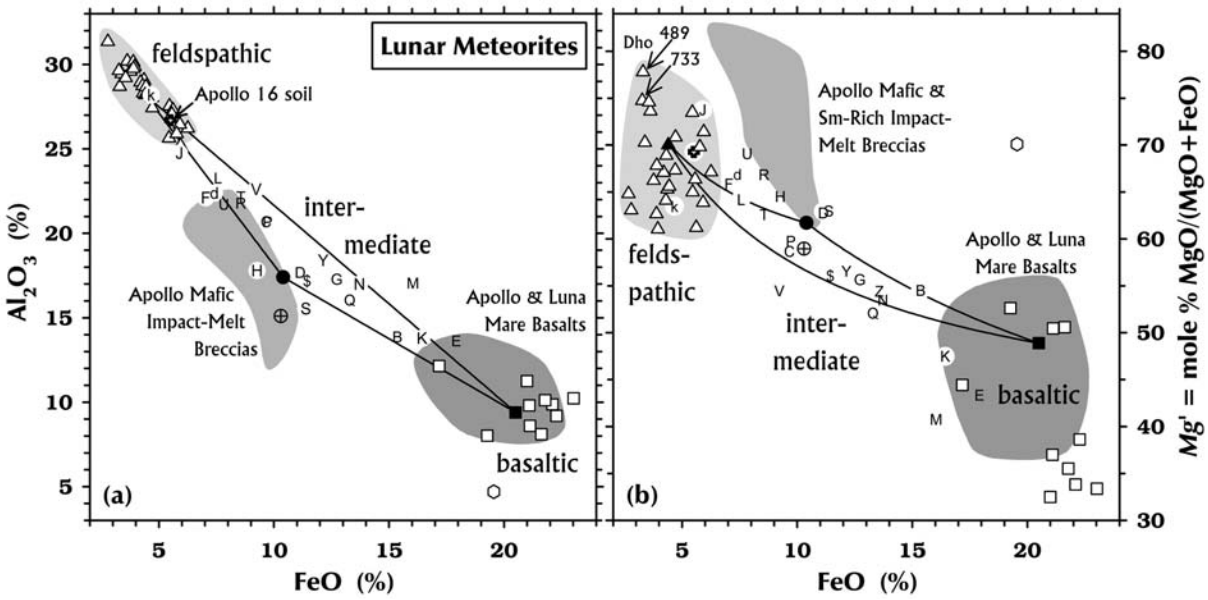

Fig. 1. a) Lunar meteorites in Al_2O_3-FeO space. The main subjects of this paper are those meteorites that plot between the fields of feldspathic lunar meteorites (triangles) and basaltic lunar meteorites (squares = unbrecciated basalts; see text for references to these data). For comparison in this and some subsequent figures, the plot also depicts the range of basalts from the Apollo and Luna missions and the mafic, Sm-rich impact-melt breccias of the Apollo collection ("LKFM" basalts; Korotev 2000), which are the main carriers of KREEP at the Apollo sites. The mare basalt fields are based on a large number of published data; see text. The symbol key for the intermediate-iron meteorites is in Table 1 and Fig. 3. The hexagon represents the olivine cumulate of NWA 773 (Fagan et al. 2003). b) *Mg′* = whole-rock Mg number (mole percent MgO/[MgO+FeO]). For this figure (but not for the values of Table 3) *Mg′* has been corrected to a zero-CM-chondrite (Fig. 8) basis using observed Ir concentrations and MgO/Ir and FeO/Ir ratios of CM chondrites (*Mg′* = 56.1; Wasson and Kallemeyn 1988). This correction leads to slightly greater *Mg′* for lunar meteorites with high Ir. Al_2O_3 and MgO data are not available for all of the meteorites of Fig. 2. See Fig. 2 for explanation of the lines and filled symbols.

et al. 2004; Arai et al. 2005a). Most of the meteorites discussed here have been discovered in the past five years. We have made preliminary reports of some of the information presented here in abstracts (Korotev and Irving 2005; Kuehner et al. 2005, 2007; Bunch et al. 2006; Korotev 2006; Zeigler et al. 2006a, 2007b; Jolliff et al. 2007, 2008, 2009; Korotev and Zeigler 2007; Korotev et al. 2007a, 2007b, 2008, 2009; O'Donnell et al. 2008).

This paper reports new bulk-composition data for meteorites, including many for which there is little or no previously published data. The goal of the paper is not so much to characterize the individual meteorites but to compare and contrast them compositionally as a diverse group and draw attention to the special or unusual features. We speculate about the nature of the breccias and possible pairing relationships on the basis of compositional characteristics and preliminary petrographic information. Some of these speculations could be tested by detailed petrographic studies and cosmic-ray exposure age measurements.

In the past, we have referred to lunar meteorites of intermediate iron concentration as "mingled" because, as polymict breccias, we have assumed them to be mixtures containing at least 10% of two or three end-member classes of lithologic components: (1) material of the FHT (Feldspathic Highland Terrane; Jolliff et al. 2000), mainly brecciated anorthosite and noritic anorthosite, (2) material of the PKT (Procellarum KREEP Terrane), usually breccia or glass of noritic composition with high concentrations of incompatible elements (alias, "KREEP;" Warren and Wasson 1979), and (3) volcanic basalt from maria or cryptomaria (Fig. 2; Korotev 2005). This "Apollo" model, which was first invoked by Goles et al. (1971) to account for compositions of Apollo 11 and 12 soils, is useful and appropriate for most polymict materials, especially regoliths, in the Apollo collection (Korotev et al. 2003a; Lucey et al. 2006). As new lunar meteorites are found, some of which must originate from points distant from the Apollo sites, the anorthosite-KREEP-basalt model may be too simplistic to apply to all brecciated meteorites and may actually obscure some important kinds of new materials. Thus, a second goal of this paper is to examine whether some meteorites might be distinct from the kinds of rocks that we know from the Apollo collection.

The complex petrologic nature of many of the meteorites, especially the fine-grained, polymict breccias, makes it difficult to reliably categorize the contributing rock types and their relative abundances. A combined chemical and petrologic approach as applied here has the advantage of broadly characterizing end-member lithologies, even though the exact mineralogy (characteristic assemblages) of each end-member cannot be uniquely specified. Exceptions include the identification of compositionally distinctive

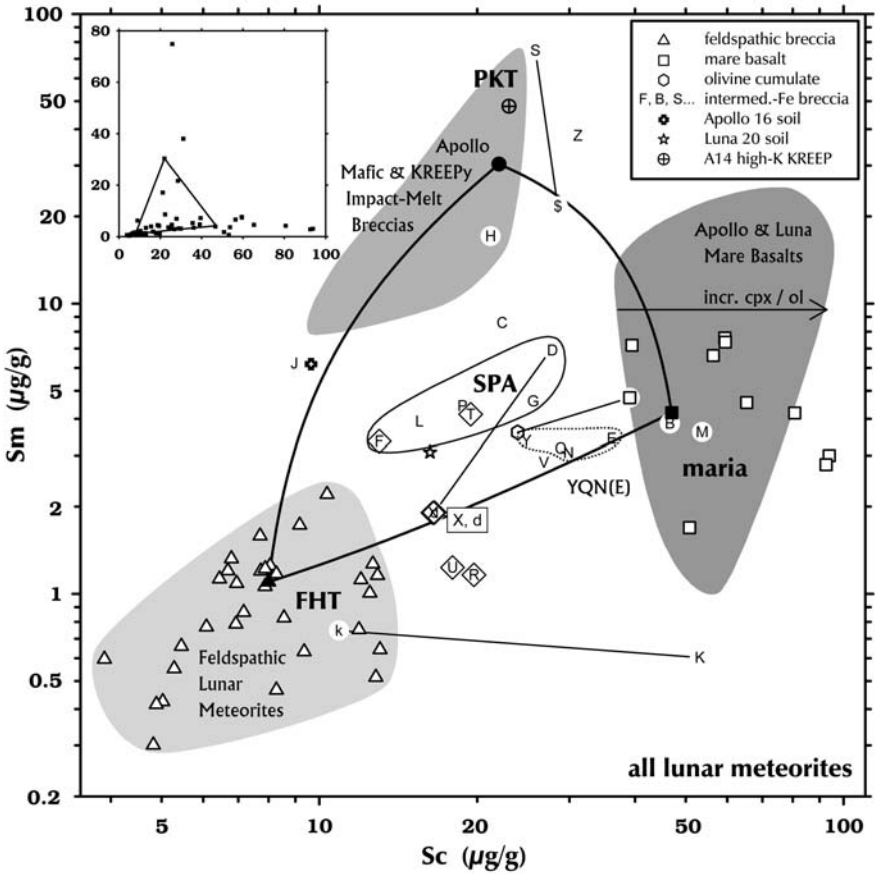

Fig. 2. Lunar meteorites in Sc-Sm space; the inset shows the same data on linear scales. Most lunar meteorites are brecciated anorthosites from the FHT (Feldspathic Highlands Terrane; triangles). A few (SaU 169 [S,$], NWA 4472/4485 [H], and Dhofar 1442 [Z]) are mafic, Sm-rich breccias that probably originate from within the PKT (Procellarum KREEP Terrane); such samples are common in the Apollo collection, mainly as mafic (noritic and troctolitic) impact-melt breccias. Ten meteorites (squares) are, or consist in large part of, unbrecciated basalts from the maria and several others are brecciated basalts with only a small fraction of nonmare material. The remaining meteorites are polymict breccias that contain a variety of lithologies (alphabetic symbols; see Table 1 for key). Straight lines connect either (1) different lithologies of multilithologic meteorites (SaU 169, NWA 773 et al.) or (2) different stones of presumably paired meteorites (Dhofar 925/961 and Kalahari 008/009). Alphabetic symbols enclosed in a diagonal square represent the high-Th/Sm meteorites of Fig. 6. The large "triangle" (distorted in logarithmic plot) is defined by the average of some feldspathic lunar meteorites (small filled triangle), the mean composition of low and very-low Ti basalts of the Apollo collection (filled square), and the mean composition of Apollo 14 soil (filled circle; Table 4). The "mean high-K KREEP" composition of Warren (1989) is shown for reference. Also shown are points for the average composition of typical, mature soil of Apollo 16 (Korotev 1997) and the soil of Luna 20 (Laul and Schmitt, 1973), both representing locations in the feldspathic highlands. Meteorites plotting in the SPA field have FeO and Th concentrations within the 2-σ range of surface composition of the South Pole-Aitken Terrane estimated by Jolliff et al. (2000).

components such as KREEP lithologies, which when in low abundance may be difficult to assess petrographically. The fact that some specimens inevitably must contain material from multiple impact mixing, re-mixing and melting events limits the degree of end-member definition that is feasible.

SAMPLES AND ANALYSIS

We obtained samples of some of the hot-desert meteorites discussed here directly from collectors and dealers. Others are portions of the type specimens deposited at Northern Arizona University and the University of Washington. Samples were usually received as sawn slices, but sometimes as chips. Some samples included the weathered exterior surface of the meteorite. Following our usual procedure (Korotev et al. 2006), we subdivided each sample into two to several subsamples of 12–36 mg each for INAA (instrumental neutron activation analysis). For subdivision, samples were wrapped in glassine weighing paper in an agate mortar, a stainless steel chisel was placed on the chip, and the chisel struck lightly with a hammer. The largest remaining fragments were broken until all fragments were less than 3 mm in diameter. Except for the subdivision procedure, we analyzed samples "as-is," i.e., the samples were not cleaned and no solvents were used. Some INAA subsamples consisted of one fragment, others of two to several fragments, and some of crumbs produced during the subdivision procedure. The number of subsamples and total

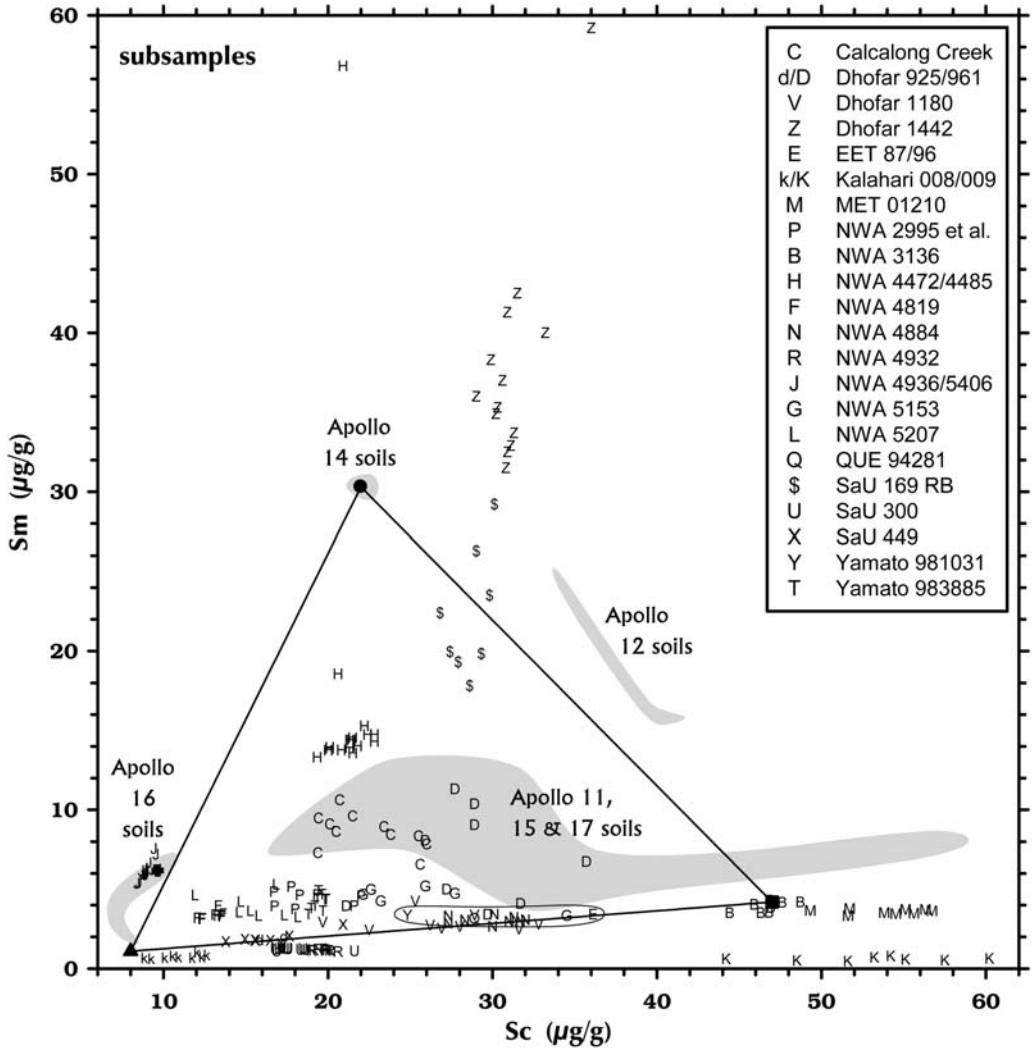

Fig. 3. A portion of Fig. 2, but with linear scales and data for subsamples of meteorites of intermediate FeO (and Sc) concentrations. The figure shows data for all analyzed subsamples of each meteorite except, to avoid congestion in this and some subsequent figures, only mean compositions are plotted for previously well studied (inside ellipse) Y = Yamato 981031, Q = QUE 94281, and E = EET 87521/96008 (Korotev et al. 2003b). Also, for the eight NWA 2995 et al. stones (P; Fig. 14), only the stone-mean data, not the data for the 54 individual subsamples are plotted. Fields for surface and trench soils of Apollo 14 (KREEP), Apollo 16 (highlands-KREEP mixtures), Apollo 11, 15, and 17 (mare-highlands-KREEP mixtures), and Apollo 12 (mare-KREEP mixtures) are shown in gray for reference. The large triangle is the same as that of Fig. 2.

analyzed mass of each meteorite is reported in Table 2, where we also report mass-weighted-mean results of INAA. The mass-weighted means, in effect, are the concentrations that we would have obtained if we had analyzed one sample consisting of the entire mass. Data for individual subsamples are presented in several of the figures.

For INAA, we sealed subsamples into tubes of ultrapure fused silica (Heraeus-Amersil Suprasil® T21, 5-mm outside diameter). The sample tubes were irradiated in 14 batches from July, 2002, through December, 2008, in the University of Missouri Research Reactor with a thermal neutron flux of 5×10^{13} cm^{-2}s^{-1} for 18 hours (Dhofar 1180, SaU 169), 24 hours (MET 01210, NWA 3136, NWA 4884), or 36 hours (all others). Each batch typically contained 48–52 unknowns and 8–9 samples of multielement standards. The principal standards for lithophile elements were chips of two synthetic glasses, designated WU-A (3 subsamples/batch) and WU-B (2 subsamples), that we have prepared and standardized against the National Bureau of Standards SRM (Standard Reference Material) 1633a, coal flyash (Korotev 1987a). Each batch contained a sample of SRM 1633a powder that was used as the standard for Sc, Sm, and Ta and a cross-check for the glass-standards. Finally, each batch contained 2–3 samples of a synthetic chemical standard for Ir and Au. Each sample tube was radioassayed by gamma-ray spectrometry at least four times between 5.5 and 28 days following the irradiation. Four gamma-ray detectors were used simultaneously. Data were reduced

Table 1. Lunar meteorites of intermediate iron composition.

	Mass of stone (g)	INAA mass (mg)	Reference	Plot symbol
Calcalong Creek	19	208	1	C
Dhofar 925/961	49/22	51/239	1	d/D
Dhofar 1180	121	196	1	V
Dhofar 1442	106	298	1	Z
EET 87521/96008	31/53	373/504	2	E
Kalahari 008 /009	598/13,500	278/265	1	k/K
MET 01210	23	240	1	M
NWA 2995 et al.	2819	1563	1	P
NWA 3136	95	230	1	B
NWA 4472/4485	64/188	323/262	1	H
NWA 4819	234	275	1	F
NWA 4884	42	266	1	N
NWA 4932	93	210	1	R
NWA 4936/5406	179	294/281	1	J
NWA 5153	50	185	1	G
NWA 5207	101	255	1	L
QUE 94281	23	464	3	Q
SaU 169 melt/reg. breccia	206	98/296	1	S/$
SaU 300	153	321	1	U
SaU 449	16.5	237	1	X
Yamato 793274/981031	9/186	0/204	2	Y
Yamato 983885	290	107	1	T

Data references: (1) This work; (2) Korotev et al. 2003b; (3) Jolliff et al. (1998). "NWA 2995 et al." includes NWA 2995, NWA 2996, NWA 3190, NWA 4503, NWA 5151, and NWA 5152, and two unnamed stones.

with the TEABAGS programs of Lindstrom and Korotev (1982).

For some meteorites, the subsamples varied considerably in composition; for others, the variation was small. For example, the RSD (relative standard deviation, $s/\bar{x}$, where s is the sample standard deviation of the concentration values obtained for the various subsamples and $\bar{x}$ is the mean) in FeO concentrations ranged from 1.8% in the impact-melt breccia lithology of SaU 169 (N = 4) to 25% in NWA (Northwest Africa) 2996 (N = 8). In lunar breccias, most compositional variation in major elements is a sampling effect resulting from differences in the abundance ratio of plagioclase to pyroxene-plus-olivine among small subsamples (Korotev 2005). For many of the meteorites discussed here, this variation, in turn, is related to differences in relative proportions of feldspathic and mafic or basaltic clasts among subsamples and the grain size of the clasts.

After activation analysis we analyzed a subset of the INAA subsamples for major elements. In order to obtain a representative major-element composition, one comparable to the INAA weighted mean (Table 2), we used the following procedure. We selected two or three INAA subsamples that spanned the range in FeO concentrations for major element analysis. We pulverized each selected subsample, fused 10–20 mg of the powder, and analyzed the resulting glasses for major elements by EPMA (electron probe microanalysis; Zeigler et al. 2005). For each meteorite we then calculated the least-squares lines (simple linear regression, Fig. 4) for the concentration of each element as a function of the FeO concentration for the analyzed subsamples. Iron is the only major element determined with high precision by both techniques. For the EPMA data, we then calculated the value of the point on the line corresponding to the mass-weighted-mean FeO concentration obtained by INAA; these are the data presented in Table 3. In practice, this entire procedure results in data that differ little from simple means calculated directly from the EPMA data.

DATA PRESENTATION AND THE APOLLO MODEL

As a means of comparing compositions of lunar meteorites to Apollo samples and the Apollo model, in some figures we plot data that we have obtained by INAA on lithic fragments in the 10–100 mg mass range from Apollo regolith samples (2–4 mm grain-size fractions). We have reported many, but not all, of these data in previous publications and reports (Jolliff et al. 1991; 1996; Jolliff and Haskin 1995; Korotev et al. 2002; Zeigler et al. 2006a). The 2361 fragments in the Apollo suite average 24 mg in mass, about the same as the lunar meteorite subsamples (28 mg).

Although the paper deals mostly with meteorites of intermediate iron concentration, we have chosen to depict Sc concentrations instead of Fe or FeO concentration on many of the plots to represent "maficness." Although Sc concentrations correlate well with those of FeO to a first approximation (R^2 = 0.86 for the meteorites of Fig. 2), interpretation of "FeO" data (total Fe as FeO) in polymict lunar samples is complicated by the fact that a significant and variable fraction of the Fe is contributed by asteroidal meteorites that have impacted the Moon, much of which occurs as metal (Korotev 1994). For

Table 2. Mass-weighted mean results of instrumental neutron activation analysis.

	Na_2O %	K_2O %	CaO %	Sc µg/g	Cr µg/g	FeO_T %	Co µg/g	Ni µg/g	As µg/g	Se µg/g	Br µg/g
Calcalong Creek	0.434	0.25	13.6	22.3	1260	9.66	25.9	113	0.37	<1	0.27
± 1	0.004	0.08	0.3	0.2	13	0.10	0.3	19	0.20	–	0.24
± 2	0.024	0.03	0.3	1.7	91	0.70	1.8	20	0.23	–	0.12
Dhofar 925	0.315	<0.3	14.9	16.6	1350	7.41	31.4	344	0.39	0.23	0.40
± 1	0.003	–	0.3	0.2	14	0.07	0.3	10	0.09	0.19	0.07
Dhofar 961	0.370	<0.7	13.6	27.8	1985	11.14	54.7	642	0.69	0.70	0.56
± 1	0.004	–	0.4	0.3	20	0.11	0.6	20	0.26	0.27	0.31
± 2	0.030	–	0.5	3.1	200	1.02	17.2	233	0.13	0.22	0.09
Dhofar 1180	0.384	<0.3	14.8	26.8	1040	9.22	18.6	128	0.35	n.a.	0.53
± 1	0.004	–	0.3	0.3	10	0.09	0.2	17	0.15	–	0.10
± 2	0.010	–	0.3	3.2	100	0.70	1.1	19	0.11	–	0.04
Dhofar 1442	0.791	0.68	11.9	31.1	1638	13.56	43.4	540	0.2	0.5	0.6
± 1	0.008	0.14	0.5	0.3	17	0.14	0.4	50	0.5	0.6	0.4
± 2	0.021	0.06	0.6	1.0	37	0.19	3.4	70	0.1	0.3	0.2
Kalahari 008	0.561	<0.5	15.4	10.9	710	4.67	10.8	61	0.32	<0.5	0.49
± 1	0.006	–	0.2	0.1	7	0.05	0.1	13	0.17	–	0.16
± 2	0.049	–	0.4	1.0	50	0.29	0.5	11	0.16	–	0.13
Kalahari 009	0.485	<1.2	11.6	53.2	2880	16.43	26.3	<150	<4.	<0.7	0.8
± 1	0.007	–	0.5	0.5	30	0.17	0.3	–	–	–	0.6
± 2	0.031	–	0.4	4.2	190	0.97	2.8	–	–	–	0.4
MET 01210	0.304	0.03	14.7	53.7	1620	16.03	26.6	180	<0.7	n.a.	<0.7
± 1	0.003	0.10	0.4	0.5	16	0.16	0.3	21	–	–	–
± 2	0.007	0.03	0.4	1.9	40	0.24	0.5	13	–	–	–
NWA 2995/6	0.471	0.18	14.3	18.8	1570	9.75	34.1	200	<0.6	n.a.	0.36
NWA 2995 et al.	0.466	0.13	14.2	18.7	1580	9.72	34.9	200	<1.0	<1.0	0.34
± 1	0.005	0.16	0.3	0.2	15	0.10	0.3	22	–	–	0.28
± 2	0.013	0.02	0.2	1.2	110	0.61	2.2	18	–	–	0.06
NWA 3136	0.295	0.14	12.4	46.6	2860	15.36	35.6	156	1.1	<0.5	0.57
± 1	0.003	0.10	0.4	0.5	30	0.15	0.4	25	0.2	–	0.19
± 2	0.009	0.05	0.2	1.0	85	0.25	2.5	16	0.4	–	0.09
NWA 4472/4485	0.600	0.49	12.5	21.2	1565	9.26	23.1	131	<1	0.08	4.4
± 1	0.006	0.22	0.4	0.2	16	0.09	0.2	22	–	0.54	0.7
± 2	0.010	0.08	0.3	0.5	40	0.15	1.0	15	–	0.06	0.9
NWA 4819	0.363	<0.5	14.9	13.0	1420	7.03	27.8	288	<1	<1	1.4
± 1	0.004	–	0.2	0.1	15	0.07	0.3	18	–	–	0.2
± 2	0.009	–	0.7	0.5	51	0.24	1.8	21	–	–	0.2
NWA 4884	0.366	<0.3	13.9	29.9	2050	13.72	43.8	153	<0.8	0.1	0.1
± 1	0.004	–	0.3	0.3	20	0.14	0.4	36	–	0.1	0.3
± 2	0.010	–	0.3	1.4	110	0.50	2.1	33	–	0.2	0.1
NWA 4932	0.307	<0.3	13.5	19.7	1500	8.55	44.3	602	0.5	0.4	1.2
± 1	0.003	–	0.2	0.20	15	0.09	0.4	26	0.2	0.2	0.2
± 2	0.007	–	0.1	0.4	47	0.30	14.5	218	0.2	0.2	0.2
NWA 4936/5406	0.525	<0.3	14.4	8.96	774	5.89	39.5	572	0.18	<0.7	0.2
± 1	0.005	–	0.3	0.09	8	0.06	0.4	15	0.13	–	0.1
± 2	0.013	–	0.2	0.19	18	0.24	9.4	143	0.06	–	0.1
NWA 5153	0.476	0.13	13.6	25.6	1960	12.72	42.4	150	<1.1	0.14	0.33
± 1	0.005	0.13	0.3	0.3	20	0.13	0.4	25	–	0.13	0.17
± 2	0.017	0.07	0.3	4.9	290	0.88	3.4	50	–	0.21	0.15
NWA 5207	0.484	0.10	14.9	15.52	1065	7.56	26.7	233	<1	<1.2	0.49
± 1	0.005	0.10	0.3	0.16	11	0.08	0.3	19	–	–	0.11
± 2	0.019	0.03	0.3	1.63	82	0.56	2.1	48	–	–	0.15
SaU 169 IMB	0.865	0.61	12.3	25.8	918	11.38	30.2	252	<1	n.a.	0.83
± 1	0.009	0.27	0.6	0.3	9	0.11	0.3	28	–	–	0.33
± 2	0.036	0.14	0.7	1.0	180	0.28	2.4	15	–	–	0.15
SaU 169 RB	0.739	0.52	12.7	28.5	1590	11.44	24.3	49	<1	<2	0.43
± 1	0.007	0.12	0.4	0.3	16	0.11	0.2	23	–	–	0.20
± 2	0.028	0.09	0.4	0.6	110	0.24	1.4	9	0.25	–	0.13
SaU 300	0.329	<0.3	13.6	17.9	1470	7.82	34.5	440	0.46	0.48	0.77
± 1	0.003	–	0.3	0.2	15	0.08	0.3	16	0.12	0.17	0.11
± 2	0.015	–	0.3	0.8	80	0.28	1.9	30	0.08	0.05	0.07
SaU 449	0.318	0.07	14.0	16.5	1370	7.86	48.4	560	0.65	<1	0.38
± 1	0.003	0.05	0.3	0.2	15	0.08	0.5	20	0.16	–	0.15
± 2	0.012	0.02	0.2	1.8	110	0.74	23.5	350	0.33	–	0.10
Yamato 983885	0.365	0.14	13.8	19.4	1490	8.56	40.3	533	<0.4	n.a.	n.a.
± 1	0.004	0.06	0.3	0.2	15	0.09	0.4	17	–	–	–
± 2	0.005	0.01	0.3	0.3	19	0.21	8.7	129	–	n.a.	n.a.

Table 2. *Continued.* Mass–weighted mean results of instrumental neutron activation analysis.

	Rb µg/g	Sr µg/g	Zr µg/g	Cs µg/g	Ba µg/g	La µg/g	Ce µg/g	Nd µg/g	Sm µg/g	Eu µg/g	Tb µg/g
Calcalong Creek	6	121	253	0.29	208	19.0	49.4	29	8.59	1.06	1.76
± 1	2	16	20	0.03	8	0.2	0.5	2	0.09	0.02	0.02
± 2	1	8	25	0.03	15	1.8	4.4	3	0.76	0.07	0.15
Dhofar 925	<3	373	62	0.09	93	4.04	10.35	6.8	1.91	0.704	0.428
± 1	–	11	9	0.02	3	0.04	0.23	0.6	0.02	0.008	0.009
Dhofar 961	<10	1180	215	0.22	320	15.4	40.0	23.2	6.90	0.815	1.439
± 1	–	25	30	0.03	8	0.2	0.4	1.6	0.07	0.017	0.017
± 2	–	463	78	0.07	87	5.2	13.3	7.8	2.27	0.103	0.459
Dhofar 1180	<8	1580	75	<0.2	537	5.30	14.1	8.9	2.84	0.90	0.64
± 1	–	30	25	–	9	0.05	0.2	1.5	0.03	0.02	0.02
± 2	–	272	15	–	300	1.04	2.7	1.7	0.44	0.04	0.08
Dhofar 1442	16	1200	1190	0.74	900	82.7	217	123	38.0	2.62	7.69
± 1	4	40	50	0.06	23	0.8	2	5	0.4	0.04	0.08
± 2	2	440	134	0.05	67	9.0	24	15	4.4	0.27	0.85
Kalahari 008	<5	200	<60	<0.1	46	1.48	3.59	2.4	0.747	1.014	0.183
± 1	–	13	–	–	4	0.02	0.13	1.0	0.008	0.013	0.008
± 2	–	9	–	–	5	0.12	0.44	0.5	0.096	0.039	0.024
Kalahari 009	<15	120	<200	<0.4	<90	0.95	2.43	<15	0.603	0.48	0.20
± 1	–	60	–	–	–	0.06	0.06	–	0.014	0.03	0.03
± 2	–	25	–	–	–	0.18	0.46	–	0.089	0.06	0.02
MET 01210	<5	150	90	<0.3	79	5.39	14.6	9.8	3.60	1.03	0.85
± 1	–	25	30	–	9	0.05	0.3	2.0	0.04	0.02	0.02
± 2	–	13	11	–	4	0.23	0.6	0.7	0.12	0.02	0.03
NWA 2995/6	<5	164	137	0.15	173	10.25	27.3	16	4.65	1.07	0.92
NWA 2995 et al.	<5	158	126	0.12	166	9.94	26.6	15.0	4.44	1.07	0.86
± 1	–	17	20	0.05	8	0.10	0.3	1.7	0.04	0.02	0.02
± 2	–	5	18	0.02	15	0.77	2.2	1.1	0.33	0.03	0.06
NWA 3136	<6	150	100	0.13	645	7.67	20.6	12.4	3.86	0.94	0.82
± 1	–	30	35	0.07	14	0.08	0.4	2.4	0.04	0.02	0.02
± 2	–	17	23	0.05	253	0.77	2.2	1.4	0.28	0.04	0.05
NWA 4472/4485	11	205	440	0.48	500	38.8	100.8	60	17.09	1.48	3.54
± 1	2	20	25	0.03	13	0.4	1.0	3	0.17	0.02	0.04
± 2	2	9	20	0.03	91	12.6	32.9	20	5.32	0.05	1.01
NWA 4819	<6	203	103	0.13	158	7.52	19.5	11.4	3.36	0.824	0.71
± 1	–	15	16	0.02	7	0.08	0.2	1.3	0.03	0.015	0.02
± 2	–	28	9	0.01	22	0.38	1.0	0.9	0.19	0.019	0.04
NWA 4884	<8	115	88	0.09	88	6.29	16.4	10.1	3.07	0.786	0.638
± 1	–	30	39	0.10	11	0.06	0.4	2.4	0.03	0.026	0.027
± 2	–	19	21	0.04	8	0.42	1.0	1.0	0.18	0.027	0.038
NWA 4932	<5	254	35	<0.15	447	2.34	6.3	3.5	1.16	0.64	0.278
± 1	–	18	25	–	9	0.03	0.2	1.9	0.01	0.02	0.014
± 2	–	26	10	–	218	0.09	0.2	0.8	0.04	0.01	0.008
NWA 4936/5406	<4	198	187	0.13	167	13.4	35.2	20.9	6.22	1.41	1.20
± 1	–	10	12	0.02	6	0.13	0.4	1.5	0.06	0.02	0.014
± 2	–	5	11	0.01	9	0.6	1.7	1.1	0.30	0.03	0.06
NWA 5153	<6	132	123	0.12	127	9.94	26.2	14.8	4.61	0.99	0.90
± 1	–	23	27	0.05	9	0.10	0.4	1.9	0.05	0.02	0.02
± 2	–	9	9	0.07	27	1.65	4.5	2.2	0.70	0.05	0.13
NWA 5207	<6	165	111	0.09	123	8.39	21.9	12.4	3.92	1.12	0.77
± 1	–	15	19	0.04	7	0.08	0.3	1.3	0.04	0.02	0.02
± 2	–	10	19	0.02	15	1.31	3.4	2.4	0.62	0.08	0.12
SaU 169 IMB	9	310	2260	0.52	1285	172	436	258	74.8	3.95	15.20
± 1	3	35	50	0.05	20	2	4	5	0.7	0.04	0.15
± 2	4	26	110	0.19	94	7	19	12	3.3	0.13	0.63
SaU 169 RB	11	233	700	0.57	627	47.5	124	72	21.7	2.23	4.53
± 1	2	21	30	0.04	12	0.5	1.3	3	0.2	0.03	0.04
± 2	2	16	90	0.12	67	4.5	12	7	2.0	0.08	0.39
SaU 300	<4	730	31	<0.1	47	2.57	6.6	3.6	1.233	0.631	0.289
± 1	–	15	15	–	5	0.03	0.2	1.0	0.012	0.012	0.011
± 2	–	124	3	–	4	0.10	0.3	0.3	0.042	0.016	0.013
SaU 449	<5	580	52	0.09	344	4.15	10.8	6.2	1.91	0.702	0.418
± 1	–	20	16	0.03	9	0.04	0.2	1.5	0.02	0.017	0.016
± 2	–	170	12	0.01	105	0.61	1.7	1.2	0.31	0.011	0.069
Yamato 983885	<6	130	123	0.20	116	9.32	24.4	13.6	3.68	0.83	0.911
± 1	–	15	15	0.03	7	0.09	0.3	1.4	0.04	0.02	0.016
± 2	–	9	13	0.02	8	0.76	2.3	1.1	0.38	0.03	0.075

Table 2. *Continued.* Mass-weighted mean results of instrumental neutron activation analysis.

	Yb µg/g	Lu µg/g	Hf µg/g	Ta µg/g	Ir ng/g	Au ng/g	Th µg/g	U µg/g	Mass 1 mg	N	Mass 2 mg/*N*
Calcalong Creek	6.71	0.920	6.77	0.90	3.4	3	3.95	1.10	208	11	19
± 1	0.07	0.009	0.07	0.03	1.1	2	0.04	0.07	–	–	–
± 2	0.50	0.066	0.66	0.08	0.4	3	0.33	0.11	–	–	–
Dhofar 925	1.82	0.252	1.61	0.230	18.3	18.6	0.94	0.45	51	2	26
± 1	0.02	0.003	0.02	0.012	0.6	0.6	0.02	0.02	–	–	–
Dhofar 961	5.48	0.762	5.39	0.61	18.3	12.0	2.86	0.98	239	9	27
± 1	0.06	0.008	0.06	0.04	1.1	1.1	0.04	0.06	–	–	–
± 2	1.64	0.224	1.92	0.21	7.4	4.3	1.02	0.27	–	–	–
Dhofar 1180	2.44	0.345	2.18	0.30	5.3	1.5	0.90	0.32	196	9	22
± 1	0.03	0.004	0.04	0.03	1.1	1.4	0.03	0.04	–	–	–
± 2	0.30	0.042	0.37	0.05	1.3	0.6	0.18	0.06	–	–	–
Dhofar 1442	27.3	3.71	29.5	3.71	22.	9.	14.4	4.0	298	13	23
± 1	0.3	0.04	0.3	0.11	2.	3.	0.2	0.2	–	–	–
± 2	2.7	0.37	3.0	0.36	4.	2.	1.1	0.3	–	–	–
Kalahari 008	0.748	0.108	0.53	0.070	1.9	1.3	0.172	0.11	238	9	31
± 1	0.013	0.003	0.02	0.014	0.7	0.8	0.014	0.04	–	–	–
± 2	0.091	0.012	0.06	0.007	0.2	1.3	0.00	0.03	–	–	–
Kalahari 009	1.25	0.190	0.40	<0.2	<9	<8	<0.2	<0.8	265	8	33
± 1	0.06	0.010	0.09	–	–	–	–	–	–	–	–
± 2	0.19	0.029	0.09	–	–	–	–	–	–	–	–
MET 01210	3.36	0.474	2.66	0.366	7.1	1.9	0.85	0.23	240	9	27
± 1	0.04	0.007	0.05	0.028	1.3	1.9	0.03	0.10	–	–	–
± 2	0.08	0.011	0.10	0.009	1.1	0.7	0.05	0.07	–	–	–
NWA 2995/6	3.16	0.439	3.61	0.42	6.0	5.0	1.73	0.50	499	16	31
NWA 2995 et al.	2.97	0.412	3.29	0.38	6.1	13.1	1.55	0.42	1563	54	29
± 1	0.03	0.006	0.05	0.03	1.1	1.6	0.04	0.06	–	–	–
± 2	0.20	0.028	0.41	0.03	0.8	7.0	0.14	0.04	–	–	–
NWA 3136	3.37	0.476	2.93	0.343	6.0	3.3	1.29	0.37	230	8	29
± 1	0.04	0.008	0.06	0.032	1.5	1.6	0.04	0.09	–	–	–
± 2	0.11	0.014	0.21	0.015	1.3	1.3	0.10	0.06	–	–	–
NWA 4472/4485	12.35	1.697	11.21	1.55	3.7	<8	6.99	1.89	584	17	34
± 1	0.12	0.017	0.11	0.05	1.4	–	0.08	0.13	–	–	–
± 2	2.13	0.257	0.39	0.07	0.6	–	0.72	0.12	–	–	–
NWA 4819	2.65	0.366	2.76	0.34	11.9	4.1	1.50	0.46	275	9	31
± 1	0.03	0.004	0.04	0.02	0.9	1.1	0.03	0.05	–	–	–
± 2	0.13	0.017	0.12	0.02	0.8	0.3	0.07	0.03	–	–	–
NWA 4884	2.35	0.33	2.25	0.26	3.2	1.2	0.93	0.26	266	9	30
± 1	0.04	0.01	0.06	0.04	2.1	2.1	0.04	0.08	–	–	–
± 2	0.09	0.02	0.33	0.03	1.1	1.0	0.06	0.02	–	–	–
NWA 4932	1.26	0.181	0.89	0.14	27.4	8.0	0.5	0.16	210	8	26
± 1	0.02	0.004	0.03	0.02	1.2	1.0	0.0	0.04			
± 2	0.04	0.005	0.04	0.01	11.5	3.9	0.04	0.02			
NWA 4936/5406	4.03	0.557	4.79	0.60	16.6	12.0	1.95	0.49	472	16	30
± 1	0.04	0.006	0.05	0.02	0.7	0.9	0.03	0.05	–	–	–
± 2	0.20	0.027	0.24	0.03	7.7	2.6	0.10	0.03	–	–	–
NWA 5153	3.15	0.431	3.27	0.40	3.6	1.8	1.54	0.43	185	6	31
± 1	0.04	0.006	0.05	0.03	1.3	1.2	0.04	0.07	–	–	–
± 2	0.43	0.054	0.35	0.07	1.8	1.1	0.32	0.14	–	–	–
NWA 5207	2.71	0.376	2.87	7.2	4.3	1.26	0.35	7.2	255	8	32
± 1	0.03	0.004	0.04	1.0	1.0	0.03	0.06	1.0	–	–	–
± 2	0.35	0.048	0.44	0.9	1.7	0.16	0.05	0.9	–	–	–
SaU 169 IMB	54.8	7.50	52.4	6.45	<20	<30	30.0	7.9	98	4	25
± 1	0.5	0.08	0.5	0.11	–	–	0.3	0.2	–	–	–
± 2	2.0	0.28	2.4	0.21	–	–	1.2	0.3	–	–	–
SaU 169 RB	16.7	2.31	17.8	2.27	<4	<8	9.05	2.62	173	13	23
± 1	0.2	0.02	0.2	0.06	–	–	0.09	0.10	–	–	–
± 2	1.3	0.18	2.0	0.17	–	–	0.89	0.26	–	–	–
SaU 300	1.275	0.183	0.97	0.132	19.1	5.5	0.53	0.25	321	11	29
± 1	0.016	0.003	0.02	0.016	0.9	0.8	0.02	0.04	–	–	–
± 2	0.027	0.004	0.04	0.006	1.9	0.4	0.03	0.02	–	–	–
SaU 449	1.72	0.247	1.48	0.22	18.5	9.8	0.87	0.39	237	8	30
± 1	0.02	0.004	0.04	0.02	1.1	1.1	0.03	0.05	–	–	–
± 2	0.21	0.030	0.22	0.03	15.7	5.5	0.10	0.06	–	–	–
Yamato 983885	3.67	0.511	3.36	0.46	23.3	8.1	2.10	0.55	107	9	12
± 1	0.04	0.005	0.04	0.03	1.1	0.8	0.03	0.04	–	–	–
± 2	0.26	0.037	0.26	0.04	7.9	1.9	0.15	0.04	–	–	–

The first line for each meteorite entry is the mass-weighted ("mass 1") mean of N subsamples. "Mass 1" is the total mass of material analyzed and "mass 2" is the average mass of an analyzed subsample. FeO_T is the total iron concentration expressed as FeO. Se and Br concentrations were not analyzed (n.a.) for all meteorites. The row "± 1" is the mean analytical uncertainty (standard deviation, based on counting statistics) for an individual subsample of a given meteorite. The row "± 2" is the 95% confidence interval of the mean (STDEV × *t*/SQRT[*N*], where *t* is the Student's *t* factor [function TINV in Excel] for *N*–1 degrees of freedom). For precisely determined elements, row "± 2" reflects sampling uncertainty (sample heterogeneity) in that the value is usually greater than 2× the standard deviation of row "± 1."

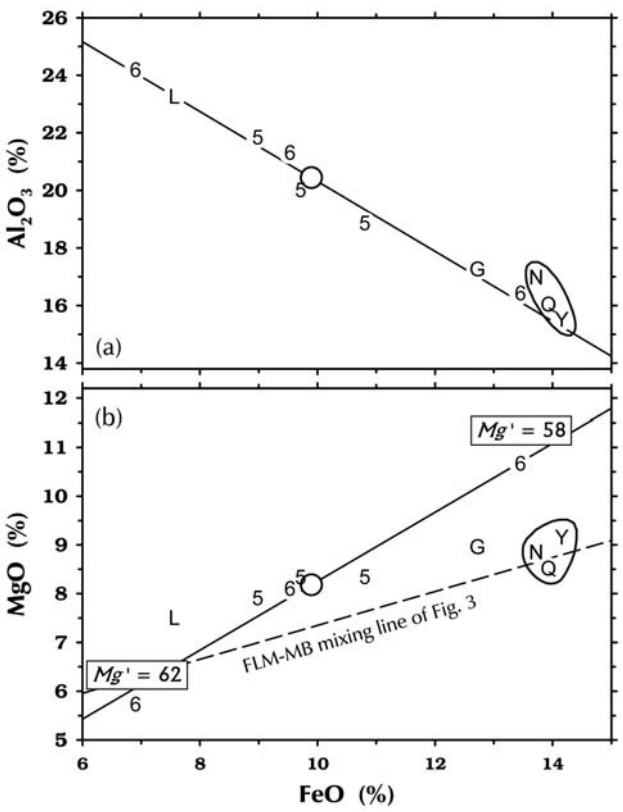

Fig. 4. Variation of FB-EPMA data for Al_2O_3 and MgO with FeO data from INAA for subsamples of paired stones NWA 2995 and NWA 2996 (symbols 5 and 6). The solid diagonal lines are simple linear regressions to the subsample data (N = six subsamples representing 191 mg of material). The circles are points on the lines corresponding to the mass-weighted mean FeO concentration of all INAA subsamples of both stones (N = 16 subsamples representing 499 mg of material). The values of Table 3 are the ordinate values of the circles on diagrams such as these. In (b), the mixing line between the feldspathic (Mg' = 69) and mare-basalt (Mg' = 49) components of Figs. 2 and 3 (Table 4) is shown by the dashed line. For comparison, the mean concentrations of the YQN meteorites (Yamato 981031 [Y], QUE 94281 [Q], and NWA 4884 [N]; Korotev et al. 2003b, and this work), NWA 5153 [G], and 5207 [L] are also shown. In (b) The YQN meteorites lie off the regression line of because they contain a substantial proportion of mare basalt with low MgO/FeO (Jolliff et al. 1998; Arai and Warren 1999).

example, two of the most feldspathic (Fe-poor) meteorites discussed here, NWA 4932 and NWA 4936, 10–12% of the iron derives from extra-lunar sources; we discuss this issue in more detail below. Scandium concentrations, on the other hand, are only insignificantly affected (<3%) by admixture of meteoritic material. Also, Sc has a greater relative range in lunar meteorites (factor of 24) than does FeO (factor of 8.6), so it is more useful for distinguishing similarities and differences among meteorites.

As noted in the introduction, regolith samples from the Apollo missions are—both lithologically and compositionally—mixtures primarily of three classes of materials: (1) feldspathic material (rocks, breccias, glass, mineral fragments) generally similar to the material composing the feldspathic lunar meteorites and much of the regolith at the Apollo 16 site (Korotev 1996, 1997), (2) mafic, KREEP-bearing basalts and impact-melt breccias, and (3) volcanic basalt and glass. As a reference frame on many of the plots presented here (e.g., Figs. 1–3), we depict this ternary mixing relationship as a triangle with apices depicted, somewhat arbitrarily, by (1) the average composition of regolith from the FHT, as derived from feldspathic lunar meteorites, most of which are regolith breccias, (2) the most Sm-rich regolith sampled by Apollo in the PKT, that from Apollo 14, and (3) the mean composition of some low-Ti and VLT (very-low Ti) basalts of the Apollo collection (Table 4). Some of the figures also depict the range of all mare basalt types of the Apollo and Luna missions (e.g., Neal 1982) and the range of mafic, KREEP-bearing impact-melt breccias of the Apollo collection (the 16 compositional groups from Apollo 14, 15, 16, and 17 of Korotev 2000, plus the "high-Th" group from Apollo 12 of Zeigler et al. 2006a). In soils and breccias from the Apollo missions, the mafic melt breccias are the main carriers of the KREEP signature. Finally, for reference, several figures present data from this laboratory for feldspathic and basaltic lunar meteorites (Jolliff et al. 2003; Korotev et al. 2003a,b, 2006; Korotev 2005; Zeigler et al. 2005, and references cited within these papers plus abstracts of Korotev and Irving 2005; Irving et al. 2006, 2008; Korotev 2006; Korotev and Zeigler 2007; Zeigler et al. 2007a, 2007b; Korotev et al. 2008, 2009; and Haloda et al. 2009).

We emphasize that for any given lunar breccia that is, in fact, mainly a mixture of feldspar-rich rocks of the Feldspathic Highlands Terrane, KREEP norites of the Procellarum KREEP Terrane, and mare basalt (which occurs in both terranes), any or all of the three components will likely have compositions different from those of the exact apices of the triangle of Figs. 1 and 2. We suspect, however, that the mean composition of each of the three actual components of any such breccia would plot somewhere in the gray fields representing the known ranges. Thus, the exact apices of the mixing triangle have no particular significance, they only provide a self consistent reference frame from figure to figure. A reviewer of this paper suggested that we should choose an extreme (low-Sc, low-Sm; an anorthosite) feldspathic lunar meteorite to represent the FHT instead of the average. The implication of such a choice would be that the feldspathic component of all lunar meteorites is anorthosite and that feldspathic lunar meteorites with high Sc (e.g., 10–15 ppm) are rich in Sc because they contain mare basalt. There is little evidence to support such a model. As we discuss here, we interpret the sample data, particularly those from lunar meteorites, to support a model in which the feldspathic highlands consists mainly of brecciated noritic and troctolitic anorthosites (Korotev and Haskin 1988; Korotev et al. 2003a) although in some regions of the crust anorthositic norite or anorthosite may prevail (Jolliff and Haskin 1995; Takeda et al. 2006). Similarly, because most of the meteorites we discuss are regolith breccia and fragmental

Table 3. Results of EPMA of fused beads.

	Calcalong Creek	Dhofar 925	Dhofar 961	Dhofar 1180	Kalahari 008	Kalahari 009	MET 01210	NWA 2995/6	NWA 3136	NWA 4472/4485
SiO_2	47.3	45.1	45.9	45.4	45.0	47.7	45.0	46.2	45.8	48.0
TiO_2	0.77	0.35	0.63	0.71	0.51	0.26	1.41	0.68	1.23	1.28
Al_2O_3	20.5	22.7	17.7	22.6	28.6	14.85	17.0	20.6	13.85	17.8
Cr_2O_3	0.19	0.21	0.29	0.14	0.11	0.40	0.24	0.23	0.42	0.23
FeO	9.66	7.41	11.14	9.22	4.67	16.43	16.03	9.75	15.36	9.26
MnO	0.14	0.11	0.16	0.15	0.07	0.25	0.21	0.15	0.25	0.14
MgO	7.51	9.00	10.31	6.17	4.62	7.95	6.22	8.08	10.33	9.38
CaO	12.9	14.2	12.65	14.9	15.1	11.1	13.3	13.5	11.7	12.1
Na_2O	0.44	0.33	0.37	0.36	0.58	0.50	0.30	0.51	0.30	0.59
K_2O	0.24	0.07	0.10	0.06	0.13	0.17	0.04	0.19	0.10	0.42
P_2O_5	0.16	0.08	0.23	0.05	0.03	0.24	0.05	0.14	0.06	0.27
Σ	99.9	99.6	99.4	99.7	99.5	100.2	99.8	100.0	99.5	99.5
Mg′	58	68	62	54	64	46	41	60	55	64

	NWA 4819	NWA 4884	NWA 4932	NWA 4936	NWA 5153	NWA 5207	SaU 169 IMB	SaU 169 RB	SaU 300	Yamato 983885
SiO_2	46.4	46.2	46.0	44.5	46.6	44.5	45.5	47.2	45.0	46.1
TiO_2	0.35	0.63	0.34	0.75	0,73	0.61	2.30	2.52	0.30	0.45
Al_2O_3	22.1	17.0	21.8	24.7	17.3	23.3	15.2	16.8	23.0	22.5
Cr_2O_3	0.20	0.30	0.22	0.11	0.29	0.16	0.13	0.24	0.22	0.22
FeO	7.03	13.7	8.55	5.94	12.7	7.56	11.38	11.35	7.82	8.56
MnO	0.10	0.18	0.12	0.08	0.18	0.11	0.15	0.16	0.12	0.11
MgO	7.41	8.85	9.15	8.60	8.95	7.50	10.84	8.15	9.00	8.13
CaO	16.0	12.4	13.0	14.4*	12.7	13.9	11.1	11.3	13.9	13.5
Na_2O	0.36	0.37	0.32	0.51	0.48	0.48	0.87	0.76	0.31	0.37
K_2O	0.15	0.07	0.12	0.13	0.11	0.10	0.41	0.52	0.05	0.13
P_2O_5	0.08	0.06	0.06	0.15	0.11	0.13	1.32	0.35	0.04	0.08
Σ	100.2	99.8	99.6	100.0	99.5	98.3	99.2	99.4	99.7	100.1
Mg′	65	53	66	72	56	64	63	60	67	63

Oxide values in mass percent; *Mg′* in mole percent. *INAA datum.

Table 4. Element concentrations in "Apollo Model" components as used in figures.

	Al_2O_3 %	FeO %	MgO %	Sc μg/g	Cr μg/g	La μg/g	Sm μg/g	Eu μg/g	Lu μg/g	Th μg/g
FHT	28.2	4.4	5.4	8.0	660	2.3	1.1	0.78	0.13	0.37
PKT	17.4	10.4	9.4	22.0	1400	66.0	30.3	2.56	3.07	14.3
Mare	9.4	20.5	11.0	47.0	4000	5.7	4.2	0.92	0.51	0.67

FHT: "Surface" composition of Table 5 of Korotev et al. (2003) based on mean of feldspathic lunar meteorites ALHA81005, MAC 88105, QUE 93069, Yamato 86032, Dar al Gani 262, Dar al Gani 400, Dhofar 025, and NWA 482. PKT: Mean concentrations of Apollo 14 soil samples based on data of Schnetzler and Nava (1971), Lindstrom et al. (1972), Philpotts et al. (1972), Rose et al. (1972), Wänke et al. (1972), Willis et al. (1972), and Laul et al. (1982). Mare: Mean of data for Apollo crystalline basalts with <5% TiO_2 from the Mare Basalt Reference Suite of the Basaltic Volcanism Study Project (1981; Tables 1.2.9.1 through 1.2.9.4).

breccias, we use a regolith to represent the Procellarum KREEP Terrane, not a high-Sm impact-melt breccia of extreme composition. Throughout this paper, when we refer to the FHT or "feldspathic highlands," we are referring generically to both the FHT,A (anorthositic) and FHT,O (outer, including nearside) of Jolliff et al. (2000; Plate 1).

RESULTS

Terrestrial Alteration of Hot-Desert Meteorites

Concentrations of As, Se, and Br in Apollo soils and breccias are typically about 0.1–0.2 μg/g (Fig. 8.25 of Haskin and Warren 1991), below our INAA detection limits in lunar samples, so we do not report data for these elements in Apollo samples. All of the meteorites of Table 2 are from hot deserts except MET (Meteorite Hills) 01210, which is from Antarctica. We obtain low but detectable concentration values for As, Br, and Se (Se was not measured in all samples) in many of the hot-desert meteorites. We assume these enrichments to be the result terrestrial contamination in the form of fracture and void-filling precipitates from ground or surface water as these elements have been reported as contaminants in other kinds of hot-desert meteorites (Dreibus et al. 2003). As noted in more detail below, nearly all of the hot-desert meteorites are also enriched in Sr and Ba for the

same reason (Crozaz and Wadhwa 2001; Barrat et al. 2003; Lee and Bland 2004).

Geochemistry and Petrography

In this section we summarize compositional aspects of the meteorites studied here (Table 2), emphasizing features that are unique to or characteristic of the meteorite and comparing them to previously described meteorites. We have not studied the petrography of all the meteorites for which we have obtained new compositional data. All of the meteorites that we have not studied petrographically have been described elsewhere, however, and we cite references to those studies. For the meteorites that we have studied petrographically, our descriptions are short because they are based only on preliminary examinations for the purpose of classification.

We discuss first the three Sm-rich meteorites, SaU 169, Dhofar 1442, and NWA 4472/4485, followed by the others in order of decreasing FeO abundance with the exception that we discuss Dhofar 925, Dhofar 961, and SaU 400 last.

Impact-Melt Breccia and Regolith Breccia—Sayh al Uhaymir 169

SaU 169 is a 206-gram stone consisting of two main lithologies, impact-melt breccia and regolith breccia, that are in sharp contact and of considerably different composition (Gnos et al. 2004; Al-Kathiri et al. 2007). Our analytical results for four subsamples (total mass: 98 mg) of the impact-melt-breccia lithology and 13 subsamples of the regolith-breccia lithology (296 mg) of SaU 169 are in reasonable agreement with those of Gnos et al. (2004). Our data for Th are different, however. We obtain 30.0 ± 0.4 μg/g Th instead of 32.7 μg/g for the impact-melt breccia and 9.7 ± 1.2 μg/g Th instead of 8.44 μg/g for the regolith breccia (uncertainties are 95% confidence limits). Similarly, our values for Zr and Hf are 0.8× for the impact-melt breccia and 1.2× for the regolith breccia compared to the values of Gnos et al. (2000). A difference in zircon abundance between the sample pairs would account for both observations.

The SaU 169 impact-melt breccia has extraordinarily high concentrations of incompatible elements, 300–1000× those of CI chondrites and 1.3–1.6× those of average high-K KREEP of Apollo 14 (Warren and Wasson 1979; Warren 1989). Among all meteorites, lunar and other, SaU 169 is the richest in REEs (rare earth elements) and other incompatible elements. The SaU 169 impact-melt breccia has other compositional features that make it distinct from all Apollo samples of otherwise similar nature with the exception of some recently recognized in the Apollo 12 regolith (Zeigler et al. 2006a). For example, in contrast to the common impact-melt breccias from Apollo 14, concentrations of siderophile elements in the SaU melt breccia are low. Both Ir (<20 ng/g) and Au (<30 ng/g) are below our detection limits (Table 2), which are abnormally high because of the high concentrations of incompatible elements. (In feldspathic lunar samples our detection limits for these elements are typically <5 ng/g). *Mg′* (whole-rock mole percent Mg/[Mg+Fe] = 63) is at the low end of the range for mafic, KREEP-rich impact-melt breccias of the Apollo missions except some from Apollo 12 (Fig. 1b). Cr/Sc is also very low (Fig. 5). Both features reflect the absence of the chemical (normative) component of high-*Mg′* olivine that is characteristic of many Apollo mafic impact-melt breccias (Korotev 2000). The melt breccia of SaU 169 has ratios of Th and U to REEs that are about 0.9× those of mafic impact-melt breccias of Apollo 14 (i.e., nominal high-K KREEP; Fig. 6a). Similarly, Eu/Sm and Ba/Sm in the SaU 169 impact-melt breccia are only 0.8× and 0.6× that of Apollo 14 KREEP. These differences suggest that the SaU 169 impact-melt breccia does not contain (or contains considerably less of) the components of granite or felsite (high Th/REE and Ba/REE compared to KREEP) and alkali anorthosite (high Eu/Sm compared to KREEP) that are characteristic of impact-melt

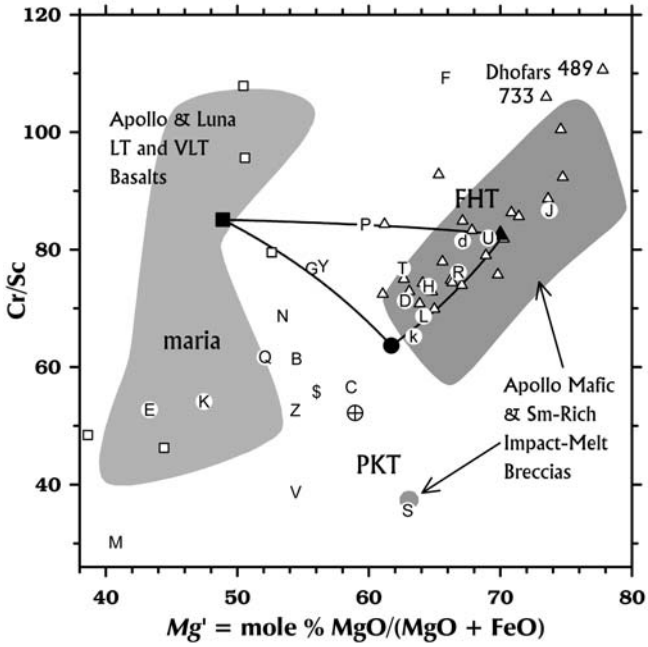

Fig. 5. Among feldspathic lunar meteorite (triangles), Cr/Sc tends to increase with *Mg′* and also with olivine (+chromite)/pyroxene (Korotev et al. 2003a). See Fig. 2 for symbol key. NWA 4819 [F] is anomalous and has the greatest Cr/Sc among meteorites studied here. Mafic meteorites MET 01210 [M], Dhofar 1180 [V], and the melt breccia lithology of SaU 169 [S] have the lowest Cr/Sc. The melt breccia lithology of SaU 169 as well as some rare compositionally equivalent fragments in the Apollo 12 regolith (Zeigler et al. 2006a) have lower Cr/Sc than any of the otherwise similar mafic, Sm-rich impact-melt breccias of the Apollo missions discussed by Korotev (2000). These melt breccias overlap with the field of feldspathic lunar meteorites (triangles) in this figure. The big "triangle" is the mixing triangle of Fig. 2. Three basaltic lunar meteorites, launch pairs Yamato 793169, Asuka 881757, and Miller Range 05035, plot off scale at *Mg′* = 33–37 and Cr/Sc = 18–22 (Warren and Kallemeyn, 1993; Koeberl et al. 1993; Korotev et al. 2003b; Korotev and Zeigler 2007). *Mg′* datum for Dhofar 1442 (Z) from Ivanova and Kononkova (in Weisberg et al. 2009).

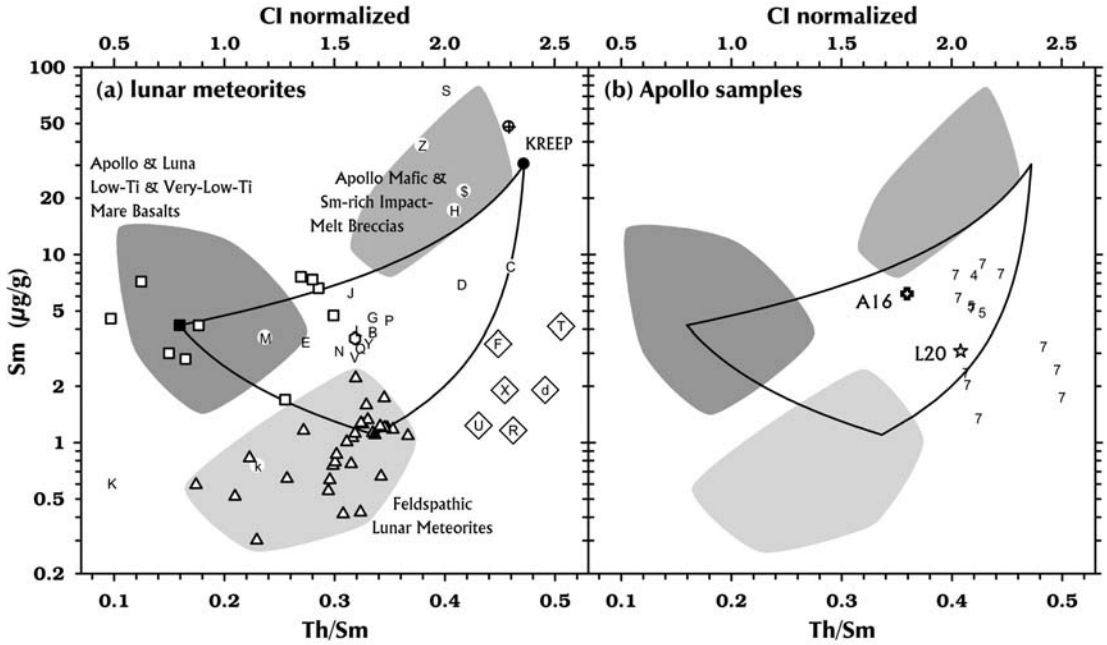

Fig. 6. a) Th/Sm in lunar meteorites. See Fig. 2 for key. The large "triangle" is the mixing triangle of Figs. 2 and 3. In this plot, the mare basalt field excludes the high-Ti basalts of Apollo 11 and 17, which have low and off-scale Th/Sm. Several lunar meteorites of intermediate iron composition (diagonal squares) have Th/Sm too great to be simple ternary mixtures of components that account for most polymict samples from the Apollo missions: Dhofar 925[d], NWA 4819[F], NWA 4932[R], SaU 300[U], SaU 449[X], and Yamato 983885[T]). b) Of the 2361 Apollo samples in the comparison suite (Fig. 18b), only 15 have the property of having high Th/Sm as well FeO and Sm concentrations (Fig. 2) in or near the range of the high-Th/Sm meteorites of (a). Most are breccias from Apollo 17 (symbol 7). Points for Apollo 16 and Luna 20 regolith, both highlands landing sites, are also shown. The CI-normalized axis is for comparison to Fig. 16a of Korotev et al. (2003a).

breccias of Apollo 12 and 14 sites (Warren et al. 1981; Jolliff et al. 1991; Jolliff 1998).

On the basis of our four subsamples, the impact-melt breccia lithology of SaU 169 is one of the most homogeneous of the samples analyzed here. Relative standard deviations for precisely determined incompatible elements, including Th, are only about 1% while those for FeO and Sc are 1.8% and 7.5% (N = 4). In contrast, the regolith breccia is not as uniform, with relative standard deviations for incompatible elements of 12–21% (N = 13). Relative standard deviations for Fe and Sc are still small, however, 3–4%. These observations suggest that if the regolith-breccia lithology of SaU 169 contains a lithologic component with substantially greater concentrations of incompatible elements, e.g., a component like the impact-melt lithology, then that component varies little in abundance among subsamples. They also suggest that if the regolith breccia contains mare basalt, then the relative abundance of the basalt is not highly variable, in contrast to several of the other meteorites discussed below. Concentrations of siderophile elements are low in the SaU 169 regolith breccia compared to most other regolith breccias (Fig. 8).

Quantitatively (mass balance) we cannot account for the composition of the regolith breccia as a mixture of known rock types, including the SaU 169 impact-melt breccia. The composition of the regolith-breccia is most similar to that of Apollo 14 regolith (Al-Kathiri et al. 2007), but is richer in Fe (1.1×), Sc (1.3×), Cr (1.2×), and Na (1.05×), and poorer in incompatible elements (0.7–0.8×). A mixture of 70% Apollo 14 soil, 30% low-Ti mare basalt, and 10% alkali anorthosite accounts reasonably well for the composition of the SaU 169 regolith-breccia. We conclude, on the basis of compositional mass balance and petrographic examination, that the large melt-breccia clast that dominates SaU 169 is not a major component of the regolith represented by the regolith-breccia lithology.

We estimate, on the basis of comparison to the Apollo 12 samples of similar composition (Zeigler et al. 2006a), that about 30% (100 μg/g) of the Sr in the impact-melt breccia lithology of SaU 169 is from terrestrial contamination.

Regolith Breccia—Dhofar 1442 [Z]

From our preliminary petrographic analysis, Dhofar 1442 is a clast-rich regolith breccia with a glassy and vesicular matrix. The lithic clast content is varied and includes basalts, moderately mafic breccias, impact spherules, and evolved lithologies such as granophyre and possibly alkali gabbronorite. Feldspathic lithic clasts, which are common in the feldspathic lunar meteorites, are largely lacking. The majority of mineral clasts are moderately ferroan pyroxene and olivine grains, with lesser amounts of plagioclase, and minor to trace amounts of Fe,Ti,Cr-oxides, silica, K-feldspar, RE-merrillite, apatite, troilite, and Fe-Ni metal. Ivanova et al. (in Weisberg et al. 2009) also report the

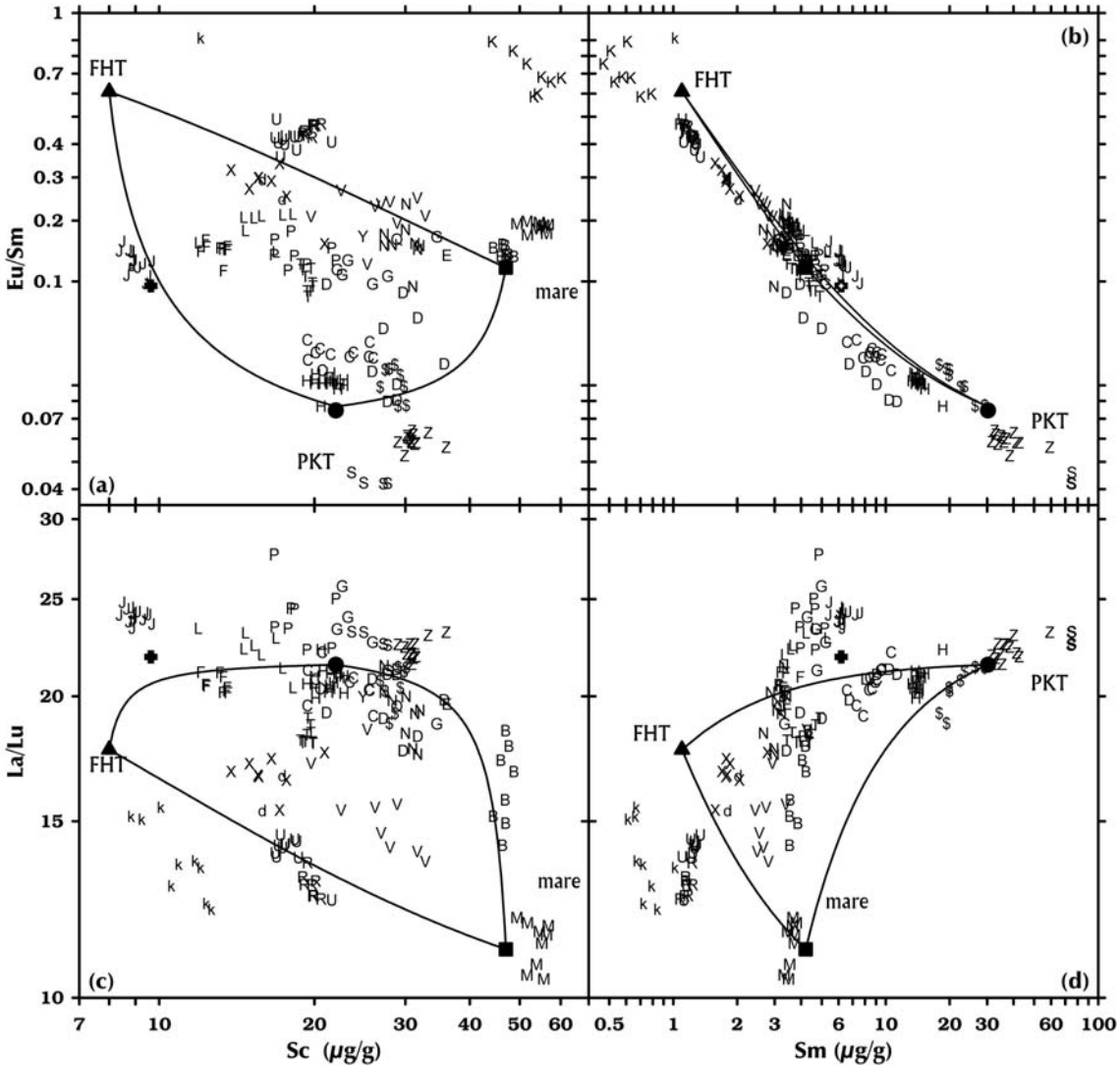

Fig. 7. Subsample data for some REE ratios in lunar meteorites of intermediate iron composition as a function of Sc and Sm concentration. The heavy + symbol near the J points (NWA 4936/5406) represents the mean composition of mature soils from Apollo 16. See Fig. 2 for explanation of lines and filled symbols. For Kalahari 008 [k], points plot off scale at Eu/Sm = 1.01–1.63 in (a) and (b); for Kalahari 009 [K], points plot off scale at La/Lu = 4.2–6.5 in (c) and (d). One anomalous (phosphate-rich) subsample of NWA 4472 [H] plots off scale at Eu/Sm = 0.03 and La/Lu = 37.

presence of "glassy spherules" and that "The lithic clast population includes anorthosites, gabbros, olivine gabbronorites, gabbro-norites and norites. KREEPy and mare basalt clasts are present." They classify the meteorite as an impact-melt breccia, but the presence of the spherules makes it a regolith breccia by definition (Stöffler et al. 1980).

Dhofar 1442 has the distinction of representing a regolith having the highest concentrations of incompatible elements of any of which we are aware. The Sm concentration, for example, is greater than that of both Apollo 14 soil and the regolith breccia of SaU 169 (Figs. 2 and 9b). Concentrations of alkali elements (K, Rb, and Cs) and REEs are in the range of "high-K KREEP" (Warren, 1989) yet concentrations of Fe, Sc, and Cr are 1.3–1.4× greater (Fig. 9a). Neither the bulk composition nor the compositional trends of the subsample data in Figs. 3 and 9 can be rationalized in terms of a mixture of rocks known from the Apollo collection. For example, soil samples from Apollo 12 are mainly KREEP-basalt mixtures (Laul and Papike 1980), leading to an anticorrelation of Sc and Sm on Fig. 3 along a trend between the fields for Apollo 14 soils and the Apollo 12 mare basalts. In Dhofar 1442, in contrast, concentrations of Sm correlate positively with those of Sc among subsamples (R^2 = 0.64; Fig. 3), suggesting that the mafic component is also the carrier of the REEs. Extrapolation of the trend of Dhofar 1442 subsamples in Fig. 3 to 47 μg/g Sc, a value typical of mare basalt (Fig. 3; Table 4), yields 91 μg/g Sm, well outside the range of known mare basalts or other common mafic lithologies in the Apollo collection. Thus, if mare basalt is in part the cause of moderately high Sc concentration, then it cannot be the major

carrier of the rare earth elements. Some nonmare component must be the carrier of the incompatible elements and that component is both more mafic and richer in incompatible elements than samples identified as "KREEP" in the Apollo collection. Among Apollo samples of which we are aware, only the rare basaltic andesite glasses in the Apollo 16 regolith (Zeigler et al. 2006b) are similar in FeO, Na_2O, and K_2O concentration.

Despite that the two most Sm-rich lunar meteorites have been found in Oman, Dhofar 1442 appears to be a different fall from SaU 169. The reported find locations are 430 km apart. Mixing trends defined by the subsamples (Fig. 9) do not overlap. Also, whereas SaU 169 is poor in siderophile elements, Dhofar 1442 is among the richest (Fig. 8). Like many other lunar meteorites from Oman, Dhofar 1442 is enriched in Sr from terrestrial alteration but is not significantly enriched in Ba (Fig. 10).

Regolith Breccia—Northwest Africa 4472 and 4485 [H]

NWA 4472 and NWA 4485 were acquired by different collectors from dealers in Morocco; the find locations are not reported (Connolly et al. 2007). The petrographic descriptions (Irving and Kuehner, in Connolly et al. 2007; Kuehner et al. 2007; Joy et al. 2008) and our chemical analyses show the two stones to be identical to each other and distinctly different from any other lunar meteorite. On the basis of the similarities we infer that the stones are paired. Concentrations of incompatible elements in NWA 4472/4485 are greater than in all other lunar meteorites except SaU 169 and Dhofar 1442 (Fig. 3), but NWA 4472/4485 is more feldspathic than the other high-Sm meteorites (Fig. 2). The composition, essentially that of a trace-element-rich norite, is intriguing because it falls in the range known as LKFM basalt ("low-K Fra Mauro;" Reid et al. 1977). Breccias and glasses of this composition are common in the Apollo collection. Among Apollo samples, NWA 4472/4485 is compositionally most similar to the group-C melt breccias of Apollo 15, the group-1S melt breccias of Apollo 16, and the aphanitic and poikilitic impact-melt breccias of Apollo 17 (Korotev 2000).

NWA 4472/4485 is a regolith breccia, however, because it contains spherules of impact glass (Joy et al. 2008). All subsamples of both stones are similar to each other in composition (compare, for example, to Dhofar 1442 and the regolith breccia portion of SaU 169 in Fig. 3), except that one of our subsamples of NWA 4472 is anomalously rich in REEs (Fig. 3) and Th, but not Zr, Hf, Ta, or U; a second subsample shows the same anomaly, but to a much lesser extent. The two anomalous subsamples must contain nuggets of RE-merrillite (Jolliff et al. 1993). The Ir concentration is low for a regolith breccia (Fig. 8).

NWA 4472/4485 is moderately enriched in Sr and, to a greater extent, Ba from terrestrial alteration (Fig. 10). A curious characteristic of both stones is that Br concentrations, 2.9 ± 0.3 μg/g for NWA 4472 and 6.2 ± 0.7 μg/g for NWA 4485, are about a factor of ten greater than we observe in other hot-desert meteorites, suggesting that both stones have been exposed to saltwater.

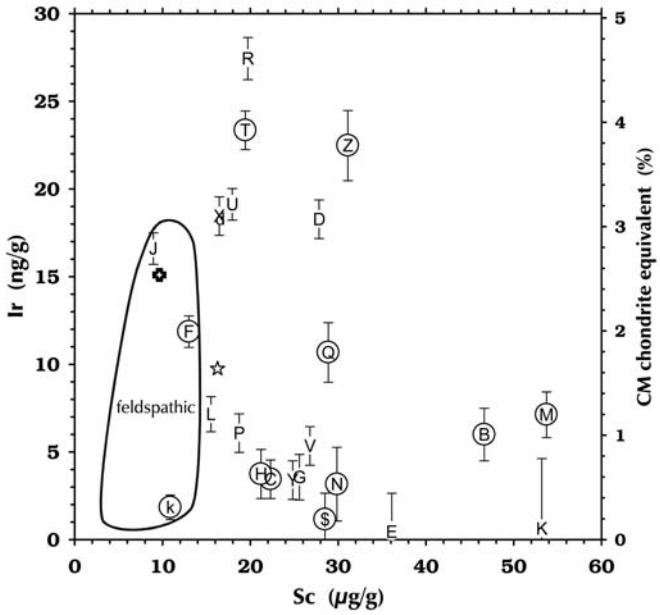

Fig. 8. Concentrations of Ir in brecciated lunar meteorites of intermediate composition. Means for the meteorites discussed here are shown as letter symbols (Table 1). Error bars represent the analytical uncertainties of Table 2 (1 standard deviation). The range for feldspathic lunar meteorites is also shown. The large + symbol represents typical soil of Apollo 16 and the star represents soil from Luna 20. Circled symbols represent regolith breccias. Wasson et al. (1975) note that the siderophile-element signature of lunar regolith most closely matches CM chondrites. A concentration of 30 ng/g Ir is equivalent to 5% meteoritic material as CM chondrite (595 ng/g Ir, Wasson and Kallemeyn 1988). Some of the meteorites plotted here contain at least some nonchondritic meteoritic material, however (Fig. 17).

Feldspathic Regolith Breccia—Kalahari 008 [k] and Basaltic Breccia—Kalahari 009 [K]

The two Kalahari stones constitute what is perhaps the most unusual lunar meteorite. Kalahari 008 (598 g) is a feldspathic breccia whereas the large Kalahari 009 stone (13.5 kg) is a monomict basaltic breccia. Yet, their reported close find proximity in the field (~50 m) and similarities in petrographic components and unusual cosmic-ray exposure history all but require that the stones are paired (Sokol et al. 2008).

Kalahari 009 is unique among basaltic lunar rocks (Sokol et al. 2008). With only 16.4% FeO, it is at the extreme low end of the range for mare basalts (Fig. 1). This feature suggests that it might contain anorthosite, but Sokol et al. (2008) do not report the occurrence of clastic anorthosite. Kalahari 009 has concentrations of incompatible elements that are very low compared to any previously known basaltic lunar meteorite or any basalt in the Apollo and Luna collections, including the VLT basalts of Apollo 17 and Luna 24 (Fig. 2). Concentrations of Th are below our detection limits; our

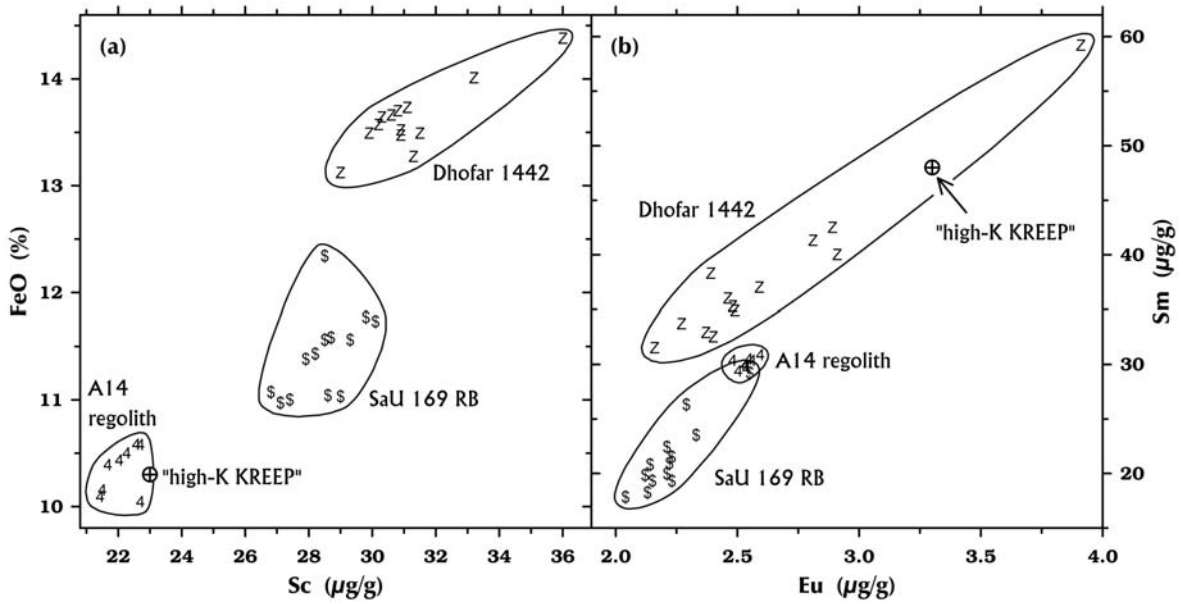

Fig. 9. Dhofar 1442 and SaU 169 are both regolith breccias. Concentrations of incompatible elements such as Sm are very high in both meteorites and most similar to regolith from Apollo 14 (b) but both meteorites are more mafic (a). There is little evidence here that SaU 169 and Dhofar 1442 are different samples of a common regolith. Apollo 14 points represent regolith samples 14003, 14141, 14148, 14149, 14156, 14163, 14240, and 14259 (unpublished data, this lab). The composition of "high-K KREEP" (Warren 1989) is shown for reference.

subsamples nominally average 0.06 μg/g Th with a sample standard deviation of 0.02 μg/g; the estimated analytical uncertainty of a single measurement, however, is 0.09 μg/g (1 standard deviation, counting statistics). Kalahari 009 has a positive Eu anomaly for the same reason that lunar anorthosites have positive Eu anomalies: concentrations of trivalent REEs were very low in the liquid from which the rock crystallized, trivalent REEs were incompatible with the major rock-forming minerals, but divalent Eu was compatible with plagioclase. The absolute concentration of Eu, 0.48 μg/g, is at the low end of the range for mare basalts and comparable only to Apollo and Luna VLT basalts (Ma et al. 1978; Wentworth et al. 1979) and lunar meteorite NWA 773, 2727, 3160, etc. (paired stones; Zeigler et al. 2007a).

Our compositional data indicate that Kalahari 008 is a typical feldspathic lunar meteorite. The stone is compositionally distinctive only in two minor aspects. First, concentrations of the plagiophile elements, Na and Eu, are greater than those of any feldspathic lunar meteorite except Dhofar 733 and NWA 4936 (Fig. 11). For Kalahari 008, this attribute reflects that the average anorthite content of the plagioclase is more albitic, ~An_{95}, as inferred from Fig. 11, than the ~An_{97} that is characteristic of feldspathic lunar meteorites. This inference is supported by the mineral composition data of Sokol et al. (2008), who obtained a mean of An_{94}. Second, Kalahari 008 has concentrations of siderophile elements at the low end of the range for feldspathic lunar meteorites that are regolith breccias (Fig. 8; also Fig. 6 of Korotev et al. 2006). This feature argues that Kalahari 008 was formed from an immature regolith, a contention consistent with the deep ejection depth inferred from cosmic-ray exposure data (Sokol et al. 2008). None of our subsamples of Kalahari 008 is anomalously rich in Sc (Fig. 3), as we sometimes observe in samples of feldspathic regoliths that contain clastic mare basalt. This observation, along with the low concentrations of Fe and Sc, suggest that Kalahari 008 contains little or no clastic mare basalt such as that composing Kalahari 009.

It is ironic that the existence of Kalahari 008/009 and other multi-lithologic lunar meteorites (Anand et al. 2003; Demidova et al. 2003; Gnos et al. 2004; Haloda et al. 2009) weakens inferences that we make here that a compositional and petrographic difference between two lunar meteorite stones provides evidence that the two stones are not paired. Nevertheless, if the Kalahari 008 and 009 stones made the Moon-Earth trip as part of a single meteoroid, that meteoroid was an unusual lunar rock.

The Kalahari stones are only weakly contaminated with Sr and Ba from terrestrial alteration (Fig. 10) and moderately contaminated with As and Br. Most of the "excess" Sr in Kalahari 008 (200 μg/g) compared to feldspathic lunar meteorites from Antarctica (140–170 μg/g) is expected on the basis of its high Na and Eu concentrations.

Mafic Regolith Breccia—Meteorite Hills 01210 [M]

MET 01210 is a well-described regolith breccia that is dominated by low-Ti mare basalt but, unlike Kalahari 009, it also contains feldspathic material (Day et al. 2006b and preliminary reports of Arai et al. 2005a; Huber and Warren 2005; Joy et al. 2006; Zeigler et al. 2007b). Our compositional

results are similar to those of Day et al. (2006b) and Joy et al. (2006), although our major-element composition (17.5% Al_2O_3, 16.0% FeO) is slightly more feldspathic (Day et al. 16.2% Al_2O_3, 16.9% FeO; Joy et al.: 16.6% Al_2O_3, 16.5% FeO). In terms of the Apollo model (Fig. 2), the breccia is an FHT-mare mixture with little PKT (KREEP) material. MET 01210 has low *Mg′* (Fig. 1b) and the lowest Cr/Sc among basaltic lunar meteorites (Fig. 5), It is also distinct in having concentrations of light REEs that are low compared to middle REEs, e.g., low La/Sm and La/Lu (Figs. 7 and 12). This feature is characteristic of basalts in the Apollo collection, but uncommon among the basaltic lunar meteorites.

Mafic Regolith Breccia—NWA 3136 [B]

NWA 3136 is also one of the most mafic meteorites of this study. It is a clast-rich regolith breccia containing mineral clasts, glass spherules and agglutinates, and other lithic clasts (<1–1000 μm grains) that are blocky to elongated and angular to subangular in a fine-grained fragmental to glassy matrix (Fig. 13). Subsamples are all similar in composition (e.g., 44–49 μg/g Sc, Fig. 2). Our sample of the meteorite is enriched in Ba from terrestrial alteration, but not grossly enriched in Sr (Fig. 10). It is also strongly contaminated with As and Br.

NWA 3136 is the first of the lunar meteorites discussed here for which we suspect that the Apollo model is inadequate. On the basis of Fig. 2, we might conclude that NWA 3136 is composed predominantly of mare basalt, like MET 01210 and Kalahari 009. In terms of the Apollo model, we can, in fact, approximate the composition reasonably well as a mixture of about 27% FHT material, 66% mare basalt, and 7% KREEP. NWA 3136 is enigmatic, however. Both the University of Washington (UWS) and Washington University authors of this paper have studied different thin sections petrographically and made preliminary reports that are not self-evidently describing the same rock. Kuehner et al. (2005) state, on the basis of two large slices (2 cm and 5 cm across), that the meteorite is a "polymict breccia consisting of mineral and lithic clasts derived predominantly from mare basalts but with a smaller proportion (~20%) of highlands lithologies." One of the mare basalts is of high-Ti affinity, a rarity in lunar meteorites. The clast is 750 μm × 400 μm in size with 200 μm × 40 μm blades of ilmenite. In Fig. 13b (taken from the UWS thin section) a clast of ophitic mare basalt is clearly visible. They also describe some clasts of nonmare lithologies: olivine-bearing norite and gabbronorite and orthopyroxene-olivine-bearing anorthosite.

In contrast, on the basis of a chip only 3.7 × 2.9 mm in cross section that was part of the sample from which the compositional data reported here derives, O'Donnell et al. (2008) report "None of the lithic clasts or glasses is highly feldspathic, nor are there any lithic mare basalt clasts or basaltic glasses. Olivine basalt and 'microgabbro' clasts reported by (Kuehner et al. 2005) are not seen in our section." Instead, they report that clasts are of four main

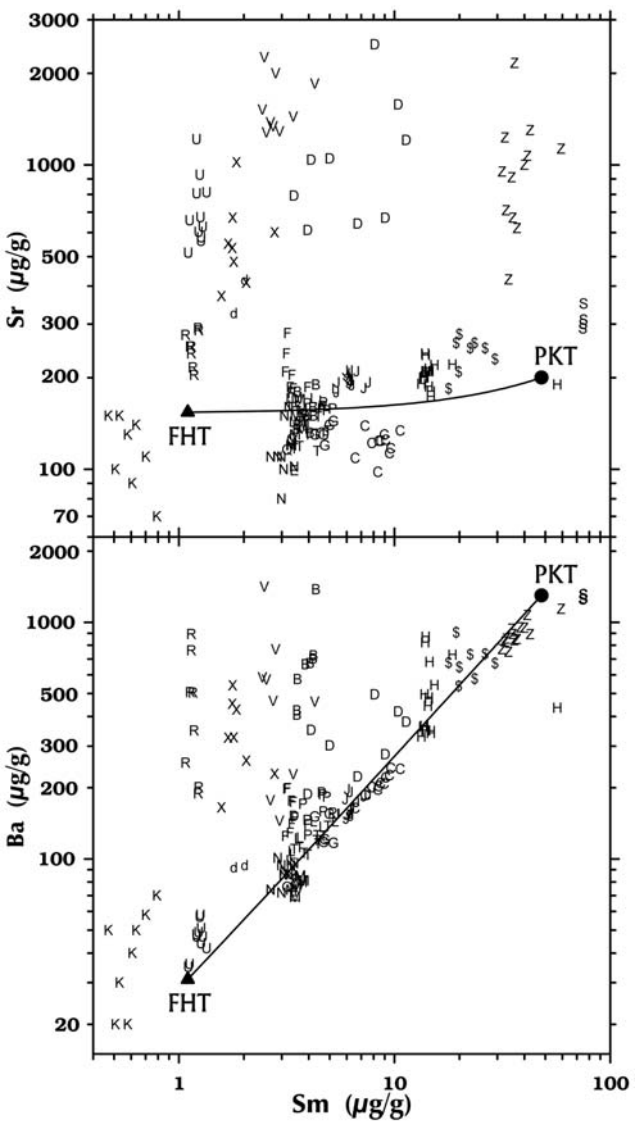

Fig. 10. Lunar meteorites from Oman, Dhofar 925 [d], Dhofar 961 [D], Dhofar 1180 [V], SaU 300 [U], and SaU 449 [X], are severely contaminated with Sr and, to a lesser extent, Ba from terrestrial alteration. SaU 169 [$,S], from northern Oman, is not so contaminated. Some meteorites from northwestern Africa, mainly NWA 3136 [B], NWA 4472/4485 [H], NWA 4819 [F], and NWA 4932 [R], are relatively more contaminated with Ba than Sr. Compare SaU 300 [U] and NWA 4932 [R], which are likely launch paired. Calcalong Creek [C], from Australia, is not obviously contaminated with either element. The lines are mixing lines between points representing mean feldspathic lunar meteorites from Antarctica (FHT, low Sm, uncontaminated) and Apollo 14 high-K KREEP (PKT, high Sm, uncontaminated). Points plotting substantially above the lines contain excess Sr or Ba from terrestrial alteration.

types of nonmare lithologies: impact-melt breccia of gabbronorite composition (most common), intergranular feldspathic basalt, shocked anorthositic norite, and shocked gabbronorite. They describe the four largest (but submillimeter) clasts in the section as intergranular olivine norite (7% FeO by modal recombination), shocked anorthositic norite (13% FeO), impact-melt breccia (12%

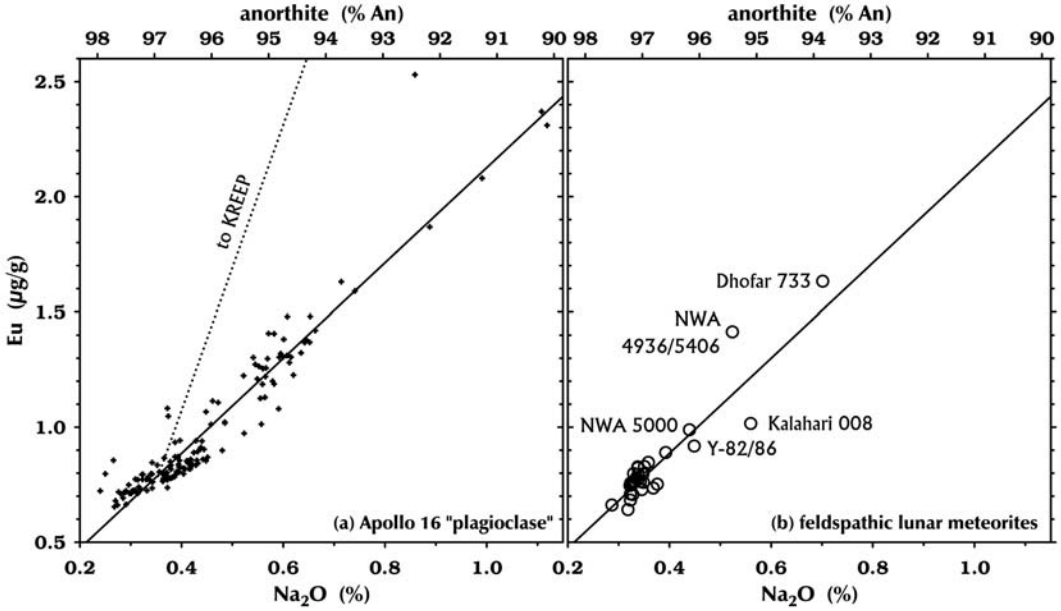

Fig. 11. a) Europium (and strontium, not shown) concentrations correlate with those of sodium in plagioclase from the Apollo 16 mission (a subset of the Apollo comparison suite of Fig. 18). The Apollo 16 samples are lithic fragments (some glassy) from the regolith with <2% FeO and <1 μg/g Sm ($N = 153$, $R^2 = 0.91$). In KREEP, the plagioclase is more albitic (e.g., Fig. 42 of Papike et al. 1998) but some Eu is also carried by RE-merrillite and apatite (Jolliff et al. 1993). The anorthite axis assumes stoichiometric plagioclase. b) Most feldspathic lunar meteorites plot along the Apollo 16 trend. NWA 4936/5406 plots off the trend because it contains a component of KREEP. KREEP-poor Dhofar 733 (Foreman et al. 2008), Kalahari 008 (Sokol et al. 2008), NWA 5000 (Irving et al. 2008), and paired Yamato stones 82192, 82193, and 86032 (Koeberl et al. 1989; Korotev et al. 1996), as well as many samples from the Apollo 16 collection, contain plagioclase somewhat more albitic, on average, than the $An_{96–97}$ plagioclase typical of the feldspathic highlands (James et al. 1989).

FeO), shocked gabbroic norite (18% FeO, compared with 15% FeO for the whole rock).

The meteorite evidently is a heterogeneous, polymict breccia, one representing a regolith unlike any in the Apollo collection. The nonmare component is mafic and highly feldspathic material is rare. Bulk composition is not particularly useful in determining the relative proportions of mare and nonmare material because of the compositional similarity between mare basalt with about 1% TiO_2 and the pyroxene-rich nonmare rocks. These same issues are important in some of the rocks we describe subsequently.

We observe minor calcite and barite in thin section and the INAA sample is among the richest in terrestrial Ba (Fig. 10).

Mafic Regolith Breccia—Northwest Africa 4884 [N]

NWA 4884, a regolith breccia (Fig. 13), is composed of abundant angular mineral and lithic clasts in a sparsely vesicular, glassy matrix. Mineral fragments include calcic plagioclase, pigeonite, augite, Ti-chromite, ilmenite (one with a baddeleyite inclusion) and a silica polymorph. Lithic clasts include several types of mare basalt, symplectitic intergrowths of Fe-rich augite + fayalitic olivine + silica polymorph, a coarse-grained dunitic or troctolitic rock containing a large metal grain (associated with rutile and secondary ilmenite), and a large breccia-within-breccia clast. Mare basalt clasts are predominant over highlands lithologies.

Both the composition and petrology of NWA 4884 are consistent with the Apollo model. The composition corresponds to a 2:3 mixture of FHT material and VLT mare basalt. There is little or no KREEP component, i.e., the composition plots along the FHT-maria join of Fig. 2. NWA 4884 is special, however, in that for lithophile elements it is indistinguishable in composition from QUE 94281 from Antarctica (Figs. 3, 7 and 14c, 14d) and thus appears to be another meteorite in the launch pairing that also includes Yamato 793274/981031 (paired stones) and possibly EET 87521/96008 (Warren and Kallemeyn 1989; Jolliff et al. 1998; Arai and Warren 1999; Korotev et al. 2003b). Following the lead of Arai and Warren (1999) we will refer to this group of meteorites as the "YQN meteorites." Our sample of NWA 4884 does differ from our sample of QUE 94281 (Jolliff et al. 1998) in having only 30% of the Ir concentration (Fig. 8), but other samples of QUE 94281 have similarly low Ir (Arai and Warren 1999).

Unlike many lunar meteorites from northwestern Africa, our sample of NWA 4884 is not strongly enriched in Ba (1.15×) from terrestrial alteration compared to QUE 94281.

Fragmental to Melt-Matrix Breccias—Northwest Africa Stones 2995, 2996, 3190, 4503, 5151, and 5152 [P]

We have studied samples of eight stones from northwestern Africa that we obtained from different

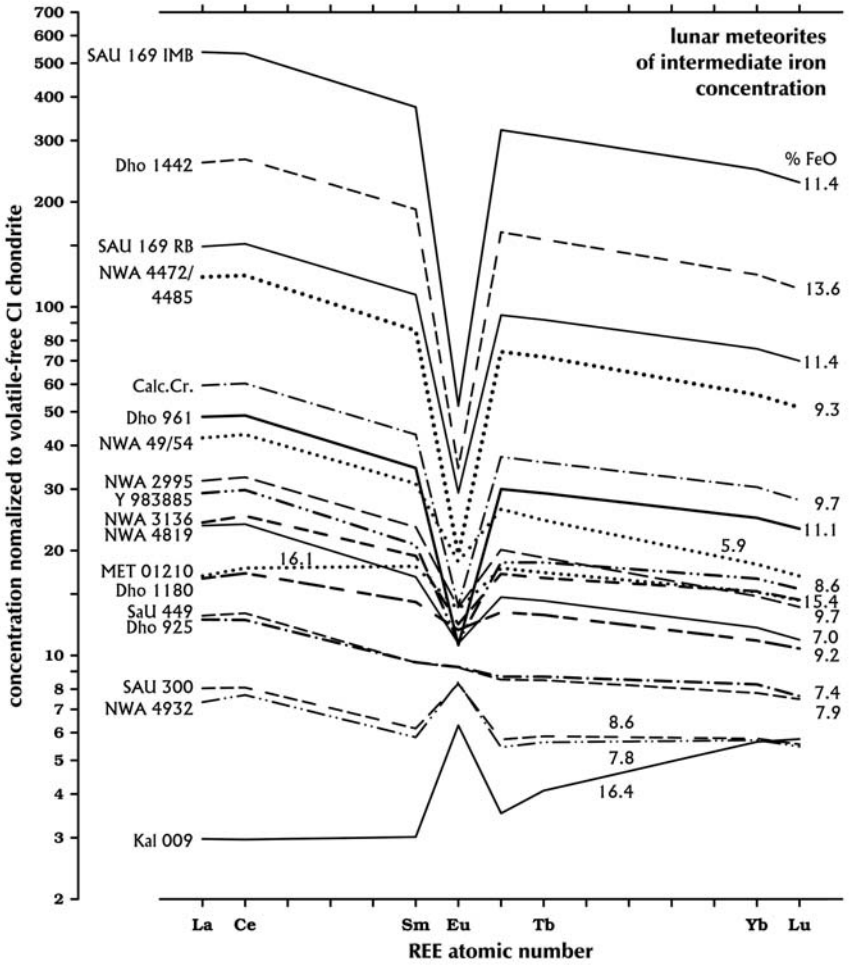

Fig. 12. Chondrite-normalized REE concentrations of lunar meteorites of intermediate iron concentration (see Fig. 12 of Korotev [2003a] for normalization technique). Iron concentrations (% FeO) are listed on the right. This stylized plot is based on data for the seven REEs of the abscissa, for which the analytical uncertainties are typically 1–4% (Table 2).

collectors and dealers, all of which are similar in composition. On the basis of the compositional and petrographic similarity, we infer that all are paired with each other, although subsequent study may show that they are not. The first of these stones to be described is NWA 2995 (Bunch et al. 2006); other named stones in the pair group are NWA 2996, NWA 3190, NWA 4503, NWA 5151, and NWA 5152. We refer to these six stones and two unnamed stones together as NWA 2995 et al.

Texturally, the NWA 2995 et al. stones range from fragmental to melt-matrix breccias (Fig. 13). They contain clasts of anorthosite, anorthositic norite, anorthositic troctolite, norite, troctolite, gabbro, granulitic breccia, mare basalt, and glass of KREEP-basalt composition. Breccia-within-breccia clasts are common and some clasts are a centimeter in size. As a consequence of the large grain size and lithologic diversity, the 54 subsamples vary considerably in composition (Figs. 14a, 14b). One INAA subsample of NWA 3190 is nearly pure plagioclase and one from NWA 5152 has the composition of a troctolitic anorthosite (e.g., high Cr/Sc). Even discounting these two clast-rich subsamples, the remaining typical subsamples vary by a factor of 2 in FeO concentration and factors of 2 to 4 in concentrations of incompatible elements.

In terms of the Apollo model (Figs. 2 and 3) and simple mass balance, the mean composition of NWA 2995 et al. corresponds approximately to a 2:1 mixture of feldspathic material and mare basalt, with about 5% KREEP. The proportion of mare basalt implied by this simple model, however, is considerably greater than we observe petrographically. We suspect that the proportion of mare material is substantially less than one-third and that the mafic character of the meteorite (7–14% FeO, Fig. 4) instead results in large part from the various nonmare mafic lithologies. For example, extrapolation of the trend of Fig. 4b to 20% FeO, a value typical of mare basalt, yields 15% MgO ($Mg' = 58$), a high value for a crystalline mare basalt and comparable only to the olivine basalts of Apollo 12. Mg' does not decrease substantially with increasing FeO among subsamples, as we would observe in an anorthosite-basalt mixtures (Fig. 4b).

The trend of Fig. 4b is more consistent with mixing between anorthosite and norites and gabbros of the ferroan-anorthositic suite.

The elements Mg, Cr, Sc, and Co all correlate positively with Fe while Na and Eu correlate negatively with Fe and Sc among subsamples of NWA 2995 et al. (Fig. 14a). The inferred feldspathic component of NWA 2995 et al. is richer in Na_2O (~0.5%) and Eu (1.2 μg/g) than are most feldspathic lunar meteorites (see Kalahari 008, above). Other compositional characteristics of NWA 2995 et al. are low concentrations of heavy REEs (high La/Lu) compared to other lunar meteorites of similar total REE concentration (Figs. 7c, 7d, and 12) and less contamination with terrestrial Ba than several other NWA lunar meteorites (Fig. 10). The least mafic subsamples of NWA 2995 et al. bear some compositional resemblance to the Luna 20 regolith, an observation that we explore in more detail below.

Fragmental to Melt-Matrix Breccia—Northwest Africa 5153 [G]

NWA 5153 may be part of the NWA 2995 et al. pair group. The stone is a fragmental to melt-matrix breccia containing clasts of ophitic pigeonite and olivine mare basalt, cataclastic gabbro, troctolite, and fragments of granophyric intergrowths of K-feldspar, felsic glasses and silica (Fig. 13). The interior is fresh and lacks alteration veins. On average, it is richer in Sc than NWA 2995 et al. but the most Sc-poor subsamples of NWA 5153 overlap in composition with the most Sc-rich subsamples of NWA 2995 et al. (Fig. 14c). On average, *Mg′* (56) is less than that of NWA 2995 et al. (60; Fig. 5) and outside the range of NWA 2996 and 2996 subsamples (58–62; Fig. 4b). Both of these observations are consistent with a greater proportion of mare basalt.

Fragmental to Melt-Matrix Breccia—Northwest Africa 5207 [L]

NWA 5153 and NWA 5207 both superficially resemble NWA 2995 and its pairs and were purchased in Morocco over the same time period, 2005–2007 (Connolly et al. 2006, 2008; Weisberg et al. 2008, 2009). In contrast to NWA 5153, NWA 5207 subsamples plot at the feldspathic (low-Sc) end of the large distribution of NWA 2995 et al. subsamples (Fig. 14c). The meteorite differs in several respects, however. *Mg′* is greater, but Cr/Sc is lower than for NWA 2995 (Fig. 5). The exterior is dark without the reddish-brown to gray–brown surface colors that are typical of most lunar meteorites from northwestern Africa. The breccia has a fragmental matrix containing a wide variety of lithic components, mainly troctolitic orthocumulates, recrystallized noritic and troctolitic anorthosites, anorthosites, gabbros and coarse- to fine-grained basalts, small lithic clasts of breccia, shock-melted lithologies, symplectites (from pyroxferroite decomposition), and green glasses of nonspherical shapes, some of which are vesicular and contain tiny metal-sulfide spherules (Fig. 13). Of the 20 green glasses for which we obtained compositional data, three were in the range of the Apollo 15 green picritic glass (7–8% Al_2O_3, 17–18% MgO; Delano and Livi 1981). The other 17 tightly clustered around 19% Al_2O_3 and 7% MgO and, consequently are likely of impact origin.

The interior weathering grade of NWA 5207 is low. With means of 127 ± 9 and 123 ± 7 μg/g Ba (Table 2), both NWA 5207 and NWA 5153 are less contaminated with Ba than is NWA 2995 et al. (range of 146–191 and mean of 170 μg/g among the eight stones).

Regolith Breccia—Calcalong Creek [C]

Calcalong Creek, a regolith breccia, is described by Marvin and Holmberg (1992) and Hill and Boynton (2003). We obtained a single chip of Calcalong Creek with vesicular fusion crust on one face. After breaking the sample into small pieces, we selected fragments rich in fusion crust as subsample A and made ten other subsamples (B–K) consisting of single chips, multiple chips, and crumbs. On average, our results for 208 mg of material are similar to those of Hill and Boynton (2003) for 64 mg ("bulk sample"), but with slightly higher concentrations of "mafic" elements (1.04–1.15× for Fe, Sc, and Cr) and slightly lower concentrations of incompatible elements (0.92–0.96×) and Na (0.89×). The subsamples (mean mass: 19 mg) vary considerably in composition, particularly for the "mafic" elements, presumably because of variation in the relative abundance of mare basalt, which has been identified in thin section (Hill and Boynton 2003). Incompatible elements vary among the subsamples (Sm: 7.4–10.7 μg/g) with the fusion-crust subsample (A) being richest. As with NWA 2995 et al. there is no correlation between incompatible element concentrations and FeO or Sc concentration (Fig. 3), indicating that the incompatible elements are carried by a third component. In terms of the Apollo model, the mean composition corresponds approximately to a 2:1:1 mixture of FHT material, VLT mare basalt, and KREEP. Although Calcalong Creek is among the richest in incompatible elements among lunar meteorites, there is some evidence, described in more detail below, that it does not contain a clastic, lithic component of KREEP basalt or norite.

Unlike lunar meteorites from Africa and Oman, Calcalong Creek (Australia) is not substantially contaminated by Sr and Ba from terrestrial alteration (Fig. 10).

Fragmental Breccia—Dhofar 1180 [V]

Dhofar 1180 was found in Oman at a point distant (>20 km) from any other lunar meteorite. The meteorite is a fragmental breccia that is unusual for a lunar breccia in having a slight preferred orientation of clasts (Fig. 13, but more evident in photographs of sawn slices). Most clasts are ferroan anorthosites; less common are mafic clasts of gabbroic anorthosites, anorthositic gabbros and norites, troctolites, olivine gabbros, and microporphyritic and fine-grained impact-melt breccias. Ophitic to subophitic basalts and symplectites are rare. Zhang and Hsu (2006, 2007) report a similar assemblage, as well as one glass clast that is rich in

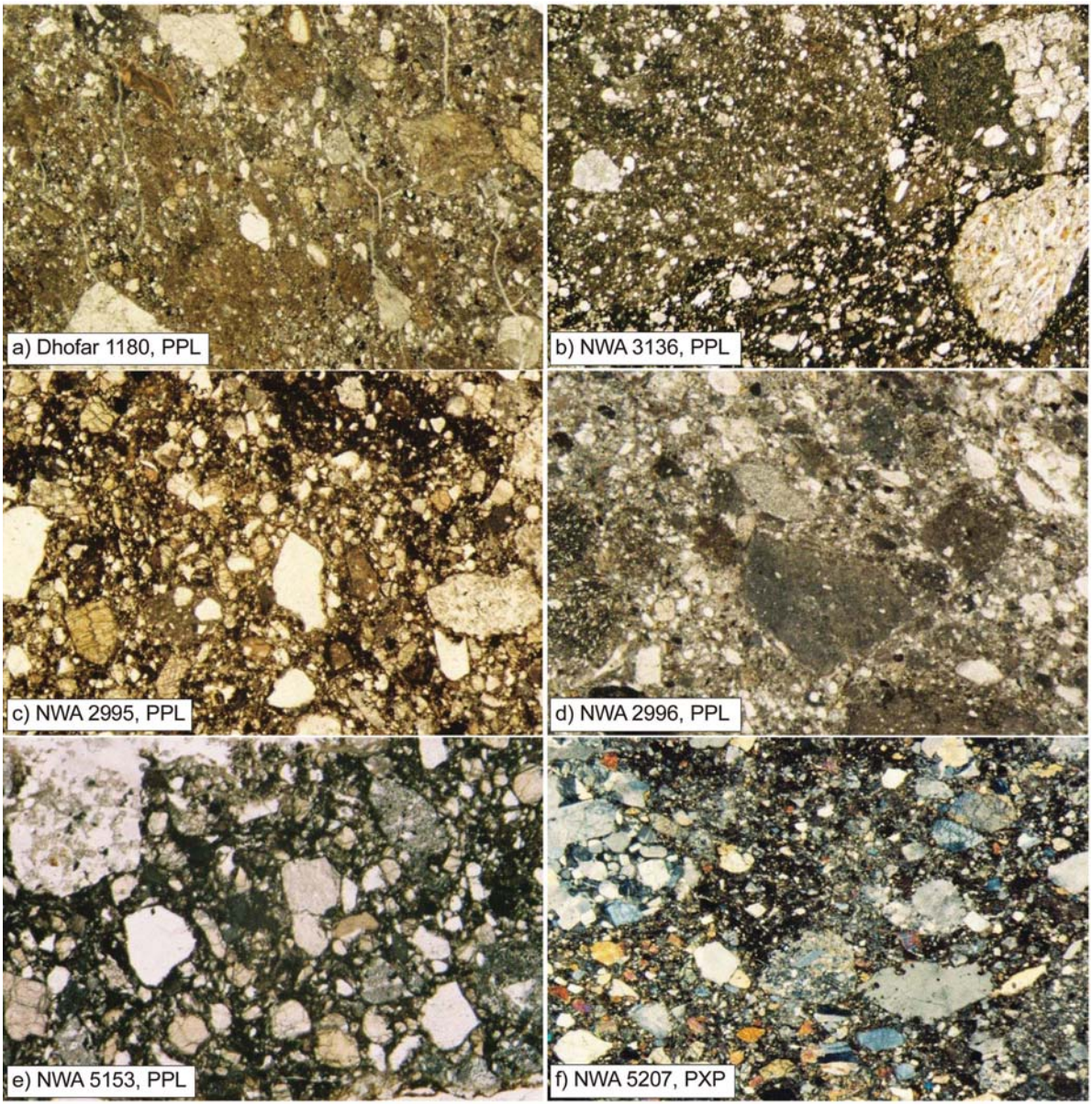

Fig. 13. a–f) Photomicrographs of thin sections of some of the breccias discussed here. The width of field is 7 mm for all images; PPL = plane polarized light, PXP = partially cross-polarized light.

incompatible elements. Although Zhang and Hsu (2007) identify this glass clast as "KREEP," it does not have a KREEP-like major-element composition. It appears to be a granite-QMG (quartz monzogabbro) immiscible-liquid assemblage of the kind discussed by Neal and Taylor (1989) and Jolliff (1998).

Dhofar 1180 is compositionally distinct from other lunar meteorites of similar major-element composition in having low *Mg′* (Fig. 1b), low Cr/Sc (Fig. 5), and low La/Lu (Fig. 7). Also, there is a wide range among subsamples of concentrations of elements associated with mafic minerals (e.g., 20–33 μg/g Sc, Fig. 3), reflecting large variation in the plagioclase to pyroxene ratio. Dhofar 1180 is one of several meteorites plotting on or near the join between the FHT and mare basalt on Fig. 2 and we might therefore assume that it is a breccia from a location where basaltic mare and feldspathic highlands materials have mixed. Like NWA 3136, however, Dhofar 1180 poses a compositional-petrographical enigma. In terms of the Apollo model, the mean composition requires ~33% of a VLT basalt, one such as Asuka 881757 (Warren and Kallemeyn 1993) or MIL 05035 (Joy et al. 2007) that has low *Mg′* and Cr/Sc. Our petrographic examination, however, suggests that mare material is rare and not nearly so abundant as one-third. Thus, an alternate possibility is that the meteorite consists mainly of brecciated plutonic rocks of the feldspathic highlands, rocks that are considerably more mafic and KREEP-poor than nonmare rocks of the Apollo collection.

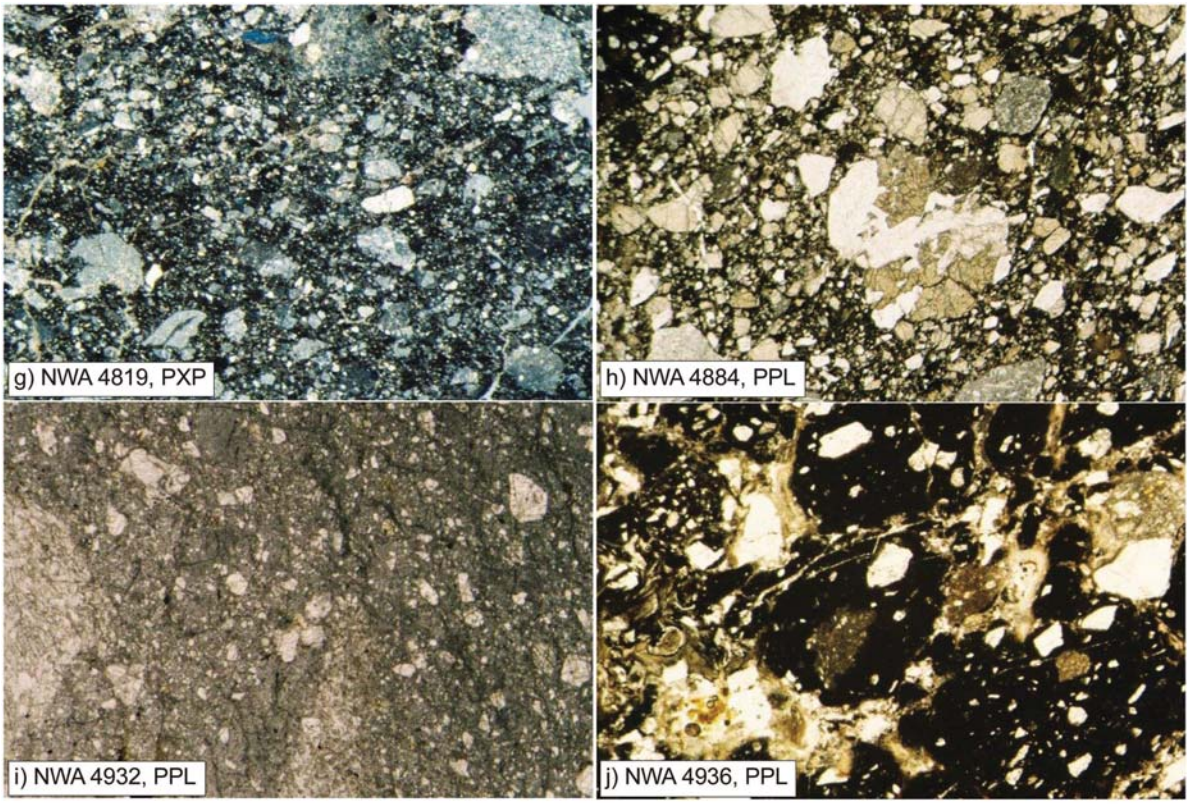

Fig. 13. g–j) Photomicrographs of thin sections of some of the breccias discussed here. The width of field is 7 mm for all images; PPL = plane polarized light, PXP = partially cross-polarized light.

Our sample of the meteorite is substantially contaminated with Sr and Ba as well as As and Br from terrestrial alteration.

Regolith Breccia—Yamato 983885 [T]

Yamato 983885 is a regolith breccia that has been described by Arai et al. (2005b) and Warren and Bridges (2004). Our compositional results are consistent with those in the reports of Kaiden and Kojima (2002), Warren and Bridges (2004), and Karouji et al. (2006). It has a major-element composition like that of Dhofar 1180 but with greater and more typical Mg' (63; Fig. 1b). Concentrations of incompatible elements are ~1.6× greater. In terms of the Apollo model, the composition corresponds to a 3:1 mixture of FHT material and VLT basalt with ~10% KREEP. Both VLT basalt and clasts identified as KREEP basalt have been observed in Yamato 983885 (Warren and Bridges 2004; Arai et al. 2005b). Our subsamples of Yamato 983885 are more similar to each other in composition (e.g., 8.2–9.0% FeO) than those of Dhofar 1180 (7.9–10.4% FeO). Compositional scatter is usually greater for fragmental breccias (e.g., Dhofar 1180) than for regolith breccias (e.g., Yamato 983885) because the protolith of a regolith breccia is finer grained than that of a fragmental breccia. Yamato 983885 is rich in siderophile elements (Warren and Bridges 2004), a feature characteristic of breccias formed from mature regolith (Korotev et al. 2006). The mean Ir concentration (23 ng/g, Table 2; 22 ng/g, Warren and Bridges 2004) corresponds to 3.9% CM chondrite (Fig. 8).

Yamato 983885 is distinct in having the greatest Th/Sm of meteorites studied here (Fig. 6a). Warren and Bridges (2004) also noted high Th and U compared to other incompatible elements. This feature cannot be explained in terms of the Apollo model as all components of the model have lower Th/Sm (Fig. 6a). Several other meteorites studied here share the same feature, and we defer discussion of the significance to a later section.

Impact-Melt Breccias—Sayh al Uhaymir 300 [U] and Northwest Africa 4932 [R]

SaU 300 is a crystalline impact-melt breccia (Hudgins et al. 2007; Hsu et al. 2008), a lithology that is not common among lunar meteorites. (There are only 3–6 among the feldspathic lunar meteorites.) It is one of the least mafic of the meteorites discussed here (Fig. 1a) and in that regard does not belong with the others because SaU 300 is not "mingled" but consists nearly entirely of material of the Feldspathic Highlands Terrane (Hsu et al. 2008). The meteorite (and its likely launch pair, NWA 4932, below) appears to be the most mafic of nominally feldspathic lunar meteorites (Fig. 1). SaU 300 is distinct, for a feldspathic lunar meteorite, in being both moderately rich in elements associated with ferromagnesian

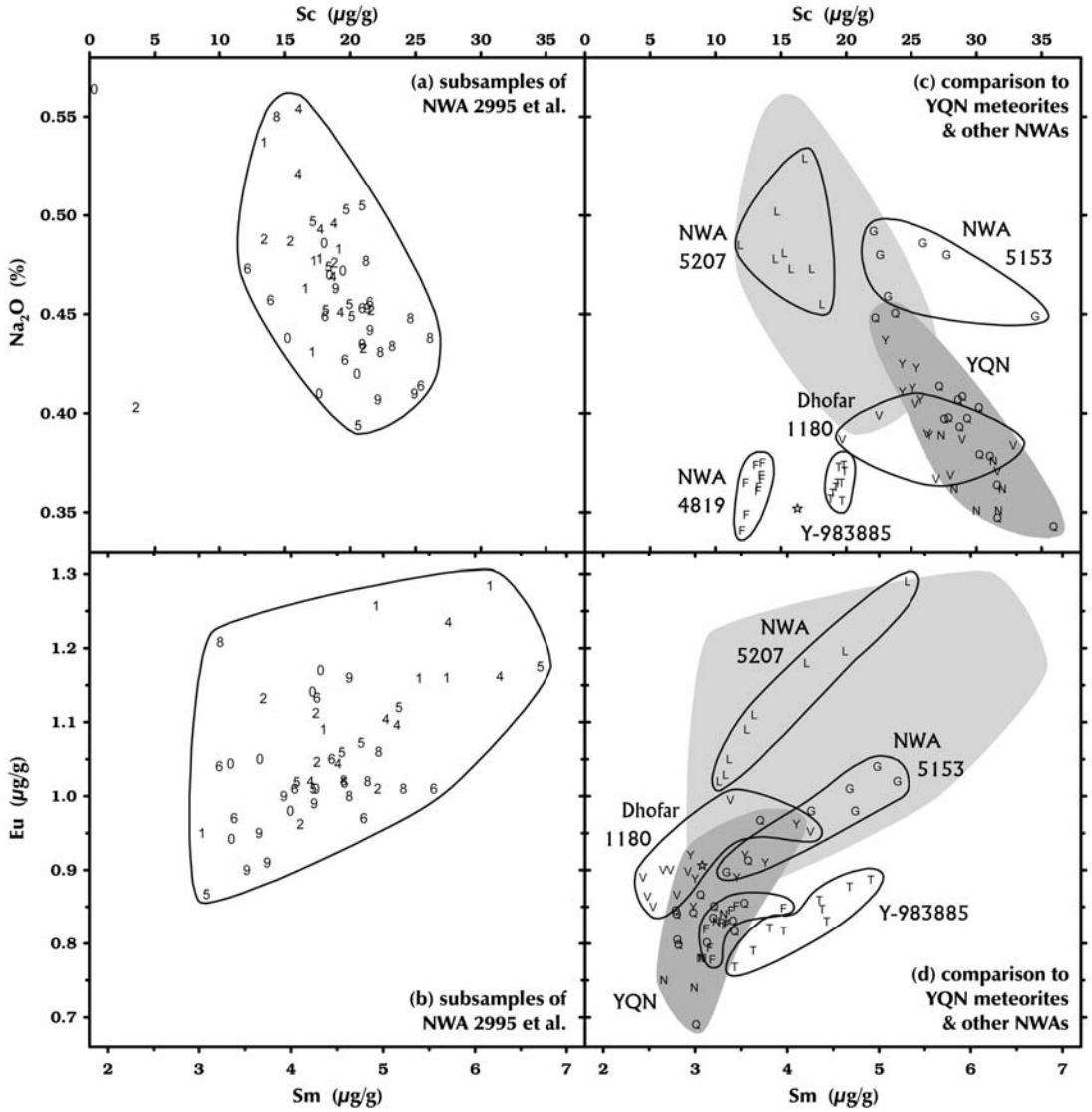

Fig. 14. a, b) Comparison of subsample data for NWA 2995 (symbol 5), NWA 2996 (6), NWA 3190 (0), NWA 4503 (4), NWA 5151 (1), NWA 5152 (2), and two unnamed stones (8 and 9) that are also likely part of the pair group. (c, d) Comparison of NWA 2995 et al. to the YQN launch-pair group (Yamato 981031, QUE 94281, and NWA 4884), NWA 4810, NWA 5153, NWA 5207, Dhofar 1180, and Yamato 983885. In (b) and (d), three anomalous subsamples of NWA 2995 et al. plot off scale. The star represents the composition of the Luna 20 soil.

minerals and poor in incompatible elements, leading to low Sm/Sc (Fig. 2). Sm/Sc (0.069) is only slightly greater than that of the plutonic anorthositic norite component of Apollo 16 sample 67513 (0.057; Jolliff and Haskin 1995), suggesting that SaU 300 is largely uncontaminated by KREEP and does not contain any significant component of regolith (Korotev et al. 2006). This inference is in agreement with the low concentrations of solar-wind gases (Hsu et al. 2008. Petrographic studies of SaU 300 have not found evidence of mare basalt (lithic clasts or mineral clasts; Hudgins et al. 2007; Hsu et al. 2008), thus the high Sc concentration must result from the moderately high abundance of nonmare mafic silicates. Whole-rock *Mg′* is 67 (68.5, if the chondritic meteorite contribution is discounted, below), a value at the high end of the range for ferroan anorthosite, but SaU 300 is more mafic than all but a few Apollo 16 ferroan-anorthositic-suite samples (Warren 1990). CaO/Al_2O_3, which is 0.58 ± 0.01 for the six well-studied feldspathic lunar meteorites from Antarctica (i.e., those with no terrestrial calcite; Korotev et al. 2003a) and 1.0–1.3 in mare basalt, is only 0.60 in SaU 300, about what would be expected for a mafic anorthosite.

NWA 4932 is also a crystalline impact-melt breccia (Fig. 13) composed of small gabbroic to troctolitic clasts (granular aggregates of rounded olivine grains and calcic plagioclase enclosed within low-Ca pyroxene with accessory Ti-chromite and troilite), sparse large grains of kamacite (up to 1 mm, partly altered to iron oxide or oxyhydroxide), and rare large grains of silica polymorph in a dominant, very fine-grained matrix of the same phases. Compositionally, our sample is slightly more mafic but

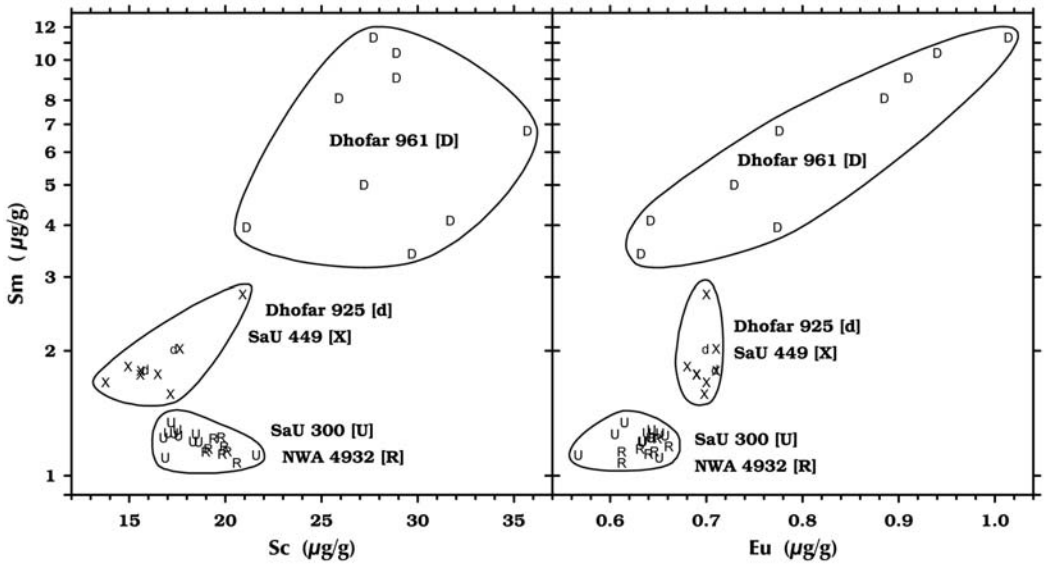

Fig. 15. The figure shows that (1) SaU 300 and SaU 449 differ in composition, (2) SaU 300 and NWA 4932 have the same composition, (3) SaU 449 and our small sample of Dhofar 925 (two subsamples) have the same composition, and (4) Dhofar 961 is compositionally distinct from Dhofar 925. The relationships depicted in these Sc-Sm and Sc-Eu plots are supported by all elements measured here that are not affected by terrestrial alteration (Fig. 10).

otherwise very similar to our sample of SaU 300. Because their compositions are similar to each other and together unique among lunar meteorites (Figs. 2, 7, and 15), the two meteorites may be launch (source-crater) paired, that is, they may have been ejected from the Moon by a single impact but as separate meteoroids that took different paths to make the Moon-Earth trip.

Like Yamato 983885, SaU 300 and NWA 4932 have ratios of Th to REEs that are greater than highly feldspathic lunar meteorites and most Apollo samples of otherwise similar composition (Fig. 6). Both meteorites are rich in siderophile elements (Fig. 8), presumably from the impactor that formed the melt from which they crystallized. Ir/Au is 3.45, i.e., the same as in H chondrites (Fig. 17). A 2.5% (SaU 300) and 3.7% (NWA 4932) component of H chondrite accounts for all of the Ir and Au and >90% of the Ni in the two meteorites. Assuming chondritic ratios of Ir/Fe in the asteroidal meteorite component of the two lunar meteorites, about 9% of the total iron in the two breccias derives from meteorites.

Compared to Apollo samples, both SaU 300 and NWA 4932 are enriched in K, Sr, and Ba as a result of terrestrial alteration (Fig. 10). SaU 300 is more enriched in Sr (5×) than NWA 4932 (1.7×) whereas NWA 4932 is more enriched in Ba (12×) than SaU 300 (1.3×). This pattern of difference is consistent among meteorites from the two regions, Oman and northwestern Africa (Korotev et al. 2003a). We observe barite in most NWA meteorites and celestite in most Dhofar meteorites. On the basis of La/Yb, Th/Yb, and U/Yb, SaU 300 is enriched in La (1.08×) and U (1.6×), but not Th (0.98×), from terrestrial alteration, compared to NWA 4932. The latter, on the other hand, is richer in K_2O (0.12%; Table 3) than SaU 300 (0.05%). Feldspathic lunar meteorites from Antarctica of similar REE concentrations have about 0.027% K_2O.

Regolith Breccia—Northwest Africa 4819 [F]

NWA 4819 is a regolith breccia with lithic clasts of ferroan-anorthositic-suite affinity, including anorthosites, fine-grained anorthositic norites, gabbros, and troctolites, as well as K-rich glass and glass spherules (Fig. 13). Pyroxene fragments are common among mineral clasts.

Compositionally, the meteorite is just outside the main cluster of feldspathic lunar meteorites in being more mafic and 3–4 times richer in incompatible elements (Fig. 2). The major-element composition is similar to that of the Luna 20 regolith (Laul et al. 1981) and the most feldspathic regolith samples of Apollo 17 (Korotev and Kremser 1992), although a bit less mafic. It is unlikely that the moderately high Fe, Sc, and Cr concentrations, compared to the more feldspathic lunar meteorite, result from a mare component as we observe no basalt clasts in thin section. Although we observe ~2% Fe-Ni metal in thin section, the INAA sample has typical concentrations of siderophile elements for a regolith breccia (Fig. 8).

NWA 4819 is compositionally unusual in two respects. First, it has anomalously high Cr/Sc (Fig. 5). High Cr/Sc usually implies a magnesian troctolite or spinel troctolite component. For example, in the most magnesian ($Mg' = 78$) of the typical feldspathic lunar meteorites, Dhofar 489 and pairs, Cr/Sc is similar at 114 (Korotev et al. 2006; Takeda et al. 2006). However, the whole-rock Mg' of NWA 4819 is only 65, a typical value for ferroan anorthosite. Second, as with Yamato 983885, SaU 300, and NWA 4932, Th/REE is (marginally)

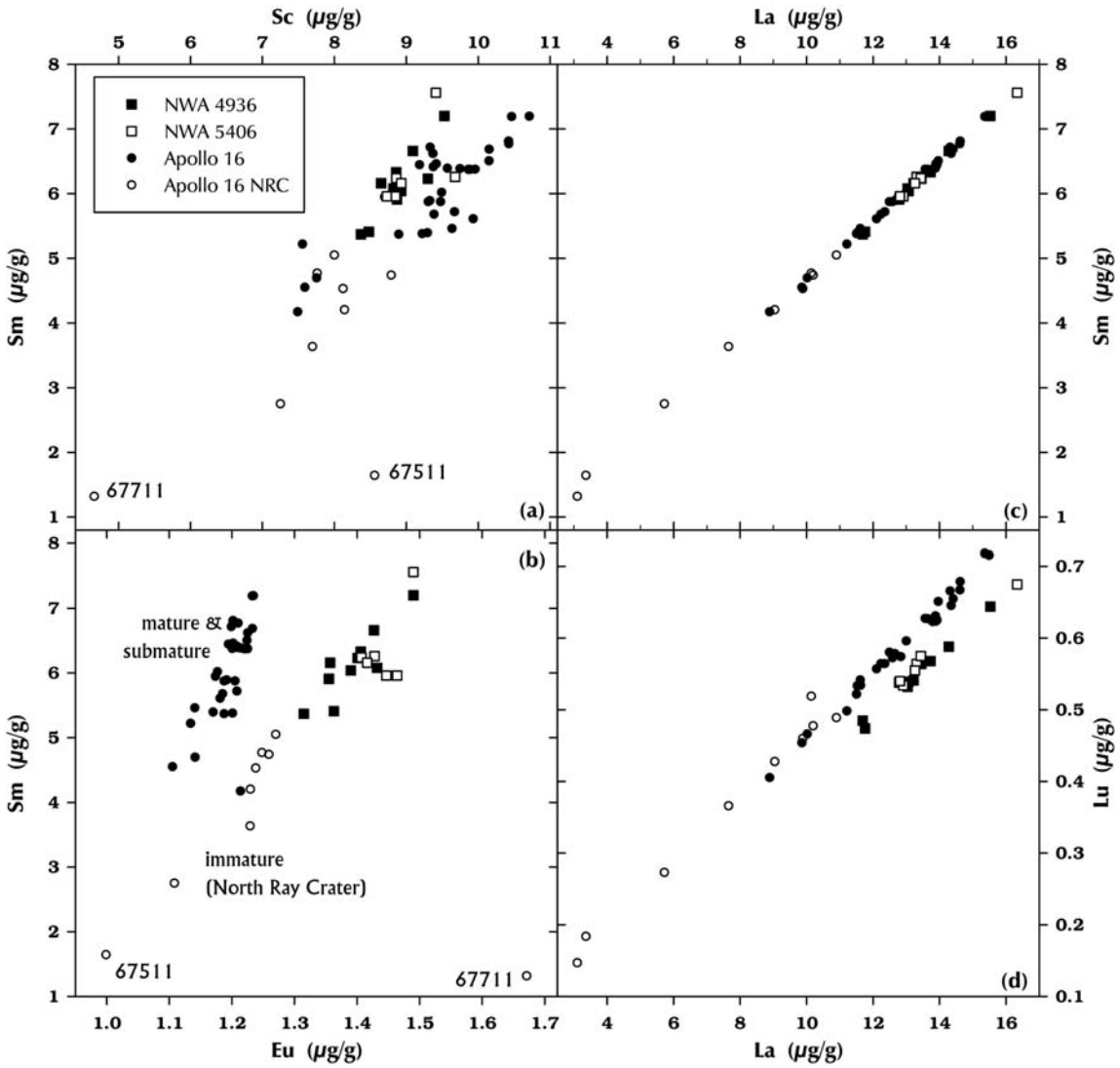

Fig. 16. Comparison of NWA 4936/5406 subsamples to Apollo 16 surface and trench soils. a) Apollo 16 regolith is richer in Sc than NWA 4936/5406 presumably because the meteorite contains a lesser proportion of mare basalt than Apollo 16 soil. b) NWA 4936/5406 is richer in Na and Eu than typical mature and submature Apollo 16 soil samples. Soils from North Ray Crater (NRC, stations 7 and 11) as well as anomalous sample 61221 are similarly rich in Eu, however. c, d) The ratios of light REEs, La/Sm, are identical but the meteorite is relatively depleted in heavy REEs (lower Lu/La) compared to Apollo 16 regolith. Each Apollo 16 point represents a regolith sample (Korotev 1997). All data from this laboratory.

greater for NWA 4819 than that of any mixture of the three components of the Apollo model of Fig. 2 (Fig. 6a).

NWA 4819 is enriched in Ba, and to a lesser extent Sr, from terrestrial alteration compared to Apollo samples of similar composition (Fig. 10).

Glassy Impact-Melt Breccia—Northwest Africa 4936 and 5406 [J]

NWA 4936/5406 is a glassy impact-melt breccia with a fine-grained matrix that includes heterogeneous "swirly" glass (schlieren) and grains of kamacitic metal (Fig. 13). Most clasts are small mineral clasts, not lithic clasts, that include anorthitic plagioclase, pigeonite, augite, sparse olivine, Mg-bearing ilmenite, kamacite, and troilite.

With only 5.9% FeO, NWA 4936/5406 is the most feldspathic of the breccias discussed here (except for Kalahari 008) and at the iron-rich end of the range for the truly feldspathic lunar meteorites (Fig. 1). We include it in the discussion because it differs from the numerous other feldspathic lunar meteorites in having substantially greater concentrations of incompatible elements, 4 to 6 times those of the FHT component of Table 4 and Fig. 2. Our sample of NWA 4936 is compositionally (e.g., Fig. 16) and texturally identical to our sample of NWA 5406, so we infer that the stones are paired.

The meteorite is distinct in that it is the first lunar meteorite for which the composition is similar to regolith from the Apollo 16 site (Figs. 2, 7, and 8), the only nonmare,

feldspathic-highlands location among the Apollo landing sites (Muehlberger et al. 1980). The Apollo 16 regolith is richer in incompatible elements than the majority of feldspathic lunar meteorites because it contains 25–30% mafic (noritic), KREEP-bearing impact-melt breccias as a result of the proximity of the site to the Procellarum KREEP Terrane and location on the Cayley Formation, an Imbrium ejecta deposit (Korotev 1997; Korotev et al. 2003a). As a consequence, the composition of Apollo 16 regolith plots along the FHT-PKT join of Fig. 2. NWA 4936/5406 is similarly "mingled." Subsamples of the meteorite also define a mixing trend between the feldspathic component and the KREEP component of Fig. 3. On the basis of the composition and texture, we suspect that the meteorite was formed mainly from immature regolith, but experienced more impact heating than breccias consisting simply of shock-compressed regolith so as to produce a glassy matrix.

The most striking similarity between NWA 4936/5406 and Apollo 16 regolith is in the absolute concentrations of incompatible elements (Figs. 3 and 16). There are some subtle, but intriguing systematic differences, however. (1) Mature regolith from Apollo 16 is richer in Sc by about 8% (Fig. 16a). This difference implies that the meteorite has a lesser proportion of mare basalt (<2%?) than the approximately 6% (Korotev 1997) inferred to be present in the Apollo 16 regolith. Less mare material is expected if the melt volume of the impact forming the NWA 4936/5406 breccia is several meters or more below the surface where admixture of mare basalt to the regolith by post-basin impacts has been minimal (Zeigler et al. 2006b). (2) The meteorite is richer in MgO (8.6%) than the Apollo 16 regolith (6.1%; Korotev 1997), leading to significantly greater Mg' for the meteorite, 72.1 compared with 66.5 for Apollo 16 (Fig. 1b). This difference all but requires that the feldspathic component of NWA 4936/54 include some type of magnesian anorthosite (Korotev et al. 2003; Takeda et al. 2006) as opposed to the ferroan anorthosite that is common at the Apollo 16 site. (3) Although ratios among light REEs are identical (e.g., La/Sm; Fig. 16c), the meteorite has ratios of heavy to light REEs (Lu/La, Fig. 16d) that are ~90% those of otherwise similar Apollo 16 regolith, leading to a heavy-REE-depleted rare-earth pattern (Fig. 12, "NWA 49/56"). (4) Finally, Concentrations of Na and Eu are about 10% and 16% greater in the meteorite than in Apollo 16 soils of similar Sm concentration (Fig. 16b). As in our discussion of Kalahari 008 and Fig. 11, this difference reflects a plagioclase component of NWA 4936/5406 that is more albitic, on average, than that of typical Apollo 16 regolith. Soil samples collected near North Ray Crater are less mature and more variable in composition than those from the central and southern part of the Apollo 16 site. Many North Ray Crater soils are similar to NWA 4936/5406 in being richer in Na and Eu (Fig. 16b) than the typical mature soils of Apollo 16. Observations 2 and 3 are both consistent with a greater olivine to pyroxene ratio in the meteorite compared to Apollo 16, that is, precursor that is more

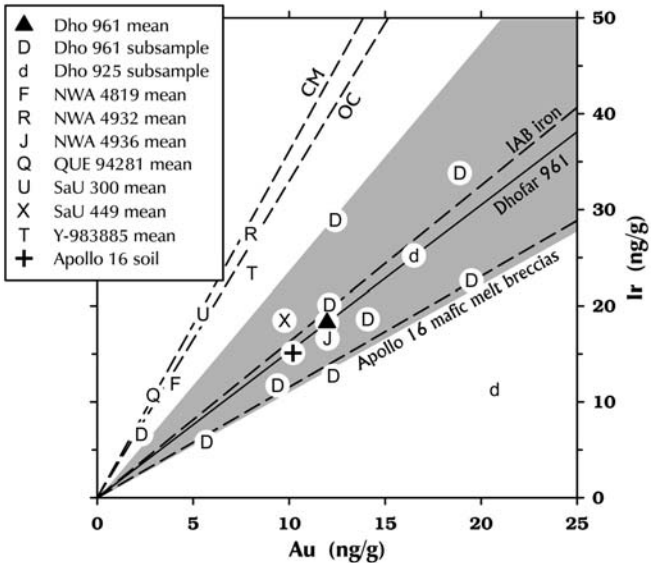

Fig. 17. Ir and Au concentrations in lunar meteorites with high concentrations of both elements (Fig. 8). Most lunar meteorites have chondritic Ir/Au because siderophile elements in most regoliths derive mainly from chondritic micrometeorites with CM-like compositions (Wasson et al. 1975). Dhofar 961, NWA 4936, and SaU 449 (Fig. 15) are unusual in having Ir/Au (and Ni/Co) more similar to group IAB irons than chondrites. In this respect, they are similar to metal-rich mafic melt breccias of Apollo 16 (Korotev 1987b, 1994). The regolith (soil) of Apollo 16 contains both the metal component and the chondritic component (Korotev 1997). The dashed lines represent (top to bottom) the average ratios for CM and ordinary chondrites (Wasson and Kallemeyn, 1988), IAB (main group) irons (Wasson and Kallemeyn 2002), and mafic, Sm-rich impact-melt breccias from Apollo 16 (Korotev 1994). The solid line represents the ratio for mean Dhofar 961. Of the 71 main-group IAB irons in the study of Wasson and Kallemeyn (2002), Ir/Au for 70% of the meteorites fall within the gray field. For the Dhofar 925 and Dhofar 961 (only) subsample data are plotted; analytical uncertainties (2σ) for both Au and Ir are about ± 2 ng/g. For the other meteorites, the mass-weighted means of Table 2 are plotted.

troctolitic. Along with observation 4, we infer that a portion of the feldspathic component of the meteorite is compositionally similar to unique lunar meteorite Dhofar 733 (Foreman et al. 2008) in being anomalously albitic (Fig. 11), magnesian (Mg' = 74.5; Fig. 1b), and having high La/Lu (off scale at Sc = 4 μg/g and La/Lu = 31 on Fig. 7c). We can, in fact, obtain a reasonable, but not perfect, match to the composition of NWA 4936/5406 with a mixture of 23% typical feldspathic lunar meteorite, 31% Dhofar 733, and 45% Apollo-16 group-2DB impact-melt breccia (Korotev 1994).

Siderophile element ratios also suggest a relationship between NWA 4936/5406 and Apollo 16. The Apollo 16 mafic melt breccias are rich in Fe-Ni metal with a meteoritic, but nonchondritic, Ir/Au ratio (Hertogen et al. 1977; Korotev 1997). In typical Apollo 16 soil, 36–66% of the Ni, Ir, and Au are carried by the ancient melt-breccia component; the remaining portion is contributed by post-basin meteorites with chondritic compositions, mainly micrometeorites (Korotev 1987c; Korotev 1997). As a consequence, the CI-

normalized Ir/Au of typical Apollo 16 regolith (0.43) is intermediate to that of the metal (0.34) and chondrites (1.0). Most lunar meteorites have Ir/Au ratios in the chondritic range (Fig. 17) because they do not contain the metal-rich, Sm-rich, melt-breccia component (Korotev et al. 2006). NWA 4936/5406, in contrast, has an intermediate ratio (0.40) like that of Apollo 16. Also, as with Apollo 16 regolith samples, absolute concentrations of siderophile elements in NWA 4936 are both high on average (e.g., 17 ng/g Ir; Fig. 8) and highly variable among subsamples (10–57 ng/g Ir) because of the nonuniform distribution of Fe-Ni metal nuggets.

We conclude that among lunar meteorites, NWA 4936 is most likely to have originated close to the Apollo 16 site, perhaps at a different location in the Cayley Formation.

Clast-Rich, Glassy-Matrix Breccias—Dhofar 925 [d] and 961 [D], and Sayh al Uhaymir 449 [X]

Dhofar stones 925, 960, and 961 were reportedly found together in the field at a point distant from other lunar meteorite stones (see Fig. 14 of Korotev et al. 2006) except for totally dissimilar Dhofar 489, a highly feldspathic impact-melt breccia with very low concentrations of incompatible elements (Takeda et al. 2006; Korotev et al. 2006). Initial studies of Dhofar 925, 960, and 961 classified the stones as feldspathic impact-melt breccias that are mutually paired on the basis of field location, texture, clast population, and mineral chemistry (Demidova et al. in Russell et al. 2004, 2005; Demidova et al. 2007).

For Dhofar 925, we obtained a sample of only 0.051 g from which we made two INAA subsamples. After INAA, we made a polished thick section of one subsample and determined major-element concentrations on the other (Table 3). For Dhofar 961, we obtained a 0.57 g slice from which we took nine ~29 mg INAA subsamples from around the edge and made a polished thick section of the remaining interior piece. Major-element data were obtained from four of the INAA subsamples. We have been unable to obtain samples of Dhofar 960 or more Dhofar 925 material.

Regarding Dhofar 925, Demidova et al. (in Russell et al. 2004) state "abundant mineral fragments and lithic clasts are set within a fine-grained impact melt matrix; the lithic clast population is dominated by impact-melt breccias and granulitic rocks of anorthositic, troctolitic, noritic, and gabbronoritic compositions; the presence of VLT mare basalt clasts and rare KREEPy and granitic fragments is a characteristic feature of this meteorite." Our small polished section of Dhofar 925 is largely consistent with this description. Our much larger sample of Dhofar 961 is dominated by large clasts of mafic impact-melt breccia (~60 vol%), with some granulitic lithic clasts (~3%), small norite and gabbronorite breccia clasts (~2%), and a few very small, aluminous basaltic vitrophyre clasts (<0.5%). The "matrix" of Dhofar 961 makes up some 33% of our section and comprises fine- to very fine-grained lithic clasts and mineral clasts welded by a small amount of inter-clastic melt. Dhofar 961 also contains impact-melt veins that are compositionally somewhat less mafic than the bulk composition of the meteorite and more like the bulk composition of Dhofar 925. Both meteorites are essentially clast-rich impact breccias that may, in fact, be regolith breccias, although we observed no regolith components such as glass spherules or agglutinate clasts in our petrographic study. Both stones contain large lithic clasts of fine-grained, mafic, crystalline impact-melt breccia. Our Dhofar 925 sample, however, contains a higher percentage of plagioclase clasts and feldspathic lithic clasts.

Dhofar 961 has the bulk composition of olivine gabbronorite. Concentrations of incompatible elements are greater than those of most meteorites discussed here (Fig. 2). Presumably because of the lithologic variety and large size of the clasts, the nine INAA subsamples vary widely in composition. The variation occurs among major elements, incompatible elements, and siderophile elements (Figs. 3, 15, and 17) is far greater in relative magnitude than is usually observed, for example, in lunar impact-melt breccias (e.g., Korotev, 1994). Our two subsamples of Dhofar 925 are similar to each other in composition and to the sample of Demidova et al. (2007) but outside the range of the Dhofar 961 subsamples for most elements in being compositionally more feldspathic (Fig. 15), consistent with their clast component proportions.

We have not studied SaU 449 petrographically. As with Dhofar 925, Ivanova and Nazarov (in Connolly et al. 2008) classify the rock as a clast-rich, feldspathic impact melt breccia that was reportedly found 4.2 km from SaU 300, a feldspathic, crystalline impact-melt breccia (Hudgins et al. 2007; Hsu et al. 2008). Although both SaU meteorites are mafic anorthosites in composition, the two stones are compositionally distinct from one another (Figs. 7 and 15). Discounting elements associated with terrestrial alteration, SaU 449 is compositionally indistinguishable from our small sample of Dhofar 925, however, for which the reported collection site is 212 km to the south. Our hand samples (sawn slices) of SaU 449 and Dhofar 925 also strongly resemble each other but neither resembles SaU 300. The similarity of Dhofar 925 and SaU 449 is unexpected in light of the compositional difference between our samples of Dhofar 925 and Dhofar 961, which were reportedly collected within 200 m of each other. We regard SaU 449 and Dhofar 925 as candidate terrestrial pairs or launch pairs. (For the record, we analyzed our sample of Dhofar 925 in February 2006, before the reported find date of SaU 449, March 19, 2006). Our compositional data do not strongly support the pairing of Dhofar 925 and Dhofar 961, but in light of the clast-rich nature of both stones (as well as the extreme differences between, for example, different portions of SaU 169 and Kalahari 008/009) they also cannot refute the pairing hypothesis. If Dhofar 925 and 961 are paired, then our sample of Dhofar 925 (and that of Demidova et al. 2007) represents a feldspathic assemblage of clasts in the Dhofar 925/960/961

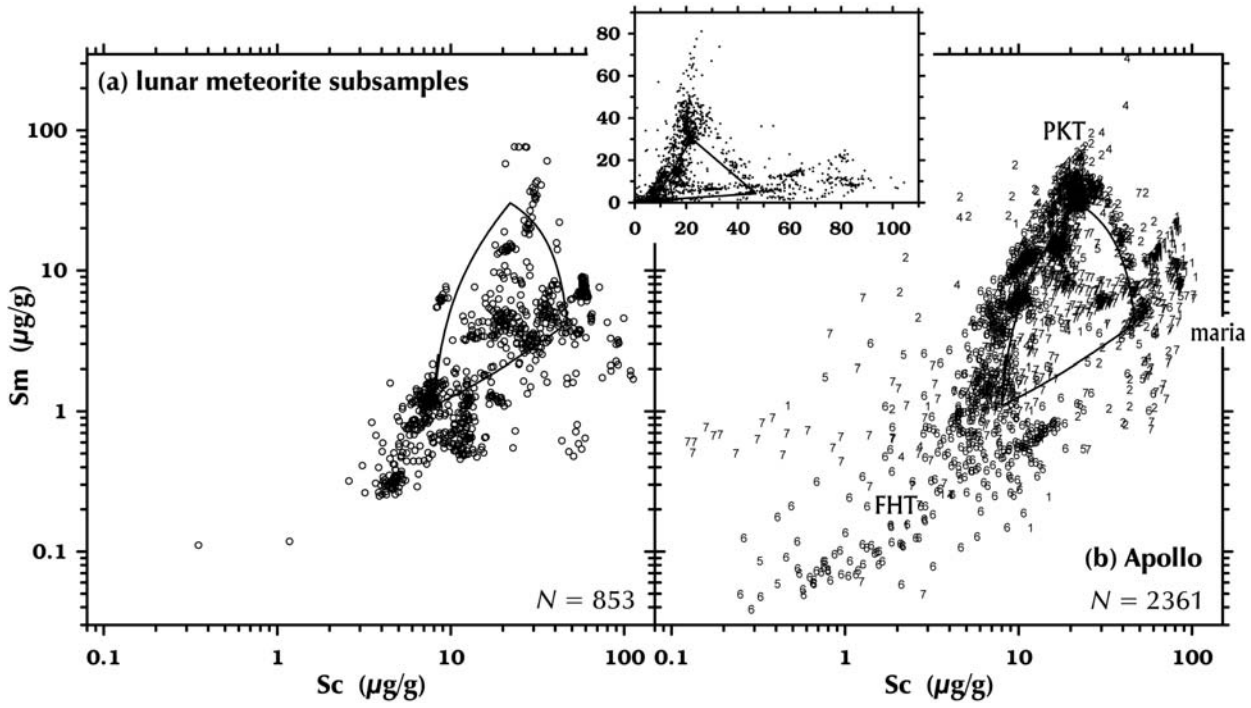

Fig. 18. Comparison of compositions of lunar meteorites with samples from the Apollo collection. All data are from this laboratory (see text). The "triangle" is the same as that of Fig. 2. a) Each point represents a subsample of a lunar meteorite. The mean mass of the subsamples is 28 mg. One-hundred ten stones from about 61 meteorites are represented. b) Each point represents a lithic fragment from an Apollo regolith sample (see text). The mean mass of the fragments is 24 mg. The symbol "1" designates Apollo 11, "2" Apollo 12, etc. The proportions of samples from each Apollo mission are 5% for Apollo 11, 11% for Apollo 12, 19% for Apollo 14, 2% for Apollo 15, 31% for Apollo 16, and 31% for Apollo 17. The inset shows the Apollo data on a linear scale.

meteorite and the meteorite is consequently even more heterogeneous than our Dhofar 961 data suggest.

Dhofar 961 differs from most other lunar meteorites in being rich in siderophile elements (Fig. 8) and in containing grains of Fe-Ni metal that are large, with diameters up to 500 μm. Nickel concentrations of the metal are typically 5.5% (EPMA). Siderophile-element ratios, e.g., Ni/Co and Ir/Au, in Dhofar 961 are different from those of most other brecciated lunar meteorites that we have studied, which have ratios similar to chondrites (Fig. 17). Concentrations of Ni and Co are strongly correlated among the subsamples ($R^2 = 0.984$, $N = 9$) and the correlation requires a metal component with mean Ni/Co of 13.7 ± 1.5. This ratio is substantially less than the chondritic ratio (20–22), but within the range of iron meteorites, e.g., IAB and IIAB (13.9 and 11.6; Mittlefehldt et al. 1998). In Dhofar 961, ratios of Ir to Au vary substantially among the subsamples. On average, the ratio is half that of CM chondrites but within the range of IAB irons (Fig. 17). Hot-desert meteorites can be seriously contaminated with gold (Korotev et al. 2003; Warren et al. 2005), but the Ir/Ni of the metal in Dhofar 961, $3.0 \pm 0.4 \times 10^{-5}$ (using the regression technique of Korotev 1994), also is not chondritic (0.61 times the CM ratio) but is in the range of IAB irons. Thus, the metal component of Dhofar 961 appears to derive from an iron meteoroid. If we assume a IAB component, then our sample of Dhofar 961 contains 0.7% metal by mass on the basis of the mean Ir concentration. There is strong evidence that the metal in mafic impact-melt breccias of Apollo 16 also derives from an iron meteorite, possibly a IAB (Korotev 1987b, 1987c, 1994; James 2002). Apollo 16 melt breccias also contain a high abundance of Fe-Ni metal, typically 0.5–2 wt% metal (Korotev 1994).

Concentrations of siderophile elements in SaU 449 are also high (Fig. 8) and siderophile-element ratios of the metal component are also nonchondritic ($Ni/Co = 15 \pm 2$; $Ir/Ni = 3.8 \pm 0.7 \times 10^{-5}$, 0.76× the CM ratio; Fig. 17). This feature is the only compositional characteristic of SaU 449 that suggests a possible relationship to Dhofar 961.

Our samples of Dhofar 925 and SaU 449 have no Eu anomaly (Fig. 12), an observation that has no special significance given that the stones are breccias. An unusual geochemical feature of Dhofar 961, however, is that it has low concentrations of plagiophile elements, Na and Eu, compared to Apollo samples of similar trivalent REE concentrations (Fig. 7b). We discuss the significance of this observation in a later section.

DISCUSSION

A New Comparison of Lunar Meteorites and Apollo Samples

There is now a sufficient number of lunar meteorites

($N \approx 65$) that a comparison of the lunar meteorite suite to the Apollo collection is more meaningful than comparisons made even six years ago ($N \approx 24$; Korotev et al. 2003a). In Fig. 18, we use Sc and Sm data to compare the composition of lunar meteorites and Apollo samples. The comparison has the advantage that we acquired all of the data in the figure by the same technique and each point represents the same mass of sample, on average. It suffers in that in neither plot (a and b) are samples represented by the points a truly random or representative subset of the Moon or the Apollo collection. In Fig. 18a, at least one stone from nearly every known lunar meteorite is represented but, as an extreme example, there is only one point representing basalt Yamato 793169 but 37 points for six stones of the LaPaz Icefield basalt. Fig. 18b is not representative in that the number distribution of fragments among the six Apollo sites is not equal and for Apollo 11, 12, 15, and 17 our sample selection was biased in favor of nonmare samples at the expense of basalt. The Apollo suite contains numerous mare basalts and breccias derived therefrom (15% of the fragments in the figure have >15% FeO), but the relative proportion of such material in the Apollo collection may be greater than in our sample set. Although there are a few points representing clasts of extreme composition in the lunar-meteorite data set, it is likely that the Apollo suite contains a greater proportion of anomalous samples because each point represents a discrete rock fragment from the regolith and few of our lunar meteorite subsamples are dominated by a single clast. Despite these limitations, it is our opinion, based on the large number of points and compositional diversity of each data set, that none of the observations we make below are grossly in error because of our imperfect sampling strategy.

Mare basalts occur in both data sets ("maria," Fig. 18b) but in detail there are no compositional matches between any meteorite basalt and an Apollo or Luna basalt. This simple observation attests to the diversity of lunar basalts, a diversity that challenges that of terrestrial basalts and, on the basis of limited sampling, considerably exceeds that of Mars. The closest match between meteorites and Apollo samples is NWA 032/479 and LaPaz Icefield 02205 (and pairs), two meteorites that are so similar they may be from the same source crater (Zeigler et al. 2005), and the Apollo 12 basalts (Righter et al. 2005; Anand et al. 2006; Day et al. 2006a; Day and Taylor 2007). Lunar meteorites have significantly extended the compositional range of mare basalts over that known from the Apollo and Luna missions and provide additional evidence that the source region of lunar basalts is nonuniform on a global scale.

Feldspathic samples that are poor in incompatible elements are common in both data sets and there are numerous small samples from Apollo 16 that are compositionally similar to the feldspathic lunar meteorites. The Apollo 16 regolith also contains numerous fragments of nearly pure plagioclase from ferroan anorthosite (very low Sc and Sm in Fig. 18b), however, and only a few of the lunar meteorite subsamples are so feldspathic. As we have noted before (Korotev et al. 2003a), there is little evidence in the lunar meteorite collection that ferroan anorthosite consisting of 98–99% plagioclase, such as is prevalent in the Apollo 16 regolith, is common throughout the feldspathic highlands.

The most noteworthy difference between the Apollo suite and the lunar-meteorite suite is that Sm-rich (>3 μg/g), nonmare samples, nearly all of which are impact-melt breccias and regolith breccias derived in part from impact-melt breccias, are common in the Apollo collection and occur at all six Apollo sites but are unusual among the meteorites. Most nonmare Apollo samples plot along the anorthosite-KREEP edge of the mixing triangle of Fig. 18b, as does the Apollo 16 regolith (Fig. 3), whereas none of the meteorites except NWA 4936/5406 plot in this location. The anorthosite-KREEP trend of the Apollo samples reflects large-scale mixing between the Feldspathic Highlands Terrane and Procellarum KREEP Terrane largely as a consequence of the impacts of the Imbrium and Serenitatis bolides into the Procellarum KREEP Terrane (Haskin 1998; Haskin et al. 1998). Few lunar meteorites originate from this mixing zone.

In the Apollo collection, binary mixtures of KREEP and mare basalt with little or no FHT material are rare (Fig. 3) and occur only at the Apollo 12 site as regolith and regolith breccias (Seddio et al. 2009). Lunar meteorites of this type are also rare, with Dhofar 1442 and SaU 169 being the only candidates, although the compositions of both are different in detail from Apollo 12 regolith. With exceedingly high concentrations of incompatible elements, SaU 169 (Gnos et al. 2004) and Dhofar 1442 must derive from the Procellarum KREEP Terrane. Likewise, the high concentrations of incompatible elements in NWA 4472/4485 and the overall similarity of the composition to impact-melt breccias from the Apollo missions (Fig. 2) argues for a PKT origin for this meteorite as well. With less than about 10% each of mare basalt and feldspathic material (Joy et al. 2008), NWA 4472/4485 is consistent with a regolith developed on a deposit of impact-melt breccia.

Although regolith breccias consisting mainly of brecciated anorthosite and basalt occur at the Apollo 11, 15, and 17 sites (Apollo soils of Fig. 3), all such Apollo breccias also contain components of KREEP impact-melt breccia, which puts the compositions in the interior of the mixing triangle not along the anorthosite-basalt join. For example, even at the Apollo 11 site in Mare Tranquillitatis, the soil is a mixture of 71–72% mare basalt and volcanic glass, 20–21 % feldspathic material, and 7–9% KREEP impact-melt breccia (by mass balance; Korotev and Gillis 2001). In contrast, a few lunar meteorites of intermediate iron concentration (MET 01210 and the YQN meteorites [likely launch pairs Yamato 793274/981031, QUE 94281, and NWA 4884], EET 87521/96008, and, possibly, Dhofar 1180 and NWA 3136) are primarily binary mixtures of anorthosite and mare basalt with little or no KREEP. Compositionally and petrographically, these meteorites are consistent with an origin from regions of

the Moon distant from the Procellarum KREEP Terrane where mare basalt has mixed with regolith of the feldspathic highlands. MET 01210 and EET 87/96 are breccias with high iron concentrations; these meteorites might derive from regolith in a maria. Some others likely derive from other types of mare-highlands mixing zones, either boundary locations like the Apollo 15 and 17 sites, or cryptomaria, i.e., old maria resurfaced with feldspathic basin ejecta (Schultz and Spudis 1979; Terada et al. 2007). The YQN meteorites may fall in this category (Jolliff et al. 1998; Arai and Warren 1999; this work).

On the basis of both composition and petrography, several meteorites of intermediate iron concentration appear to differ from rocks of the Apollo collection in being breccias derived mainly from anorthosites and more mafic lithologies of the feldspathic highlands, with little admixed Sm-rich material from the Procellarum KREEP Terrane (<3%?) or mare volcanic material. If this surmise is correct, then several of these meteorites contain or represent lithologies that are rare in the Apollo collection. As we have noted in some descriptions above, if Fig. 3 is interpreted in light of the Apollo model, where a meteorite with 30–35 μg/g Sc, for example, is an approximately 50:50 mixture of feldspathic and mare material, then clastic mare basalt is not nearly as common in some meteorites as the figure implies. Meteorites in this category include Calcalong Creek, Dhofar 925, Dhofar 961, Dhofar 1180, NWA 2995 et al. NWA 3136, NWA 4819, NWA 4932, NWA 5207, SaU 300, SaU 449, and Yamato 983885. Six of these twelve meteorites are those that have Th/Sm greater than any mixture of the three Apollo model components (Fig. 6). Thus, incompatible elements in these meteorites are not supplied mainly by KREEP or mare basalt because the meteorites plot outside the mixing triangle of Fig. 6a. The meteorites are mafic not because they contain mare basalt but because they contain norites, gabbronorites, and troctolites of the feldspathic crust. These lithologies apparently have higher Th/Sm than most rocks in the Apollo collection. Several granulitic breccias of the Apollo collection have high Th/Sm (Korotev et al. 2003a), but all such samples are more feldspathic (<12 μg/g Sc) than the high-Th/Sm meteorites of Fig. 6. Mafic, high-Th/Sm rocks must dominate at the Luna 20 site as well, where the regolith also has high Th/Sm compared, for example, to Apollo 16 regolith (Fig. 6b). Luna 20 regolith, which consists mainly of nonmare material ejected from the Crisium basin with only a small mare component (Heiken and McEwan 1972; Spudis and Pieters 1991), likely contains material from the lower crust. Thus several of the intermediate-iron lunar meteorites may well also be rich in mafic material of the lower crust. If so, then it is significant that these meteorites are both low in incompatible elements and not highly magnesian. For the six high-Th/Sm lunar meteorites of Fig. 6a, *Mg′* is in the range of ferroan anorthosites (mean: 65, range: 60–68).

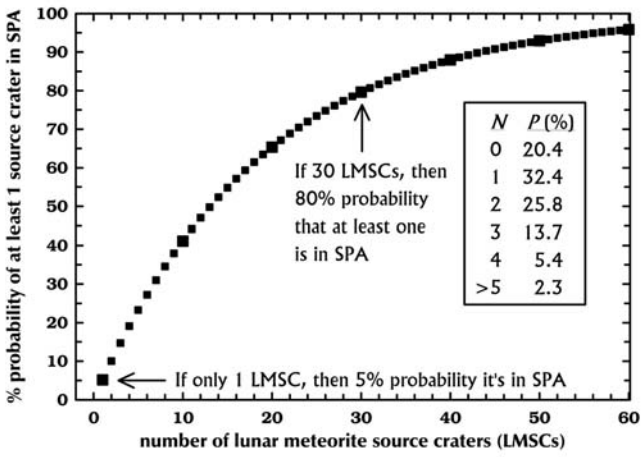

Fig. 19. The figure shows that if 5.3% of the Moon's surface is in the inner SPA basin (Jolliff et al. 2000) and if lunar meteorites originate from randomly distributed locations on the lunar surface, then on the basis of Poisson statistics (e.g., Walpole and Meyers 1993, p. 134; $x = 0.053$) there is a 79.6% probability that at least one lunar meteorite originates from the inner SPA basin even if there are as few as 30 lunar-meteorite source craters (LMSCs). The table (inset) shows that under these conditions (i.e., 30 LMSCs), for example, there is a 25.8% probability that exactly two derive from SPA and a 47.2% probability that two or more derive from SPA. If the number of source craters is greater than 30, then all the probabilities are also greater. Our analysis assumes that over the past several million years, there has been an equal probability for crater formation at any point on the lunar surface and that meteorites launched from anywhere have an equal probability of reaching Earth. The first assumption is not absolutely correct in that the polar (equatorial) rate is reduced (enhanced) by 10% (5%) relative to the global average (Le Feuvre and Wieczorek 2008) and the cratering rate of the leading (Mare Orientale) hemisphere is 1.28× that of the trailing (Mare Marginis) hemisphere (Gallant et al. 2009). Neither of these differences will strongly affect our SPA estimates. There is no difference in cratering rate (Gallant et al. 2009) or delivery efficiency between the nearside and farside meteorites (Gladman et al. 1995; Gladman, personal communication), although there will be a slightly greater but unquantified delivery efficiency for meteorites launched from the trailing hemisphere (Gladman et al. 1995; Gladman, personal communication).

Are There Lunar Meteorites from the South Pole-Aitken Basin?

Jolliff et al. (2000) advocated that the geochemical anomaly (moderately mafic with moderate concentrations of Th) that constitutes the interior of the South Pole-Aitken basin can be regarded as a geologic terrane distinct from the Feldspathic Highlands Terrane (feldspathic and low concentrations of Th) because of its large size, distinct geochemistry, and ancient age. The inner South Pole-Aitken Terrane constitutes 5.3% of the lunar surface (Jolliff et al. 2000). The number of lunar meteorites is now about 65, and when the obvious cases of launch pairing are taken into account, the meteorites may represent as many as about 50 craters on the Moon and probably not less than 30. Thus,

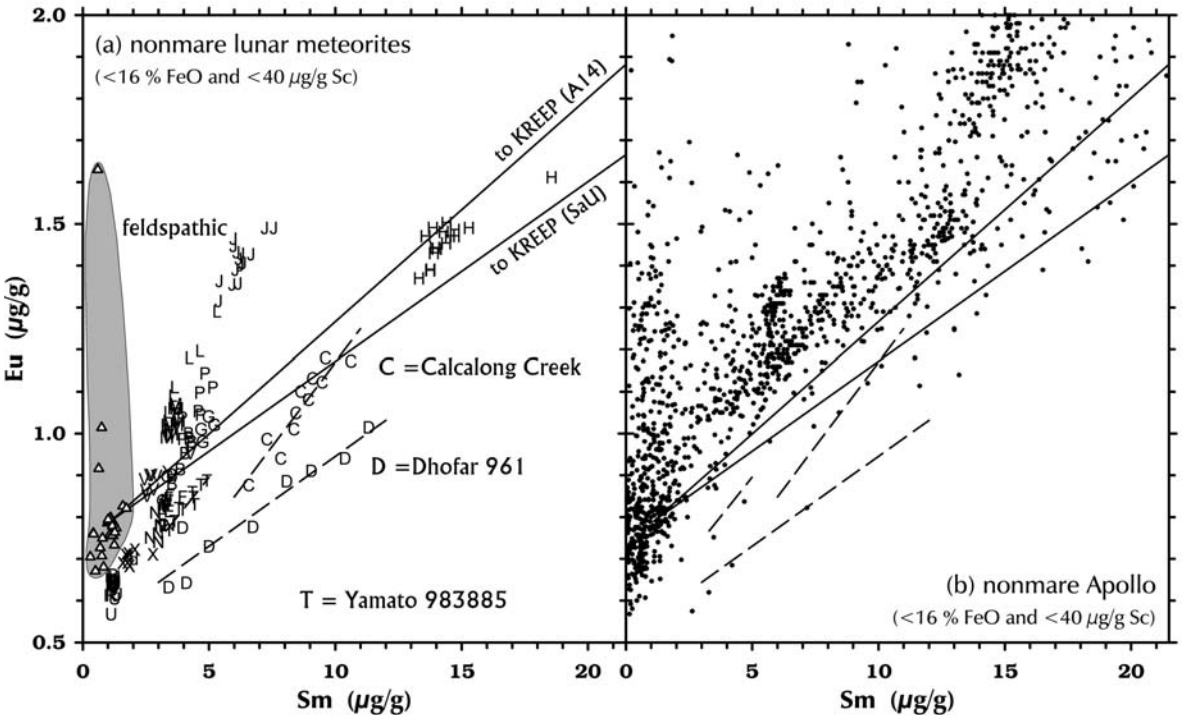

Fig. 20. Variation of Eu with Sm among (a) subsamples of lunar meteorites (<16% FeO) and (b) comparison to Apollo samples of similar composition and mass. See Table 1 for legend. The dashed lines are regression lines through the points for Dhofar 961 (D), Calcalong Creek (C), and Yamato 983885 (T) subsamples. In (b), the points represent nonmare lithic fragments from Apollo regoliths (low-Sm subset of data of Fig. 18b; $N = 1344$). The solid lines are mixing lines between typical feldspathic lunar meteorites representing the Feldspathic Highlands Terrane (Korotev 2003a) and two forms of KREEP with differing Eu/Sm ratios, high-K KREEP of Apollo 14 (Warren 1989) and SaU 169 (Fig. 7b), representing the PKT. The figure shows that the Sm-bearing component of Dhofar 961 has lower Eu/Sm than does KREEP as known from the PKT.

simply on the basis of statistics, it is highly likely (>80%; Fig. 19) that one or more meteorites originates from within the South Pole-Aitken basin. If so, which ones and how can we tell?

Because of their intermediate compositions, several lunar meteorites discussed in this paper are SPA candidates. Using FeO and Th data obtained from orbit (Lucey et al. 1988; Lawrence et al. 2000), Jolliff et al. (2000) estimate the mean composition of inner South Pole-Aitken to be 10.1 ± 4.2% FeO and 1.9 ± 0.8 μg/g Th (uncertainties are two standard deviations). Estimates based on newer analysis of the Lunar Prospector gamma-ray data (Prettyman et al. 2006) are not significantly different (Jolliff et al. 2009). Concentrations of both elements in SPA are considerably greater than those of the Feldspathic Highlands Terrane, and the Th concentration is considerably less than that of the Procellarum KREEP Terrane. The SPA concentrations are similar to some meteorites that plot in the interior of the mixing triangle of Fig. 2: Dhofar 961 [D]; NWA 2995 [P] et al. NWA 4819 [F], NWA 5153 [G], NWA 5207 [L], and Yamato 983885 [T]. All the meteorites are breccias, so two end-member possibilities can account for a meteorite of this composition: (1) In terms of the Apollo model, the meteorite is a mixture of rocks of more extreme composition, e.g., anorthosite, KREEP, and mare basalt. For example, some regolith samples from Apollo 15 (station 2 on Apennine Front) and 17 (station 6 on North Massif) plot in the SPA region of Fig. 2 because they are mixtures of anorthosite, KREEP, and mare basalt, although they were formed in or near the Procellarum KREEP Terrane. (2) The meteorite is a breccia dominated by gabbronorite with moderate concentrations of incompatible elements. The latter hypothesis is consistent with what we would expect for a breccia containing both mare and nonmare components from the South Pole-Aitken Terrane (Pieters et al. 2001).

One, and possibly two or more, of the SPA-candidate meteorites has some geochemical characteristics that suggests that it does not come from the Procellarum KREEP Terrane, at least not from the vicinity of the Apollo sites. The most likely candidate is Dhofar 961, which has a low concentration of Eu in comparison to Apollo samples of similar Sm concentration (Figs. 7b and 20). Sm and Eu concentrations in nonmare samples of the Apollo collection (Fig. 20), that is, samples from in or near the Procellarum KREEP Terrane, are largely consistent with mixtures of noritic anorthosite (5–10 μg/g Sc, very low Sm, low Eu) and KREEP (20–30 μg/g Sc, high Sm and Eu). Most ferroan anorthosite from the Apollo missions contains 0.8 ± 0.1 ppm Eu, and this range is typical of the feldspathic lunar meteorites (Fig. 20). Some feldspathic meteorites and

Apollo samples are richer in Eu because they contain plagioclase that is more albitic than the An_{97} plagioclase typical of ferroan anorthosite (Fig. 20a). Nonmare Apollo samples that are poorer in Eu with respect to the anorthosite-KREEP mixing lines of Fig. 20 are mafic samples for which both Sm and Eu are effectively diluted with olivine or pyroxene. This is why, for example, the mafic anorthosites SaU 300 and NWA 4932 plot below the field of typical feldspathic lunar meteorites at 0.6 μg/g Eu in Fig. 20a. The Dhofar 961 subsamples plot along a line distinct from that of the Apollo samples, one parallel to the Apollo trend but at lower Eu concentration (Fig. 20a). Put another way, we are unaware of any sample in the Apollo collection that is compositionally and petrologically similar to Dhofar 961. Only a few Apollo samples plot in the Dhofar-961 portion of the diagram (Fig. 20b). In detail, none is similar to Dhofar 961. This distinction argues that Dhofar 961 is not a mixture of anorthosite and KREEP, as known from the PKT.

Our working hypothesis is that the large variation in incompatible elements among the Dhofar 961 subsamples (Fig. 15) does not reflect variable abundance of high-Sm KREEP, as with the Apollo samples, but nonuniform distribution (on the size scale of our small subsamples) of the residual components (e.g., trapped liquid) from which the igneous precursor (or precursors) of the Dhofar 961 breccia was formed. The low Eu concentration of Dhofar 961 is not consistent with either KREEP, as we know it from the Apollo sites, or mafic, magnesian-suite rocks of the Apollo collection, which are also likely products of the Procellarum KREEP Terrane (Korotev et al. 2006). If Dhofar 961 does not contain KREEP, then it probably does not originate from near the Procellarum KREEP Terrane. If it is not from the Procellarum KREEP Terrane, then the South Pole-Aitken basin is the next most likely region of origin because it is the only other large region of the Moon with moderately high concentrations of FeO and Th.

Anorthosite-KREEP mixing also does not account for the trend of the Calcalong Creek subsamples, which are also depleted somewhat in Eu (Fig. 20a). Although we and others have claimed that Calcalong Creek "contain(s) . . . KREEP" (Korotev et al. 2003a) and, thus, likely originates from near the Procellarum KREEP Terrane, that hypothesis is not supported by the Sm-Eu systematics of the subsamples, which do not plot along or parallel to the Apollo mixing trend. It is also (marginally) one of the high-Th/Sm samples of Fig. 6b. Calcalong Creek does contain clasts of mare basalt, which complicates evaluation in terms of Fig. 20. However, a component of mare basalt will decrease, not increase Th/Sm of a mixture (Fig. 6a). Hill and Boynton (2003) describe "an incompatible-element-rich VLT basalt" clast in Calcalong Creek, thus the trend of the subsamples on Fig. 20a could reflect mixing between a low-Eu/Sm nonmare component and a high Eu/Sm basalt component, given that most mare basalts have greater Eu/Sm than nonmare samples of similar Sm concentration. However, Sm does not increase with Sc among the subsamples of Calcalong Creek (Fig. 3), so basalt is not the main carrier of incompatible elements. Marvin and Holmberg (1992) note that they could not identify in thin section the lithologic carrier of the inferred KREEP component of Calcalong Creek. Fig. 20a implies, however, that, as with Dhofar 961, high-Sm KREEP as known from the Apollo sites is not the cause of the elevated concentrations of incompatible elements in Calcalong Creek and, possibly, also Yamato 983885.

CONCLUSIONS

Approximately one quarter of lunar meteorites are breccias with 7–17% FeO, that is, they have compositions intermediate to those of the numerous feldspathic lunar meteorites (3–7% FeO) and the basaltic lunar meteorites (18–22% FeO). Despite that all are polymict breccias, lunar meteorites of intermediate iron concentration are diverse, both petrographically and compositionally. Even among this small subset of lunar meteorites, the diversity exceeds that of meteorites from any other meteorite parent body. Some of the intermediate-iron breccias are, in fact, mixtures that consist mainly of brecciated anorthosite from the feldspathic highlands and basalt from the maria. In this respect they are like regolith breccias from the Apollo 11, 15, and 17 sites. The Apollo samples, however, all have greater concentrations of incompatible elements than binary mixtures of anorthosite and basalt because they also contain KREEP basalt or KREEP-bearing, mafic impact-melt breccia, lithologies that are common among nonmare rocks of the Apollo landing sites. Several of the anorthosite-basalt lunar meteorites, however, do not have substantially greater concentrations of incompatible elements than do mixtures of anorthosite and basalt. Thus these meteorites, which include EET 87521/96008, MET 01210, and likely launch pairs, Yamato 793274/981031, QUE 94281, and NWA 4884, do not contain any substantial proportion of KREEP and likely originate from mare-highlands mixing zones distant from the Procellarum KREEP Terrane.

The range of concentrations of incompatible elements in the intermediate-iron meteorites is large, e.g., a factor of 124 for Sm. Two of the intermediate-iron breccias, NWA 4472/4485 (glassy-matrix breccia) and SaU 169 (regolith breccia), have concentrations of incompatible elements that are much greater (17 and 22 μg/g Sm) than that of any anorthosite-basalt mixture (1–3 μg/g Sm). Among small subsamples of these meteorites, there is no correlation between concentrations of incompatible elements and elements associated with mafic phases. The meteorites consist mainly of some brecciated form of KREEP norite or basalt; both have compositions like those of samples in the Apollo collection. Like the Apollo samples, they likely originate from within or near the Procellarum KREEP Terrane. Another Sm-rich meteorite, Dhofar 1442 (39 μg/g Sm, regolith breccia), is dominated by a KREEP-like component that is more mafic

than any rock from the Apollo collection but nevertheless likely originates from the Procellarum KREEP Terrane.

A number of intermediate-iron lunar meteorites with low-to moderate concentrations of incompatible elements (Calcalong Creek, Dhofar 925, Dhofar 961, Dhofar 1180, NWA 2995 et al. NWA 3136, NWA 4819, NWA 4932, NWA 5207, SaU 300, SaU 449, and Yamato 983885) differ from Apollo samples in that they consist at least in part of mafic, but ferroan, lithologies of the feldspathic highlands, possibly material of the lower crust excavated by basin forming impacts. A number of these meteorites have greater Th/Sm than KREEP-bearing rocks of the Apollo collection, and this ratio may be a signature of lower-crustal mafic rocks containing little or no KREEP.

Some meteorites of intermediate iron concentrations and moderate concentrations of incompatible elements, most notably Dhofar 961 but to a lesser extent Calcalong Creek and Yamato 983885 (4–9 μg/g Sm), also have compositions, as well as compositional variation among subsamples, that is not consistent with an anorthosite-basalt-KREEP mixture in that no such mixture can account for the low concentration of europium in the meteorite. If these breccias are mixtures that do not contain a component of high-Sm KREEP, then they may originate from the South Pole-Aitken basin, with Dhofar 961 being the most likely SPA candidate.

On the basis of petrographic similarity and nearly identical compositions, NWA 4472 is paired with NWA 4485, NWA 4936 is paired with NWA 5406, and the following NWA stones are likely pairs: NWA 2995, 2996, 3190, 4503, 5151, and 5152. Dhofar 925 is likely paired, either terrestrially or by lunar launch, with SaU 449. If Dhofar 961 is also paired with Dhofar 925, then the meteorite is highly heterogeneous. NWA 4819 may be launch paired with SaU 300. NWA 4884 is almost certainly launch paired with Queen Alexandra Range 94281. NWA 4936 is the first lunar meteorite to have a composition similar to Apollo 16 soil. As noted by Sokol et al. (2008), Kalahari 009 (16.4% FeO) derives from a basalt that has lower concentrations of incompatible elements (e.g., ~0.5 μg/g Sm) than any previously known basalt from the Moon. Kalahari 008 is a typical feldspathic lunar meteorite (4.7% FeO). Our compositional data provide little or no evidence supporting or refuting the hypothesis that the Kalahari stones are paired.

Acknowledgments—We thank Martin Altmann, Rainer Bartoschewitz, Addi Bischoff, Dolores Hill, Beda Hoffman, Jim Strope, the National Institute of Polar Research (Japan), and the Antarctic Search for Meteorites program (NSF/NASA) for meteorite samples. A. B. Foreman, S. M. Kuehner, S. P. O'Donnell, and J. H. Wittke assisted with analyses and characterization. The work has benefited greatly by reviews of J. M. D. Day, K. H. Joy, H. Takeda, and A. H. Treiman and discussion with B. Gladman, for which we are grateful. This work was funded mainly by NASA grant NNX07AI44G.

Editorial Handling—Dr. Allan Treiman

REFERENCES

Al-Kathiri A., Gnos E., and Hofmann B. A. 2007. The regolith portion of the lunar meteorite Sayh al Uhaymir 169. *Meteoritics & Planetary Science* 42:2137–2152.

Anand M., Taylor L. A., Misra K. C., Demidova S. I., and Nazarov M. A. 2003. KREEPy lunar meteorite Dhofar 287A: A new lunar mare basalt. *Meteoritics & Planetary Science* 38:485–499.

Anand M., Taylor L. A., Floss C., Neal C. R., Terada K., and Tanikawa S. 2006. Petrology and geochemistry of LaPaz Icefield 02205: A new unique low-Ti mare-basalt meteorite. *Geochimica et Cosmochimica Acta* 70:246–264.

Arai T. and Warren P. H. 1999. Lunar meteorite Queen Alexandra Range 94281: Glass compositions and other evidence for launch pairing with Yamato 793274. *Meteoritics & Planetary Science* 34:209–234.

Arai T., Misawa K., and Kojima H. 2005a. A new lunar meteorite MET 01210: Mare breccia with a low-Ti ferrobasalt (abstract #2361). 36th Lunar and Planetary Science Conference. CD-ROM.

Arai T., Otsuki M., Ishii T., Mikouchi T., and Miyamoto M. 2005b. Mineralogy of Yamato 983885 lunar polymict breccia with KREEP basalt, a high-Al basalt, a very low-Ti basalt and Mg-rich rocks. *Antarctic Meteorite Research* 18:17–45.

Barrat J. A., Jambon A., Bohn M., Blichert-Toft J., Sautter V., Göpel C., Gillet Ph., Boudouma O., and Keller F. 2003. Petrology and geochemistry of the unbrecciated achondrite Northwest Africa 1240 (NWA 1240): An HED parent body impact melt. *Geochimica et Cosmochimica Acta* 67:3959–3970.

Basaltic Volcanism Study Project. 1981. *Basaltic volcanism on the terrestrial planets*. New York: Pergamon Press, Inc. 1286 p.

Bunch T. E., Wittke J. H., and Korotev R. L. 2006. Petrology and composition of lunar feldspathic breccias NWA 2995, Dhofar 1180 and Dhofar 1428 (abstract #5254). *Meteoritics & Planetary Science* 41:A31.

Connolly H. C. Jr., Zipfel J., Grossman J. N., Folco L., Smith C, Jones R. H., Righter K., Zolensky M., Russell S. S., Benedix G. K., Yamaguchi A., and Cohen B. A. 2006. The Meteoritical Bulletin, No. 90, 2006 September. *Meteoritics & Planetary Science* 41: 1383–1418.

Connolly H. C. Jr., Zipfel J., Folco L., Smith C., Jones R. H., Benedix G., Righter K., Yamaguchi A., Chennaoui Aoudjehane H., and Grossman J. N. 2007. The Meteoritical Bulletin, No. 91, 2007 March. *Meteoritics & Planetary Science* 42:413–466.

Connolly H. C. Jr., Smith C., Benedix G., Folco L., Righter K., Zipfel J., Yamaguchi A., and Chennaoui Aoudjehane H. 2008. The Meteoritical Bulletin, No. 93, 2008 March. *Meteoritics & Planetary Science* 43:571–632.

Crozaz G. and Wadhwa M. 2001. The terrestrial alteration of Saharan shergottites Dar al Gani 476 and 489: A case study of weathering in a hot desert environment. *Geochimica et Cosmochimica Acta* 65:971–977.

Day J. M. D., Taylor L. A., Floss C., Patchen A. D., Schnare D. W., Pearson D. G. 2006a. Comparative petrology, geochemistry and petrogenesis of evolved, low-Ti lunar mare basalt meteorites from the LaPaz Icefield, Antarctica. *Geochimica et Cosmochimica Acta* 70:1581–1600.

Day J. M. D., Floss C., Taylor L. A., Anand M., and Patchen A. D. 2006b. Evolved mare basalt magmatism, high Mg/Fe feldspathic crust, chondritic impactors, and the petrogenesis of Antarctic lunar breccia meteorites Meteorite Hills 01210 and Pecora Escarpment 02007. *Geochimica et Cosmochimica Acta* 70:5957–5989.

Day J. M. D. and Taylor L. A. 2007. On the structure of mare basalt lava flows from textural analysis of the LaPaz Icefield and Northwest Africa 032 lunar meteorites. *Meteoritics & Planetary Science* 42:3–17.

Delano J. W. and Livi K. 1981. Lunar volcanic glasses and their constraints on mare petrogenesis. *Geochimica et Cosmochimica Acta* 45:2137–2149.

Demidova S. I., Nazarov M. A., Anand M., and Taylor L. A. 2003. Lunar regolith breccia Dhofar 287B: A record of lunar volcanism. *Meteoritics & Planetary Science* 38:501–514.

Demidova S. I., Nazarov M. A., Lorenz C. A., Kurat G., Brandstätter F., and Ntaflos Th. 2007. Chemical composition of lunar meteorites and the lunar crust. *Petrology* 15:386–407.

Dreibus G., Huisl W., Spettel B., Haubold R., and Jagoutz E. 2003. Chemical alterations in martian meteorites from cold and hot deserts (abstract #10642). EGS-AGU-EUG Joint Assembly.

Elphic R. C., Lawrence D. J., Feldman W. C., Barraclough B. L., Maurice S., Binder A. B., and P. G. Lucey. 2000. Lunar rare earth distribution and ramifications for FeO and TiO_2: Lunar Prospector neutron spectrometer observations. *Journal of Geophysical Research* 105:20,333–20,345.

Fagan T. J., Taylor J. G., Keil K., Hicks T. L., Killgore M., Bunch T. E., Wittke J. H., Mittlefehldt D. W., Clayton R. N., Mayeda T. K., Eugster O., Lorenzetti S., and Norman M. D. 2003. Northwest Africa 773: Lunar origin and iron-enrichment trend. *Meteoritics & Planetary Science* 38:529–554.

Foreman A. B., Korotev R. L., Jolliff B. L., and Zeigler R. A. 2008. Petrography and geochemistry of Dhofar 733—An unusually sodic, feldspathic lunar meteorite (abstract #1853). 39th Lunar and Planetary Science Conference. CD-ROM.

Gallant M., Gladman B., and Ćuk M. 2009. Current bombardment of the Earth–Moon system: Emphasis on cratering asymmetries. *Icarus*, doi:10.1016/j.icarus.2009.03.025.

Gladman B. J., Burns J. A., Duncan M. J., and Levison H. F. 1995. The dynamical evolution of lunar impact ejecta. *Icarus* 118:302–321.

Gnos E., Hofmann B. A., Al-Kathiri A., Lorenzetti S., Eugster O., Whitehouse M. J., Villa I., Jull A. J. T., Eikenberg J., Spettel B., Krähenbühl U., Franchi I. A., and Greenwood G. C. 2004. Pinpointing the source of a lunar meteorite: Implications for the evolution of the Moon. *Science* 305:657–659.

Goles G. G., Duncan A. R., Lindstrom D. J., Martin M. R., Beyer R. L., Osawa M., Randle M., Meek L. T., Steinborn T. L., and McKay S. M. 1971. Analyses of Apollo 12 specimens: Compositional variations, differentiation processes, and lunar soil mixing models. Proceedings, 2nd Lunar Science Conference. pp. 1063–1081.

Greshake A., Irving A. J., Kuehner S. M., Korotev R. L., Gellissen M., and Palme H. 2008, Northwest Africa 4898: A new high-alumina mare basalt from the Moon (abstract #1631). 39th Lunar and Planetary Science Conference. CD-ROM.

Haloda J., Tycova P., Jakes P., Gabzdyl P., and Kosler J. 2006. Lunar meteorite Northeast Africa 003-B: A new lunar mare basaltic breccia (abstract #2311). 37th Lunar and Planetary Science Conference. CD-ROM.

Haloda J., Týcová P., Korotev R. L., Fernandes V. A., Burgess R., Thöni M., Jelenc M., Jakeš P., Gabzdyl P., and Košler J. 2009. Petrology, geochemistry, and age of low-Ti mare-basalt meteorite Northeast Africa 003-A: A possible member of the Apollo 15 mare basaltic suite. *Geochimica et Cosmochimica Acta* 73:3450–3470.

Haskin L. A. 1998. The Imbrium impact event and the thorium distribution at the lunar highlands surface. *Journal of Geophysical Research* 103:1679–1689.

Haskin L. A. and Warren P. H. 1991. Lunar chemistry. In *Lunar sourcebook*, edited by Heiken G., Vaniman D., and French B. M., Cambridge: Cambridge University Press. pp. 357–474.

Haskin L. A., Korotev R. L., Rockow K. M., and Jolliff B. L. 1998. The case for an Imbrium origin of the Apollo Th-rich impact-melt breccias. *Meteoritics & Planetary Science* 33:959–975.

Heiken G. and McEwan M. C. 1972. The geologic setting of the Luna 20 mission. *Earth and Planetary Science Letters* 17:3–6.

Hertogen J., Janssens M.-J., Takahashi H., Palme H., and Anders E. 1977. Lunar basins and craters: Evidence for systematic compositional changes of the bombarding population. Proceedings, 8th Lunar Science Conference. pp. 17–45.

Hill D. H. and Boynton W. V. 2003. Chemistry of the Calcalong Creek lunar meteorite and its relationship to lunar terranes. *Meteoritics & Planetary Science* 38:595–626.

Hsu W., Zhang A., Bartoschewitz R., Guan Y., Ushikubo T., Krähenbühl U., Niedergesaess R., Pepelnik R., Reus U., Kurtz T., and Kurtz P. 2008. Petrography, mineralogy, and geochemistry of lunar meteorite Sayh al Uhaymir 300. *Meteoritics & Planetary Science* 43:1363–1381.

Huber H. and Warren P. H. 2005. MET 01210: Another lunar mare meteorite (regolith breccia) with extensive pyroxene exsolution, and not part of the YQ launch pair (abstract 2401). 36th Lunar and Planetary Science Conference. CD-ROM.

Hudgins J., Walton E., and Spray J. 2007. Mineralogy, petrology and shock history of lunar meteorite Sayh al Uhaymir 300: A crystalline impact-melt breccia. *Meteoritics & Planetary Science* 42:1763–1779.

Irving A. J., Kuehner S. M., Korotev R. L., Rumble D. III, and Hupé G. M. 2006. Mafic granulitic impactite NWA 3163: A unique meteorite from the deep lunar crust (abstract #1365). 37th Lunar and Planetary Science Conference. CD-ROM.

Irving A. J., Kuehner S. M., Korotev R. L., Rumble D. III, and Hupé A. C. 2008. Petrology and bulk composition of large lunar feldspathic leucogabbroic breccia Northwest Africa 5000 (abstract 2186). 39th Lunar and Planetary Science Conference. CD-ROM.

James O. B. 2002. Distinctive meteoritic components in lunar "cataclysm" impact-melt breccias (abstract #1210) 33rd Lunar and Planetary Science Conference. CD-ROM.

James O. B., Lindstrom M. M., and Flohr M. K. 1989. Ferroan anorthosite from lunar breccia 64435: Implications for the origin and history of lunar ferroan anorthosites. Proceedings, 19th Lunar and Planetary Science Conference. pp. 219–243.

Jolliff B. L. 1998. Large-scale separation of K-frac and REEP-frac in the source regions of Apollo impact-melt breccias, and a revised estimate of the KREEP composition. *International Geology Review* 10:916–935.

Jolliff B. L. and Haskin L. A. 1995. Cogenetic rock fragments from a lunar soil: Evidence of a ferroan noritic-anorthosite pluton on the Moon. *Geochimica et Cosmochimica Acta* 59:2345–2374.

Jolliff B. L., Korotev R. L., and Haskin L. A. 1991. Geochemistry of 2–4 mm particles from Apollo 14 soil (14161) and implications regarding igneous components and soil-forming processes. Proceedings, 21st Lunar and Planetary Science Conference. pp. 193–219.

Jolliff B. L., Haskin L. A., Colson R. O., and Wadhwa M. 1993. Partitioning in REE-saturating minerals: Theory, experiment, and modelling of whitlockite, apatite, and evolution of lunar residual magmas. *Geochimica et Cosmochimica Acta* 57:4069–4094.

Jolliff B. L., Rockow K. M., Korotev R. L., and Haskin L. A. 1996. Lithologic distribution and geologic history of the Apollo 17 site: The record in soils and small rock particles from the highlands massifs. *Meteoritics & Planetary Science* 31:116–145.

Jolliff B. L., Rockow K. M., and Korotev R. L. 1998. Geochemistry and petrology of lunar meteorite Queen Alexandra Range 94281, a mixed mare and highland regolith breccia, with special emphasis on very-low-Ti mafic components. *Meteoritics &*

Planetary Science 33:581–601.
Jolliff B. L., Gillis J. J., Haskin L. A., Korotev R. L., and Wieczorek M. A. 2000. Major lunar crustal terranes: Surface expressions and crust-mantle origins. *Journal of Geophysical Research* 105: 4197–4416.
Jolliff B. L., Korotev R. L., Zeigler R. A., Floss C., and Haskin L. A. 2003. Northwest Africa 773: Lunar mare breccia with a shallow-formed olivine-cumulate component, very-low-Ti (VLT) heritage, and a KREEP connection. *Geochimica et Cosmochimica Acta* 67:4857–4879.
Jolliff B. L., Zeigler R. A., Korotev R. L., and Carpenter P. K. 2007. Lunar meteorite Dhofar 961, mafic impact-melt breccia: Petrographic components and possible provenance (abstract #5311). Meteoritics & Planetary Science 42:A77.
Jolliff B. L., Zeigler R. A., Korotev R. L., Carpenter P. K., Vicenzi E. P., and Davis J. M. 2008. Mafic impact-melt components in lunar meteorite Dhofar 961 (abstract #2519). 39th Lunar and Planetary Science Conference. CD-ROM.
Jolliff B. L., Korotev R. L., Zeigler R. A., and Prettyman T. H. 2009. Connecting lunar meteorite Dhofar 961 to the South Pole-Aitken basin through Lunar Prospector gamma-ray data (abstract #2555). 40th Lunar and Planetary Science Conference. CD-ROM.
Joy K. H., Crawford I. A., and Russell S. S. 2006. The petrography and geochemistry of lunar meteorite regolith breccia MET 01210 (abstract). *Meteoritics & Planetary Science* 41:5221.
Joy K. H., Crawford I. A., Kearsley A. T., Fernandes V. A., Burgess R., and Irving A. J. 2008. The petrography and composition of lunar meteorite Northwest Africa 4472 (abstract #1132). 39th Lunar and Planetary Science Conference. CD-ROM.
Kaiden H. and Kojima H. 2002. Yamato 983885: A new lunar meteorite found in Antarctica (abstract #1958). 33rd Lunar and Planetary Science Conference. CD-ROM.
Karouji Y., Arai T., and Ebihara M. 2006. Chemical composition of another KREEP-rich lunar regolith breccia Yamato 983885 (abstract #1919). 37th Lunar and Planetary Science Conference. CD-ROM.
Koeberl C., Warren P. H., Lindstrom M. M., Spettel B., and Fukuoka T. 1989. Preliminary examination of the Yamato-86032 lunar meteorite: II. Major and trace element chemistry. *Proceedings of the NIPR Symposium on Antarctic Meteorites* 2:15–24.
Koeberl C., Kurat G., and Brandstätter F. 1991. Lunar meteorites Yamato 793274: Mixture of mare and highland components, and barringerite from the Moon. *Proceedings of the NIPR Symposium on Antarctic Meteorites* 3:33–55.
Koeberl C., Kurat G., and Brandstätter F. 1993. Gabbroic lunar mare meteorites Asuka-881757 (Asuka-31) and Yamato 793169: Geochemical and mineralogical study. *Proceedings of the NIPR Symposium on Antarctic Meteorites* 6:14–34.
Korotev R. L. 1987a. National Bureau of Standards coal flyash (SRM 1633a) as a multi-element standard for instrumental neutron activation analysis. *Journal of Radioanalytical and Nuclear Chemistry, Articles* 110:59–177.
Korotev R. L. 1987b. The meteoritic component of Apollo 16 noritic impact melt breccias. Proceedings, 17th Lunar and Planetary Science Conference. *Journal of Geophysical Research* 92:E491–E512.
Korotev R. L. 1987c. The nature of the meteoritic components of Apollo 16 soil, as inferred from correlations of iron, cobalt, iridium, and gold with nickel. Proceedings, 17th Lunar and Planetary Science Conference. *Journal of Geophysical Research* 92:E447–E461.
Korotev R. L. 1994. Compositional variation in Apollo 16 impact-melt breccias and inferences for the geology and bombardment history of the Central Highlands of the Moon. *Geochimica et Cosmochimica Acta* 58:3931–3969.
Korotev R. L. 1996. On the relationship between the Apollo 16 ancient regolith breccias and feldspathic fragmental breccias, and the composition of the pre-basin crust in the Central Highlands of the Moon. *Meteoritics & Planetary Science* 31:403–412.
Korotev R. L. 1997. Some things we can infer about the Moon from the composition of the Apollo 16 regolith. *Meteoritics & Planetary Science* 32:447–478.
Korotev R. L. 2000. The great lunar hot spot and the composition and origin of the Apollo mafic ("LKFM") impact-melt breccias. *Journal of Geophysical Research* 105:4317–4345.
Korotev R. L. 2005. Lunar geochemistry as told by lunar meteorites. *Chemie der Erde* 65:297–346.
Korotev R. L. 2006. New geochemical data for a some poorly characterized lunar meteorites (abstract #1404). 27th Lunar and Planetary Science Conference. CD-ROM.
Korotev R. L. and Gillis J. J. 2001. A new look at the Apollo 11 regolith and KREEP. *Journal of Geophysical Research* 106: 12,339–12,353.
Korotev R. L. and Haskin L. A. 1988. Europium mass balance in polymict samples and implications for plutonic rocks of the lunar crust. *Geochimica et Cosmochimica Acta* 52:1795–1813.
Korotev R. L. and Irving A. J. 2005. Compositions of three lunar meteorites: Meteorite Hills 01210, Northeast Africa 001, and Northwest Africa 3136 (abstract #1220). 36th Lunar and Planetary Science Conference. CD-ROM.
Korotev R. L. and Kremser D. T. 1992. Compositional variations in Apollo 17 soils and their relationship to the geology of the Taurus-Littrow site. Proceedings, 22nd Lunar and Planetary Science Conference. pp. 275–301.
Korotev R. L. and Zeigler R. A. 2007. Keeping up with the lunar meteorites (abstract #1340). 38th Lunar and Planetary Science Conference. CD-ROM.
Korotev R. L., Jolliff B. L., and Rockow K. M. 1996. Lunar meteorite Queen Alexandra Range 93069 and the iron concentration of the lunar highlands surface. *Meteoritics & Planetary Science* 31:09–924.
Korotev R. L., Zeigler R. A, Jolliff B. L, and Haskin L. A. 2002. Lithologies of the Apollo 12 regolith (abstract #1395). 33rd Lunar and Planetary Science Conference. CD-ROM.
Korotev R. L., Jolliff B. L., Zeigler R. A., Gillis J. J., and Haskin L. A. 2003a. Feldspathic lunar meteorites and their implications for compositional remote sensing of the lunar surface and the composition of the lunar crust. *Geochimica et Cosmochimica Acta* 67:4895–4923.
Korotev R. L., Jolliff B. L., Zeigler R. A., and Haskin L. A. 2003b. Compositional constraints on the launch pairing of three brecciated lunar meteorites of basaltic composition. *Antarctic Meteorite Research* 16:152–175.
Korotev R. L., Zeigler R. A., and Jolliff B. L. 2006. Feldspathic lunar meteorites Pecora Escarpment 02007 and Dhofar 489: Contamination of the surface of the lunar highlands by post-basin impacts. *Geochimica et Cosmochimica Acta* 70:5935–5956.
Korotev R. L., Bartoschewitz R., Kurtz Th., and Kurtz P. 2007a. Sayh al Uhaymir 300—The most mafic of the feldspathic lunar meteorites (abstract #5006). *Meteoritics & Planetary Science* 42: A86.
Korotev R. L., Zeigler R. A., and Jolliff B. L. 2007b. Do we have a meteorite from the South Pole-Aitken basin of the Moon? (abstract #5257). *Meteoritics & Planetary Science* 42:A87.
Korotev R. L., Irving A. J., and Bunch T. E. 2008. Keeping up with the lunar meteorites—2008 (abstract #1209). 39th Lunar and Planetary Science Conference. CD-ROM.
Korotev R. L., Zeigler R. A., Irving A. J., and Bunch T. E. 2009. Keeping up with the lunar meteorites—2009 (abstract #1137). 40th Lunar and Planetary Science Conference. CD-ROM.
Kuehner S.M., Irving A. J., Rumble D., III, Hupé A. C., and Hupé

G. M. 2005. Mineralogy and petrology of lunar meteorite NWA 3136: A glass-welded mare regolith breccia of mixed heritage (abstract #1228). 36th Lunar and Planetary Science Conference. CD-ROM.

Kuehner S. M., Irving A. J., Korotev R. L., Hupé G. M., and Ralew S. 2007. Zircon-baddeleyite-bearing silica+K-feldspar granophyric clasts in KREEP-rich lunar breccias Northwest Africa 4472 and 4485 (abstract #1516). 38th Lunar and Planetary Science Conference. CD-ROM.

Laul J. C. and Schmitt R. A. 1973. Chemical composition of Luna 20 rocks and soil and Apollo 16 soils. *Geochimica et Cosmochimica Acta* 37:927–942.

Laul J. C. and Papike J. J. 1980. The lunar regolith: Comparative chemistry of the Apollo sites. Proceedings, 12th Lunar and Planetary Science Conference. pp. 1307–1340.

Laul J. C., Papike J. J., and Simon S. B. 1981. The lunar regolith: Comparative studies of the Apollo and Luna sites. Chemistry of soils from Apollo 17, Luna 16, 20, and 24. Proceedings, 12th Lunar and Planetary Science Conference. pp. 389–407.

Laul J. C., Papike J. J., and Simon S. B. 1982. The Apollo 14 regolith: Chemistry of cores 14210/14211 and 15220 and soils 14141, 14148, and 14149, Proceedings, 13th Lunar and Planetary Science Conference. pp. A247–A259.

Lawrence D. J., Feldman W. C., Barraclough B. L., Binder A. B., Elphic R. C., Maurice S., Miller M. C., Prettyman, and T. H. 2000. Thorium abundances on the lunar surface. *Journal of Geophysical Research* 105:20,307–20,331.

Lee M. R. and Bland P. A. 2004. Mechanisms of weathering of meteorites recovered from hot and cold deserts and the formation of phyllosilicates. *Geochimica et Cosmochimica Acta* 68:893–916.

Le Feuvre M. and Wieczorek M. A. 2008. Non-uniform cratering of the terrestrial planets. *Icarus* 197:291–306.

Lindstrom D. J. and Korotev R. L. 1982. TEABAGS: Computer programs for instrumental neutron activation analysis. *Journal of Radioanalytical Chemistry* 70:39–458.

Lindstrom M. M., Duncan A. R., Fruchter J. S., McKay S. M., Stoeser J. W., Goles G. G., and Lindstrom D. J. 1972. Compositional characteristics of some Apollo 14 clastic materials, Proceedings, 3rd Lunar Science Conference. pp. 1201–1214.

Lucey P. G., Blewett D. T., and Hawke B. R. 1998. Mapping the FeO and TiO_2 content of the lunar surface with multispectral imagery. *Journal of Geophysical Research* 103:3679–3699.

Lucey P., Korotev R. L., Gillis J. J., Taylor L. A., Lawrence D., Elphic R., Feldman B., Hood L. L., Hunten D., Mendillo M., Noble S., Papike J. J., and Reedy R. C. 2006. Chapter 2. Understanding the lunar surface and space-moon interactions. In *New views of the Moon*, edited by Jolliff B. L., Wieczorek M. A., Shearer C. K., and Neal C. R. Reviews in Mineralogy and Geochemistry, vol. 60. Washington, D.C.: Mineralogical Society of America. pp. 83–219.

Ma M.-S., Schmitt R. A., Taylor G. J., Warner R. D., Lange D. E., and Keil K. 1978. Chemistry and petrology of Luna 24 lithic fragments and <250 μm soils: Constraints on the origin of VLT mare basalts. In *Mare Crisium: The view from Luna 24*, edited by Merrill R. B. and Papike J. J. New York: Pergamon Press. pp. 569–592.

Marvin U. B. and Holmberg B. B. 1992. Highland and mare components in the Calcalong Creek lunar meteorite (abstract). Proceedings, 23rd Lunar and Planetary Science Conference. pp. 849–850.

Mittlefehldt D. W., McCoy T. J., Goodrich C. A., and Kracher A. 1998. Chapter 4. Non-chondritic meteorites from asteroidal bodies. In *Planetary materials*, edited by Papike J. J. Reviews in Mineralogy, vol. 36. Washington, D.C.: Mineralogical Society of America. pp. 4-1–4-195.

Muehlberger W. R., Hörz F., Sevier J. R., and Ulrich G. E. 1980. Mission objectives for geological exploration of the Apollo 16 landing site. In *Proceedings of the Conference on the Lunar Highlands Crust*, edited by Papike J. J. and Merrill R. B. New York: Pergamon Press. pp. 1–49.

Neal C. R. and Taylor L. A. 1989. Definition of pristine, unadulterated urKREEP composition using the "K-frac/REEP-frac" hypothesis (abstract). 20th Lunar and Planetary Science Conference. pp. 772–773.

Neal C. R. and Taylor L. A. 1992. Petrogenesis of mare basalts: A record of lunar volcanism. *Geochimica et Cosmochimica Acta* 56:2177–2211.

O'Donnell S. P., Jolliff B. L., Zeigler R. A., and Korotev R. L. 2008. Identifying the mafic components in lunar regolith breccia NWA 3136 (abstract #2507). 39th Lunar and Planetary Science Conference. CD-ROM.

Papike J. J., Ryder G., and Shearer C. K. 1998. Chapter 5. Lunar Samples. In *Planetary materials*, edited by Papike J. J. Reviews in Mineralogy, vol. 36. Washington, D.C.: Mineralogical Society of America. pp. 5-1–5-234.

Philpotts J. A., Schnetzler C. C., Nava D. F., Bottino M. L., Fullagar P. D., Thomas H. H., Schuhmann S., and Kouns C. W. 1972. Apollo 14: Some geochemical aspects. Proceedings, 3rd Lunar Science Conference. pp. 1293–1305.

Pieters C. M., Head J. W. III, Gaddis L., Jolliff B., and Duke M. 2001. Rock types of South Pole-Aitken basin and extent of basaltic volcanism. *Journal of Geophysical Research* 106:28,001–28,022.

Prettyman T. H., Hagerty J. J., Elphic R. C., Feldman W. C., Lawrence D. J., McKinney G. W., and Vaniman D. T. 2006. Elemental composition of the lunar surface: Analysis of gamma ray spectroscopy data from Lunar Prospector. *Journal of Geophysical Research* 111, No. E12, E12007 10.1029/2005JE002656.

Reid A. M., Duncan A. R., and Richardson S. H. 1977. In search of LKFM. Proceedings, 8th Lunar Science Conference. pp. 2321–2338.

Righter K., Collins S. J., and Brandon A. D. 2005. Mineralogy and petrology of the LaPaz Icefield lunar mare basaltic meteorites. *Meteoritics & Planetary Science* 40:1703–1722.

Rose H. J. Jr., Cuttitta F., Annell C. S., Carron M. K., Christian R. P., Dwornik E. J., Greenland L. P., and Ligon D. T. Jr. 1972. Compositional data for twenty-one Fra Mauro lunar materials. Proceedings, 3rd Lunar Science Conference. pp. 1215–1229.

Russell S. S., Folco L., Grady M. M., Zolensky M., Jones R., Righter K., Zipfel J., and Grossman J. N. 2004. The Meteoritical Bulletin, No. 88, 2004 September. *Meteoritics & Planetary Science* 39:A215–A272.

Russell S. S., Zolensky M., Righter K., Folco L., Jones R., Connolly Jr. H. C., Grady M. M., and Grossman J. N. 2005. The Meteoritical Bulletin, No. 89, 2005 September. *Meteoritics & Planetary Science* 40:A201–A263.

Schnetzler C. C. and Nava D. F. 1971. Chemical composition of Apollo 14 soils 14163 and 14259. *Earth and Planetary Science Letters* 11:345–350.

Schultz P. H. and Spudis P. D. 1979. Evidence for ancient mare volcanism. Proceedings, 10th Lunar and Planetary Science Conference. pp. 2899–2918.

Seddio S. M., Korotev R. L., Jolliff B. L., and Zeigler R. A. 2009. Petrographic diversity in Apollo 12 regolith rock particles (abstract #2415). 40th Lunar and Planetary Science Conference. CD-ROM.

Sokol A. K., Fernandes V. A., Schulz T., Bischoff A., Burgess R., Clayton R. N., Münker C., Nishiizumi K., Palme H., Schultz L.,

Weckwerth G., Mezger K., and Horstmannaan M. 2008. Geochemistry, petrology and ages of the lunar meteorites Kalahari 008 and 009: New constraints on early lunar evolution. *Geochimica et Cosmochimica Acta* 72:4845–4873.

Spudis P. and Pieters C. 1991. Chapter 10. Global and regional data about the Moon. In *Lunar sourcebook*, edited by Heiken G., Vaniman D., and French B. M. Cambridge: Cambridge University Press. pp. 595–632.

Stöffler D., Knöll H.-D., Marvin U. B., Simonds C. H., and Warren P. H. 1980. Recommended classification and nomenclature of lunar highlands rocks–A committee report. In *Proceedings of the Conference on the Lunar Highlands Crust*, edited by Merrill R. B. and Papike J. J. Houston: Lunar and Planetary Institute. pp. 51–70.

Takeda H., Yamaguchi A., Bogard D. D., Karouji Y., Ebihara M., Ohtake M., Saiki K., and Arai T. 2006. Magnesian anorthosites and a deep crustal rock from the farside crust of the moon. *Earth and Planetary Science Letters* 247:171–184.

Terada K., Anand M., Sokol A. K., Bischoff A., and Sano Y. 2007. Cryptomare magmatism 4.35 Gyr ago recorded in lunar meteorite Kalahari 009. *Nature* 450:849–853.

Walpole R. E. and Meyers R. H. 1993. *Probability and Statistics for Engineers and Scientists*, 5th ed. New York: Macmillan. 766 p.

Wänke H., Baddenhausen H., Balacescu A., Teschke F., Spettel B., Dreibus G., Palme H., Quijana-Rico M., Kruse H., Wlotzka F., and Begemann F. 1972. Multielement analyses of lunar samples and some implications of the results. Proceedings, 3rd Lunar Science Conference. pp. 1251–1268.

Warren P. H. 1989. KREEP: Major-element diversity, trace-element uniformity (almost). In *Workshop on Moon in Transition: Apollo 14, KREEP, and Evolved Lunar Rocks*, edited by Taylor G. J. and Warren P. H. LPI Technical Report 89-03. Houston: Lunar and Planetary Institute. pp. 149–153.

Warren P. H. 1990. Lunar anorthosites and the magma-ocean plagioclase-flotation hypothesis: Importance of FeO enrichment in the parent magma. *American Mineralogist* 75:46–58.

Warren P. H. and Bridges J. C. 2004. Lunar meteorite Yamato-983885: A relatively KREEPy regolith breccia not paired with Y-791197 (abstract #5095). 67th Annual Meeting of the Meteoritical Society. CD-ROM.

Warren P. H. and Kallemeyn G. W. 1989. Elephant Moraine 87521: The first lunar meteorite composed of predominantly mare material. *Geochimica et Cosmochimica Acta* 53:3323–3300.

Warren P. H. and Kallemeyn G. W. 1991. Geochemical investigations of five lunar meteorites: Implications for the composition, origin and evolution of the lunar crust. *Proceedings of the NIPR Symposium on Antarctic Meteorites* 4:91–117.

Warren P. H. and Kallemeyn G. W. 1993. Geochemical investigations of two lunar mare meteorites: Yamato-793169 and Asuka-881757. *Proceedings of the NIPR Symposium on Antarctic Meteorites* 6:35–57.

Warren P. H. and Wasson J. T. 1979. The origin of KREEP. *Reviews of Geophysics and Space Physics* 17:73–88.

Warren P. H., Taylor G. J., Keil K., Marshall C, and Wasson J. T. 1981. Foraging westward for pristine nonmare rocks: Complications for petrogenetic models. Proceedings, 12th Lunar Planetary Science Conference, Part 2. pp. 21–40.

Warren P. H., Ulff-Møller F., and Kallemeyn G. W. 2005 "New" lunar meteorites: Impact melt and regolith breccias and large-scale heterogeneities of the upper lunar crust. *Meteoritics & Planetary Science* 40:989–1014.

Wasson J. T. and Kallemeyn G. W. 1988. Compositions of chondrites. *Philosophical Transactions of the Royal Society of London, Series A* 325:535–544.

Wasson J. T. and Kallemeyn G. W. 2002. The IAB iron-meteorite complex: A group, five subgroups, numerous grouplets, closely related, mainly formed by crystal segregation in rapidly cooled melts. *Geochimica et Cosmochimica Acta* 66: 2445–2473.

Wasson J. T., Boynton W. V., Chou C.-L., and Baedecker P. A. 1975. Compositional evidence regarding the influx of interplanetary materials onto the lunar surface. *The Moon* 13:121–141.

Weisberg M. K., Smith C., Benedix G., Folco L., Righter K., Zipfel J., Yamaguchi A., and Chennaoui Aoudjehane H. 2008. The Meteoritical Bulletin, No. 94, September 2008. *Meteoritics & Planetary Science* 43:1551–1588.

Weisberg M. K., Smith C., Benedix G., Folco L., Righter K., Zipfel J., Yamaguchi A., and Chennaoui Aoudjehane H. 2009. The Meteoritical Bulletin, No. 95. *Meteoritics & Planetary Science* 44:429–462.

Wentworth S., Taylor G. J., Warner R. D., Keil K., Ma M.-S., and Schmitt R. A. 1979. The unique nature of Apollo 17 VLT basalts. Proceedings, 10th Lunar Planetary Science Conference. pp. 207–223.

Willis J. P., Erlank A. J., Gurney J. J., Theil R. H., and Ahrens L. H. 1972. Major, minor, and trace element data for some Apollo 11, 12, 14, and 15 samples. Proceedings, 3rd Lunar Science Conference. pp. 1269–1273.

Zeigler R. A., Korotev R. L., Jolliff B. L., and Haskin L. A. 2005. Petrology and geochemistry of the LaPaz Icefield basaltic lunar meteorite and source-crater pairing with Northwest Africa 032. *Meteoritics & Planetary Science* 40:1073–1102.

Zeigler R. A., Korotev R. L., and Jolliff B. L. 2006a. Geochemistry and petrography of high-Th, mafic impact-melt breccia from Apollo 12 and Sayh al Uhaymir 169 (abstract #2366). 37th Lunar and Planetary Science Conference. CD-ROM.

Zeigler R. A., Korotev R. L., Jolliff B. L., Haskin L. A., and Floss C. 2006b. The geochemistry and provenance of Apollo 16 mafic glasses. *Geochimica et Cosmochimica Acta* 70:6050–6067.

Zeigler R. A., Korotev R. L., and Jolliff B. L. 2007a. Petrography, geochemistry, and pairing relationships of basaltic lunar meteorite stones NWA 773, NWA 2700, NWA 2727, NWA 2977, and NWA 3160 (abstract #2109). 38th Lunar and Planetary Science Conference. CD-ROM.

Zeigler R. A., Korotev R. L., and Jolliff B. L. 2007b. Miller Range 05035 and Meteorite Hills 01210: Two basaltic lunar meteorites, both likely source-crater paired with Asuka 881757 and Yamato 793169 (abstract #2110). 38th Lunar and Planetary Science Conference. CD-ROM.

Zhang A. and Hsu W. 2006. Petrographic and mineralogical studies of the lunar meteorite Dhofar 1180 (abstract #5170). *Meteoritics & Planetary Science* 41:A197.

Zhang A. and Hsu W. 2007, A KREEP clast in the lunar meteorite Dhofar 1180 (abstract #1108). 38th Lunar and Planetary Science Conference. CD-ROM.